IT'IS FOUNDATION
Foundation for Research on Information Technologies in Society

Prof. Dr. Niels Kuster

Director, IT'IS Foundation
Professor, Swiss Federal Institute of Technology – ETH Zurich
Phone +41 44 245 9690 · customized@itis.swiss

Final Report of Project CRR-816

Modelling of Total Exposure in Hypothetical 5G Mobile Networks for Varied Topologies and User Scenarios

Sven Kuehn, Serge Pfeifer, Beyhan Kochali, Niels Kuster

A report on behalf of the Swiss Federal Office for the Environment (FOEN).

Zurich, 24 June 2019

The names of IT'IS and any of the researchers involved may be mentioned only in connection with statements or results from this report.

Imprint

Client:	Swiss Federal Office for the Environment (FOEN) Noise and NIR Division, CH-3003 Bern The FOEN is an office of the Federal Department of the Environment, Transport, Energy and Communications (DETEC)
Contractor:	Foundation for Research on Information Technologies in Society (IT'IS)
Authors:	Sven Kuehn, Serge Pfeifer, Beyhan Kochali, Niels Kuster
FOEN support:	Alexander Reichenbach
Note:	This study was commissioned by the Swiss Federal Office for the Environment (FOEN). The contractor is solely responsible for the content.
Date:	24 June 2019
Version:	V 1.0r2764

Executive Summary

In January 2019, the Swiss Federal Office for the Environment (FOEN) mandated the IT'IS Foundation to evaluate the total human exposure in hypothetical 5G mobile networks for varied topologies and user scenarios to identify factors that would minimize the total exposure of the population. In this study, *total exposure* is defined as the combined exposure from network base stations, the user's own device, as well as bystanders' mobile devices.

The influence of various factors on total exposure in mobile communication networks (as defined above) was modeled and analyzed with the help of the Monte Carlo simulation technique. Total exposure is described as the local peak specific absorption rate (SAR) spatially averaged over any 10 g of tissue mass ($\mathrm{psaSAR_{10g}}$) averaged over a period of 6 minutes. The unit $\mathrm{psaSAR_{10g}}$ was chosen because it defines the governing basic restriction for wireless exposure as the whole-body average SAR limits (wbaSAR) are intrinsically met if the limits of local exposure are satisfied. The averaging duration of 6 minutes constitutes the internationally accepted averaging time to prevent thermal hazards at frequencies below 6 GHz as instant values have little justifications. However, it should be noted that some regulators define shorter averaging time periods, e.g., the US Federal Communications Commission (FCC) of 100 s.

In a first step, we analyzed the tissue-specific exposure as a function of frequency. The preliminary dosimetric study showed that exposure of the human brain to the 3.6 GHz band, that has been recently added to the Swiss mobile communication frequencies, is reduced by a factor of >6 for the tissue averaged SAR when compared to mobile network operation at <1 GHz. This reduction is due to the smaller penetration depth at higher frequencies. This conclusion, however, does not apply to exposed tissues close to the surface or skin (eyes, testicles, etc.) when the peak SAR in this tissue is evaluated. The peak SAR in the grey matter remains in approximately the same order of magnitude (±3 dB) over all frequencies but the area of high exposure is reduced at 3.6 GHz.

In a second step, we used data measured in 4G systems and analyzed the latest mobile network standards to extrapolate the exposures for various 5G network scenarios. These measured data were also used to extrapolate the exposure to the future development of data usage in 5G networks.

Specifically, we analyzed the effect on the total exposure of (i) the network topology by varying the cell size and amount of indoor coverage in the network, as well as the usage of (ii) an individual's own device, and (iii) devices of close bystanders.

The results – based on simulations of more than 200 different exposure scenarios – reveal that, for all user types, except for non-users (including passive mobile phone users and users dominantly using downlink data traffic, e.g., video streaming), total exposure is dominated by the person's own mobile device. Compared to non-users, the exposure is increased (i) for light users (with 100 MByte uplink data per day) by 6 – 10 dB (or a factor of 4 to 10), (ii) for moderate users (with 1 GByte uplink data per day) by 13 – 25 dB (or a factor of 20 to >300), and (iii) for heavy users by 15 – 40 dB (or a factor of 30 to >10000). Further, the results show that peak exposure of non-users is not defined by exposure to base stations but by exposure to mobile devices of close bystanders in urban areas resulting in 6 dB (or a factor of 4) higher exposure than from a nearby base station antenna.

While a reduction of the mobile cell size leads to a reduction in total exposure by a factor of 2 to10 for people actively using their mobile devices, this might also lead to a small increase by a factor of 1.6 in total exposure of non-users due the generally increased incident signal levels from the surrounding base stations.

Similarly, the exposure of active users can be reduced by a factor of 4 to 600 by increasing the indoor network coverage. Yet, in line with the results for the mobile cell sizes, increased indoor

coverage will also lead to increased exposure of non-users by a factor of 2 to 10. This increase, however, starts at a level 1000 times lower than the typical total exposure of active users.
The results of this study show that the personal mobile device is the dominant exposure source for active mobile network users. Besides a person's own usage behavior, total exposure is also closely linked to the network infrastructure. Generally speaking, a network with a lower path loss, i.e., smaller cells and additional indoor coverage, helps to reduce total exposure.
The exposure per transmitted bit is reduced by a factor of <3 by the increased spectral efficiency of the 5G technology, and the reduced penetration depth associated with the new bands at 3.5 – 3.8 GHz.
The results presented above are limited due to the network data that has been used and the definition of total exposure as stated in this report. Furthermore, it only considers time-averaged (6 min) and not instant exposures. This study does not consider (i) the effect of upcoming massive MIMO systems in 5G networks, (ii) alternative data transmission links, for instance the use of Wireless Local Area Network (WLAN), and (iii) millimeter wave frequencies in 5G mobile networks.

Contents

1 List of Abbreviations and Acronyms

Δ	power control reduction factor
$\Delta_{\text{data}_{\text{4G5G}}}$	factor to describe the increase in required data capacity from LTE to 5G
$\Delta_{\text{eff}_{\text{4G5G}}}$	factor to describe the increase in spectral efficiency from LTE to 5G-NR
DC_{own}	duty-cycle of the users own mobile data transmission
S	power density in W/m^2
UL_{rf}	uplink radiation factor (loss)
5G	5th generation wireless mobile network
5G-NR	5G new radio
CDF	cumulative distribution function
EMF	electromagnetic fields
ERP	effective radiated power
FDD	frequency division duplex
ICNIRP	International Commission on Non-Ionizing Radiation Protection
LTE	Long-Term Evolution
MIMO	multiple-input and multiple-output
PL	path loss
$\text{psaSAR}_{\text{10g}_{\text{mobile}}}$	10 g peak spatial average SAR from own mobile phone measured at maximum output power
$\text{psaSAR}_{\text{10g}}$	peak spatial specific absorption rate averaged over 10 g
PSU	places with sensitive use
RF	radiofrequency
RSRP	reference signal received power
$\text{SAR}_{\text{10g}_{\text{base station}}}$	SAR from base station antennas
$\text{SAR}_{\text{10g}_{\text{bystander}}}$	SAR caused by bystander mobile devices
$\text{SAR}_{\text{10g}_{\text{mobile}}}$	SAR from own mobile phone
SDL	supplemental downlink
TDD	time division duplex
UE	user equipment
UMTS	Universal Mobile Telecommunications Service
wbaSAR	whole-body average SAR

2 Introduction and Background

The Swiss Federal Office for the Environment (FOEN) mandated the IT'IS Foundation to evaluate the total combined exposure from base stations and mobile devices used close to the human body for various topologies and usage scenarios of hypothetical 5G networks to identify factors that minimize the total exposure of the population.
The Swiss Federal Office for Communications recently licensed various frequency bands to the Swiss Mobile Communication Network Operators [1] (see Tab. 1). These bands, together with existing technology-neutrally licensed frequency bands, pave the way for the introduction of 5G mobile communication in Switzerland.

	Salt	Sunrise	Swisscom
700 MHz FDD	20 MHz	10 MHz	30 MHz
700 MHz SDL	0	10 MHz	0
1400 MHz SDL	10 MHz	15 MHz	50 MHz
2.6 GHz TDD	0	0	0
3.5 — 3.8 GHz TDD	80 MHz	100 MHz	120 MHz

Table 1: Additionally awarded frequency bands for the introduction of 5G mobile communication in Switzerland [1]; FDD refers to frequency division duplex, SDL to supplemental downlink, and TDD to time division duplex

At the same time, according to the three network operators, current Swiss regulations for base station safety [2] are an impedance to the introduction of 5G technologies in Switzerland. The emission limits for electromagnetic fields (EMF) in the radiofrequency (RF) range are generally based on the guidelines of the International Commission on Non-Ionizing Radiation Protection (ICNRIP) [3]. For base station sites (with more than 6 W effective radiated power (ERP)) there is, however, a precautionary limit [2] – of a factor of 10 in terms of incident electric field or a factor of 100 in terms of incident power density – lower than the limits of the ICNIRP [3] guidelines. This precautionary limit applies to all places where people are likely to be present for a long duration, such as their homes and offices, as well as special locations like schools and playgrounds. These locations are usually referred to as *places with sensitive use* (PSU).
It is important to note that, based on the site definition of [4], base station antennas within a site perimeter reaching from a few meters to up to a range of 70 m or more may have to be combined into a single site. In addition, [2, 4] do not foresee temporal averaging (i.e., the instantaneous maximum possible root mean square value of the incident electric field is measured with the site operating at maximum output power) and require the assessment of the spatial peak incident field, which is justified given the likelihood of partial body exposure by localized peak fields [5]. In contrast, [3] allows temporal averaging over a time-frame of 6 minutes. Some regulators defines shorter averaging time, e.g., FCC (USA) of 100 s. It should also be noted that for highly dynamic networks instant exposure levels have little correlation with the safety guidelines and the underlying biological effects.
To date, most existing base station sites in urban and suburban areas in Switzerland exhibit a utilization level of close to 100% with respect the precautionary limit. While, during the transition from the Universal Mobile Telecommunications Service (UMTS) protocol to Long-Term Evolution (LTE) technology, a large part of the increased data traffic requirements were absorbed by the much better spectral efficiency of LTE [6]. On the other hand, the increase in spectral efficiency due to the transition from LTE to 5G New Radio (5G-NR) is expected to be smaller, and, thus, traffic increase will have to be absorbed with the wider bandwidth

and, ultimately, higher output power of the base station sites due to the sensitivity limit of the mobile devices. Most of the bandwidth is allocated in the frequency range around 3.6 GHz, which is subject to higher path loss than the existing lower frequency bands used for 2G to 4G communications and, consequently, requires higher output power for the same coverage area.
Swiss operators argue that for the introduction of 5G, an increase of the precautionary limit in the range of 12 dB or a factor of 16 in power is required. FOEN, in response to a mandate of the Swiss government, has established a dedicated working group to address the needs and risks associated with future mobile networks in Switzerland.
This study has been performed as part of this working group to identify possibilities to reduce the total exposure of the Swiss population. The study aims to support decision making during the review of the precautionary limits for non-ionizing radiation from mobile network base station sites.

3 Objectives

The overall objective of this study is to perform an evaluation of the total human exposure in 5G networks for different topologies and user scenarios to identify factors that minimize the total exposure of the population. Specifically, the following variables are considered:

- network topology:
  - the use of existing base station site infrastructure
  - the increase in wide-band coverage due to wider use of indoor coverage
- geographical location:
  - rural
  - suburban
  - urban
- uplink data usage (and time-course of usage):
  - light user: 100 MB/d
  - moderate user: 1 GB/d
  - heavy user: 10 GB/d
  - non-user
- bands licensed in Switzerland (700 MHz – 3.6 GHz, i.e., excluding millimeter-wave frequencies)
- mobile device exposure
- population density
- bystander exposure

The results obtained reflect the total exposure – defined as the combined exposure from network base stations, the user's own mobile device, as well as mobile devices from bystanders – in 5G networks with respect to the peak specific absorption rate spatially averaged over 10 g (psaSAR_{10g}) induced in any location of the human body over a 6-minute temporal averaging period.

4 Methods

This section describes the proposed methods for evaluating the total exposure in 5G networks as outlined in Section 3.

4.1 Initial Situation

In the following, the main prerequisites and constraints under which the study is performed are summarized:

Time Constraint: Due to the urgency of the topic (first 5G implementations are ready to be used) and the tight schedule of the working group initiated by FOEN, this study had to be completed within only a few weeks. Consequently, large scale simulations such as propagation and exposure modelling could not be performed in the allocated time-frame.

5G Network Performance Data: As there is very little reliable data on the performance behavior of 5G networks in real implementations to date, we extrapolated performance behavior from LTE network data.

5G Performance Requirements: Based on input from Swiss mobile operators, their performance targets for 5G networks is to provide data rates of 100 MBit/s *everywhere* and 3 GBit/s in peak locations. It is important to note that the *everywhere* requirement is about a factor of 10 – 20 higher than that for current LTE networks.

Absolute versus Relative Evaluation: This study is not designed to draw conclusions about absolute levels of exposure but rather to differentially evaluate the various scenarios of 5G networks, which is why other sources of exposure (e.g., WiFi, radio, and TV broadcast, etc.) are excluded.

Network Topology: In Switzerland, 5G networks will rely on a hybrid network topology. Therefore, the main focus of this study is on the effect on total exposure of the percentage of indoor cells used in such a hybrid network. The study does not look into the realisation of the network coverage but supposes that the RSRP can be achieved.

4.2 Frequency Dependence of Absorption in Sensitive Tissue Regions

The 5G network implementation in Switzerland adds a novel frequency band at around 3.6 GHz. The absorption characteristics in the human body are very frequency dependent [7]. In the initial part of the study, we analyzed the exposure levels in human brain tissue, which is dominated by an individual's own mobile device usage against the head, based on the method described in [7]. However, we extended the work of [7] to the newly added frequencies at 3.6 GHz.

4.3 Monte Carlo Study Concept

In this study, we:

1. derive a closed-form expression for the total psaSAR_{10g} with respect to the study input variables
2. describe the study input variables by means of probability distributions and constants
3. combine the different probability distributions by means of the Monte Carlo Simulation technique
4. provide results by means of statistical summaries (histograms)

4.4 Expression for Total psaSAR$_{10g}$

In this section, an expression for the total SAR$_{10g}$ is derived, with all input variables based on probability distributions or constants that are defined in the subsequent sections.
The SAR$_{10g}$ is defined as:

$$SAR_{10g_{total}} = SAR_{10g_{mobile}} + SAR_{10g_{basestation}} + SAR_{10g_{bystander}} \quad (1)$$

where SAR$_{10g_{mobile}}$ is the 10 g SAR in the body of the user caused by exposure to the uplink signal of his/her own mobile device, SAR$_{10g_{base\ station}}$ is the 10 g SAR caused by exposure to the base station downlink signal, and SAR$_{10g_{bystander}}$ is the exposure caused by the mobile uplink signal of the mobile devices of bystanders. Note: for simplicity and due to relatively homogenous exposure from bystanders and base stations, it is assumed in the equation that the absorbed energy is summed at the same location over the 6 minute averaging period.

4.4.1 SAR from Own Mobile Phone

The SAR from a person's own mobile phone depends on the measured peak spatial average SAR ($psaSAR_{10g_{mobile}}$) at maximum output power (Section 4.7), its relative transmit power $\left(\Delta = \frac{P_{tx}}{P_{tx_{max}}}\right)$, and the duty cycle of the user's own data transmission usage (DC$_{own}$).

$$SAR_{10g_{mobile}} = psaSAR_{10g_{mobile}} \cdot \Delta \cdot DC_{own} \quad (2)$$

In this context, DC$_{own}$ is the duty-cycle dependent on the user's own data uplink usage averaged over 6 minutes (see Section 4.8). Note: As the power control in 5G (LTE) is data rate / resource block dependent, Δ would also be a function of the data usage, which is neglected here. The maximum output power of a user's equipment (UE) can range between 23 dBm (200 mW) and -40 dBm (0.1 μW). Measurements in real networks [8] show, however, that instantaneous output power levels from UE are in the range between -15 and 23 dBm or a power control range of approximately 0 to -40 dB (1 to 1/10000). UE power control in UMTS, LTE, and 5G-NR is implemented in a very similar fashion [9]. As an approximation to keep the model simple, we assume that the power control is inversely proportional to the path loss (PL) for a given reference signal received power (RSRP) and proportional to the amount of allocated resource blocks. In this model, it is assumed that the resource block allocation remains the same for different data usage behaviors for a given scenario and, hence, the effect of the occupied bandwidth on the UE output power is excluded.
With the assumption taken above:

$$\Delta = (1-N) \cdot \frac{PL_{loc}(RSRP_{loc})}{PL_{max}} + N \cdot \frac{PL_{indoor}(RSRP_{indoor})}{PL_{max}} | \Delta \in [0.0001; 1] \quad (3)$$

In the above equation, PL is the path loss probability distribution (Figure 2) for a given scenario (loc = {urban, suburban, rural}), and PL_{max} is the path loss level when the UE goes to maximum output power (see Section 4.5). Each path loss data sample is linked to a RSRP data sample in the data set. The model has been implemented in a way that a random RSRP and PL pair is drawn, i.e, coherent PL and RSRP pairs. N ($\in [0; 1]$) is a scaling factor that differentially increases coverage by indoor cells. Note: the factor (1-N) may not be fully realistic as in a real network umbrella cells would always be present as well. In this model, we assume that uplink traffic is fully routed through the additional indoor cells. As defined before, Δ is limited to take values between 0.0001 – 1 (or -40 – 0 dB), only.

4.4.2 SAR from Base Station

The SAR from the base station can be calculated on basis of the incident power density (S) and a transformation as described in Section 4.6

$$SAR_{10g_{basestation}} = S \cdot CF \tag{4}$$

CF is a factor used to convert incident power density to localized $psaSAR_{10g}$.
The incident power density can be determined from the RSRP data provided in Section 4.5:

$$S = \frac{((1-N) \cdot RSRP_{loc} + N \cdot RSRP_{indoor}) \cdot 12 \cdot M_{RB} \cdot \frac{1}{\Delta_{eff_{4G5G}}} \cdot \Delta_{data_{4G5G}} \cdot UL_{rf}}{A_e} \tag{5}$$

$$A_e = \frac{\lambda^2}{4\pi} \cdot G \tag{6}$$

As before, a scaling factor N is used to differentially include indoor coverage systems in the network topology. As the RSRP is determined per resource element (bandwidth), it must be multiplied by a factor of 12 for each resource block bandwidth, as this data originates from LTE. Note: while in LTE, each resource block can only have 12 subcarriers of 15 kHz bandwidth per resource block; there are more options in 5G-NR. This is, however, not considered to be relevant here. M_{RB} is the number of resource blocks occupied in the downlink. Publication [10] reports an average per user downlink data rate of approximately 20 Mbps in an LTE cell with 100% load and 15 MHz bandwidth and an RSRP of -100 dBm at the cell edge and 2x2 MIMO. Based on this information, we observe that an LTE cell with 75 resource blocks in the downlink can achieve a per user downlink capacity of 20 Mbps with a cell edge RSRP of < -120 dBm and no MIMO present. The factor $\Delta_{\text{eff}_{4G5G}}$ is the increase in spectral efficiency between 5G and LTE. Based on [11], $\Delta_{\text{eff}_{4G5G}}$ is assumed to be 3. The factor of 3 can be disputed, especially in initial implementations of 5G networks [12]. However, in this study design with emphasis on relative statements the same factor applies to mobile stations and base stations and is therefore not relevant. $\Delta_{\text{data}_{4G5G}}$, the increase in data capacity required for transitioning from LTE to 5G, is expected to be at least 5 with respect to the reference LTE cell, i.e., 100 Mbps.
UL_{rf} is the uplink radiation factor accounting for propagation losses in the UE and the users body. A_{e} is the effective aperture of the UE antenna that measures the RSRP. We apply the A_{e} of a dipole antenna at 2 GHz.

In summary, following constants are used in the power density calculation:

M_{RB}	75
$Delta_{eff_{4G5G}}$	3
$\Delta_{data_{4G5G}}$	5
UL_{rf}	6 dB
$12 \cdot M_{RB} \cdot \frac{1}{\Delta_{eff_{4G5G}}} \cdot \Delta_{data_{4G5G}}$	$12 \cdot 75 \cdot \frac{1}{3} \cdot 5 \cdot 4 = 6000$
A_e	$\frac{0.15^2 m^2}{4\pi} \cdot 1.64 = 0.0029\, m^2$

Which may be simplified to:

$$S = \frac{((1-N) \cdot RSRP_{loc} + N \cdot RSRP_{indoor}) \cdot 6000}{0.0029\, m^2} \tag{7}$$

$$E = \sqrt{S \cdot Z} \tag{8}$$

For N = 0 and an RSRP of -65 dBm ($3 \cdot 10^{-10}$ W) close to the cell center the power density becomes 0.64 mW/m^2 or 0.5 V/m, which is a realistic value for close to a base station antenna in Switzerland. Note: this study concept excludes exposure through a possible wireless backhaul.

4.4.3 SAR from Bystander

Exposure caused by a single bystander is approximated by the following expression:

$$SAR_{bystander} = \Delta \cdot DC_{bystander} \cdot 0.2W \cdot \frac{1}{UL_{rf}} \cdot \frac{1}{4\pi r^2} \cdot CF \quad (9)$$

which is based on the assumption that the bystander is transmitting with the same power control level Δ as the subject's own mobile phone, but with a distinctly different bystander duty-cycle $DC_{bystander}$. The maximum output power of the bystander's UE is assumed to be 0.2 W [8], with an estimated uplink radiation factor UL_{rf} (loss) of 6 dB or 4 based on various studies in this area [13], [14], [15]. Based on the assumption of an isotropic free-space propagation ($\frac{1}{4\pi r^2}$) – for the average population density scenarios defined in Section 4.5 – a circular intersubject distance was found:

rural $r = 25\,\mathrm{m}$

suburban $r = 10\,\mathrm{m}$

urban $r = 5\,\mathrm{m}$

train / urban center $r = 1\,\mathrm{m}$

As before, CF is the factor used for conversion from incident power density to localized SAR. Note: even for larger inter-subject distances, we did not take into account attenuation by buildings, et cetera. Except for the train / urban center scenario, all above distances would immediately result in contributions from bystander exposures lower than those caused by a nearby base station.

4.5 Swisscom LTE Path Loss Data

This section summarizes the RSRP and path loss data for different geographical locations and topologies in the Swisscom LTE network. Shown in Figure 1 are the cumulative distribution functions of the path loss and, in Figure 2, the RSRP. As the frequency allocation (with the exception of the newly added 3.6 GHz band) will not change for 5G in Switzerland, we assumed that the distributions of RSRP and path loss are not likely to change dramatically in the near future.
The categorization was performed on the basis of the number of citizens within 500 m of a base station:

0 – 800 citizens rural, assuming 400 citizens, or $2000\,\mathrm{m}^2$ per citizen on average

801– 4000 citizens suburban, assuming 2500 citizens, or $300\,\mathrm{m}^2$ per citizen on average

4001 – and higher numbers of citizens urban, assuming 10000 citizens, or $80\,\mathrm{m}^2$ per citizen on average

4.5.1 Cell Edge Definition

For the definition of the cell edge, we use the observation that uplink performance is inversely correlated with the path loss and that the path loss is inversely correlated with the downlink parameter (RSRP) [16]. Assuming the cell edge at the 5th percentile of the individual cumulative distribution function (CDF) in Figure 2, we obtain the following cell edge definitions.

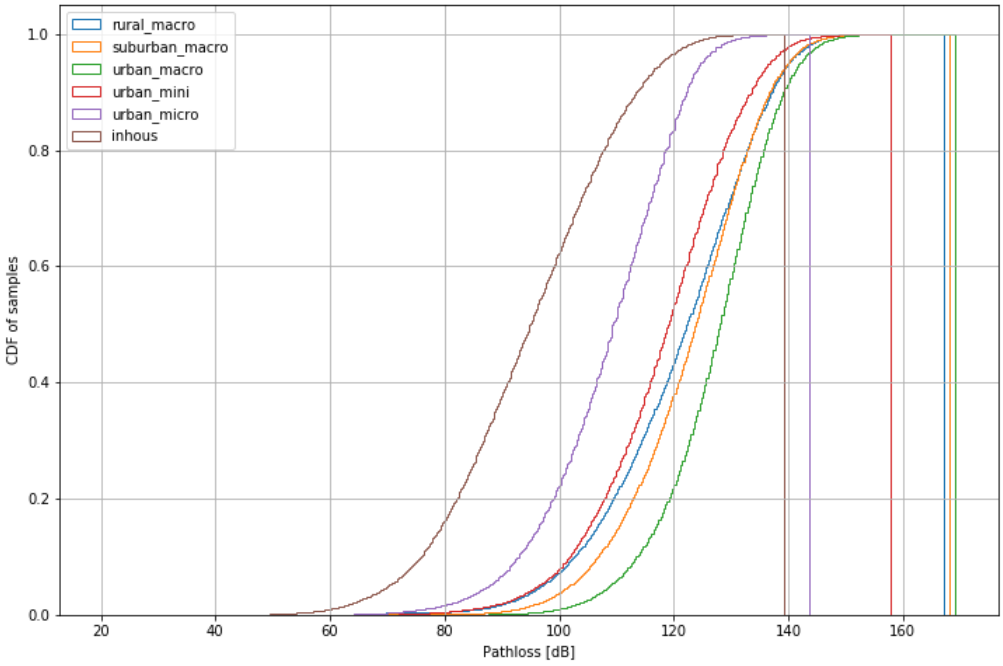

Figure 1: Swisscomm path loss data for different geographical locations

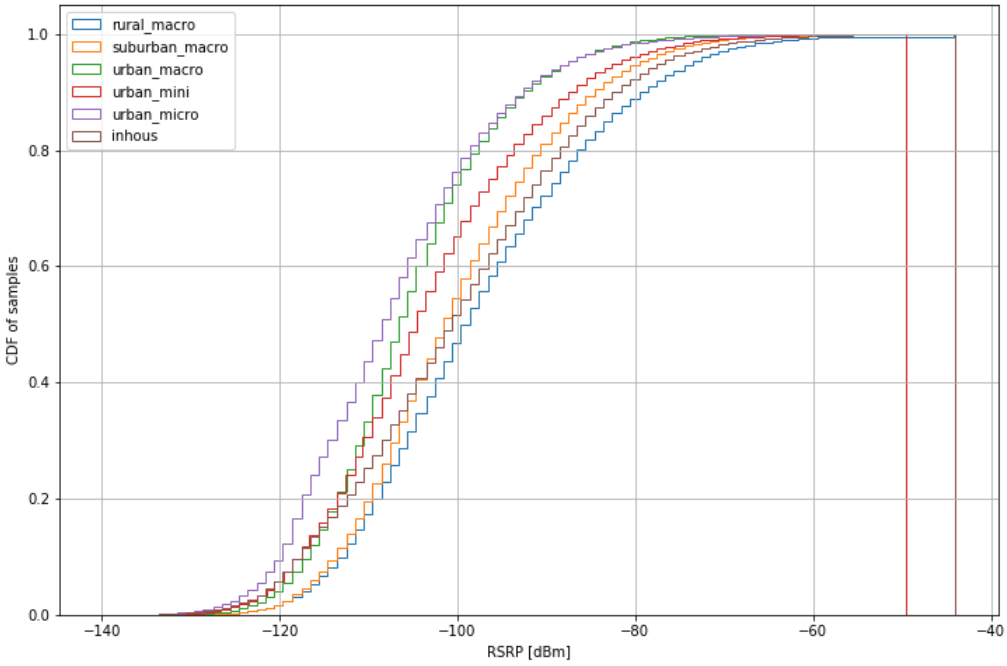

Figure 2: Swisscomm RSRP data for different geographical locations

$RSRP_{celledge_{rural-macro}}$	-117 dBm
$RSRP_{celledge_{suburban-macro}}$	-117 dBm
$RSRP_{celledge_{urban-macro}}$	-120 dBm
$RSRP_{celledge_{urban-mini}}$	-121 dBm
$RSRP_{celledge_{urban-micro}}$	-123 dBm
$RSRP_{celledge_{inhouse}}$	-120 dBm

In the Monte Carlo simulation, the cell edge is used to define the levels up to which the RSRP values (paired with the path loss) are taken into account by sampling.
Figure 1 summarizes the path loss data. It is obvious that different topologies have very different path losses; especially the path losses for indoor coverage are substantially lower. As the network will – among other optimizations – try to keep the incoming power at the base station constant, the UE undergoes a power control. We assume that the power control is proportional to the path loss, i.e., that the UE output power is high for a high level of path loss.
For the mobile phone power control calculation, we assume that the UE attains the maximum output power at a path loss of $\mathrm{PL}_{\max} = 140$ dB. Consequently, with 40 dB power control range, the UE will be at minimum output power at 100 dB path loss. This means that, for indoor coverage, the mobile phone operates at minimum output power >60% of the time.

4.5.2 Global Cell Shrinking

To evaluate the impact of global shrinking of the mobile network cell size, we simulated the increase of the cell edge definition values. Assuming free-space propagation, a reduction of the cell radius by a factor of 2 would result in a 6 dB higher RSRP cell edge value. In reality, however, the effect would be different due to signal attenuation other than free-space propagation. For this study, we assume two reduction factors, corresponding to 6 and 12 dB higher RSRP values at the cell edge. It should be noted that cell size shrinking while maintaining the same base station power (as in this experiment) may lead to higher interferences between site. However, due to the inherent power limitations imposed by ONIR this is not expected to have a large impact in Switzerland.

$RSRP_{celledge_{reduction1}}$	6 dB
$RSRP_{celledge_{reduction2}}$	12 dB

4.6 Far-field Exposure to SAR Transformation

In this section, we describe the transformation factor for converting a far-field incident field to induced SAR averaged over 10 g of tissue. The transformation is based on data in [17]: an average conversion factor of 0.054 $\frac{W}{kg}/\frac{W}{m^2}$ is applied. The standard deviation with respect to psaSAR_{10g} over all models, frequencies, and tested incidences is as small as 2 dB. Based on the overall uncertainties in this study, we do not include the variability of the psaSAR_{10g} in the human body in the statistical modelling.

CF	0.054 $\frac{W}{kg}/\frac{W}{m^2}$

4.7 Mobile Device SAR Data

About 90% of the Swiss smartphone market is taken by three device vendors: Apple, Samsung, and Huawei. We have analyzed the full psaSAR test reports [18] of the latest models from these three vendors with more than 2000 SAR measurements in total covering the frequency range from 700 MHz – 2.6 GHz. We found that the average psaSAR values from the phones of these vendors are 0.16, 0.3, and 0.52 W/kg, respectively. The standard deviation of the SAR test results over all test orientations and frequencies was found to be on the order of 3 dB. Over all

test configurations, only the test distance shows a correlation with the SAR value. Due to the relatively small variations, an average $\text{psaSAR}_{10\text{g}_{\text{mobile}}}$ value of 0.33 W/kg was selected, and the statistical distribution of the UE psaSAR is not included in the Monte Carlo analysis.

$psaSAR_{10g_{mobile}}$	0.33 W/kg

4.8 Usage Behavior (Duty-Cycle)

In this section, we describe the derivation of the probability functions of the duty cycles in the uplink for users and non-users.
As there is no data in the literature covering analysis of uplink usage statistics in modern (4G) mobile networks, we generated hypothetical usage patterns for the following user types:

user 0 : non-user,

user 1 : 100 MByte/day,

user 2 : 1 GByte/day,

user 3 : 10 GByte/day.

For these users, we generated uplink data traffic as summarized in Table 2. The traffic is quantized in atomic units that are transmitted at the maximum possible data rate at once, e.g., uploading a video and streaming units that require a certain data rate for a specific duration (e.g., a video call).

Table 2: Uplink data traffic definition for user types 1 – 3. Atomic transmission units are transmitted at maximum data rate. Streaming data units are transmitted at a constant data rate for the duration of use.

	uplink service	unit	MB /unit	user 1 units	user 2 units	user 3 units	user 1 /MB	user 2 /MB	user 3 /MB
atomic	cloud services, social media	message	0.05	10	50	1000	0.5	2.5	50
		file	50	1	5	100	50	250	5000
		picture	5	8	20	250	40	100	1250
		video	100	0	2	20	0	200	2000
stream	augmented, virtual reality	10 min	1	0	6	24	0	6	24
	voice call	10 min	6	1	2	12	6	12	72
	video call [1]	10 min	150	0	3	12	0	450	1800
	system	1 h	1	4	8	16	4	8	16

As the next step, we randomly distributed the required atomic and streaming data units for each user type over a 14 h time-frame from 8am to 10pm, with a resolution of 1 s referred to a $DR_{required}$(t, user) being the required data rate in each second. As the data rate may be limited due to the signal quality, we then filtered the peak data rate of $DR_{required}$(t, user) with the

following rates per path loss:

path loss |dB	$DR_{max}(PL)$ max. data rate /Mbps
≥130	10
<130	15
<120	20
<110	30
<100	45
<90	60
<80	90
<70	120
<60	180

These data rates were chosen based on an uplink to downlink ratio of 1/10, a minimum downlink data rate requirement of 100 Mbps at the cell edge, and a maximum downlink data rate of approximately 2 Gbps. In case the available data rate (depending on the RSRP) is insufficient at any instant in time, the transmission duration is prolonged at the maximum rate until all data is transmitted. In the simulations it is assumed that all cell-types can reach their full theoretical capacity in future, even though this may not be the case for all types to date.
The resulting filtered data rate time course is referred to as $DR_{required_{limited}}$(t, user, PL). For each instant in time, we calculated the duty cycle (DC) of the UE with respect to the maximum possible data rate for each RSRP range:

$$DC(t, user, PL) = \frac{DR_{required_{limted}}(t, user, PL)}{DR_{max}(PL)} \tag{10}$$

The time course is then subdivided into 6 minute intervals over which the average duty cycle $DC_{6min\text{-}avg}$(N, user, PL) is calculated:

$$DC_{6min-avg}(N, user, PL) = \frac{\sum_{t=0}^{360} DC(t, user, PL)}{360s}\Bigg|_{N=0}^{140} \tag{11}$$

resulting in 140 samples of 6 minute averaged duty-cycles for each user type and RSRP level to be used in the Monte Carlo simulation. The resulting distributions are summarized in Figure 3.

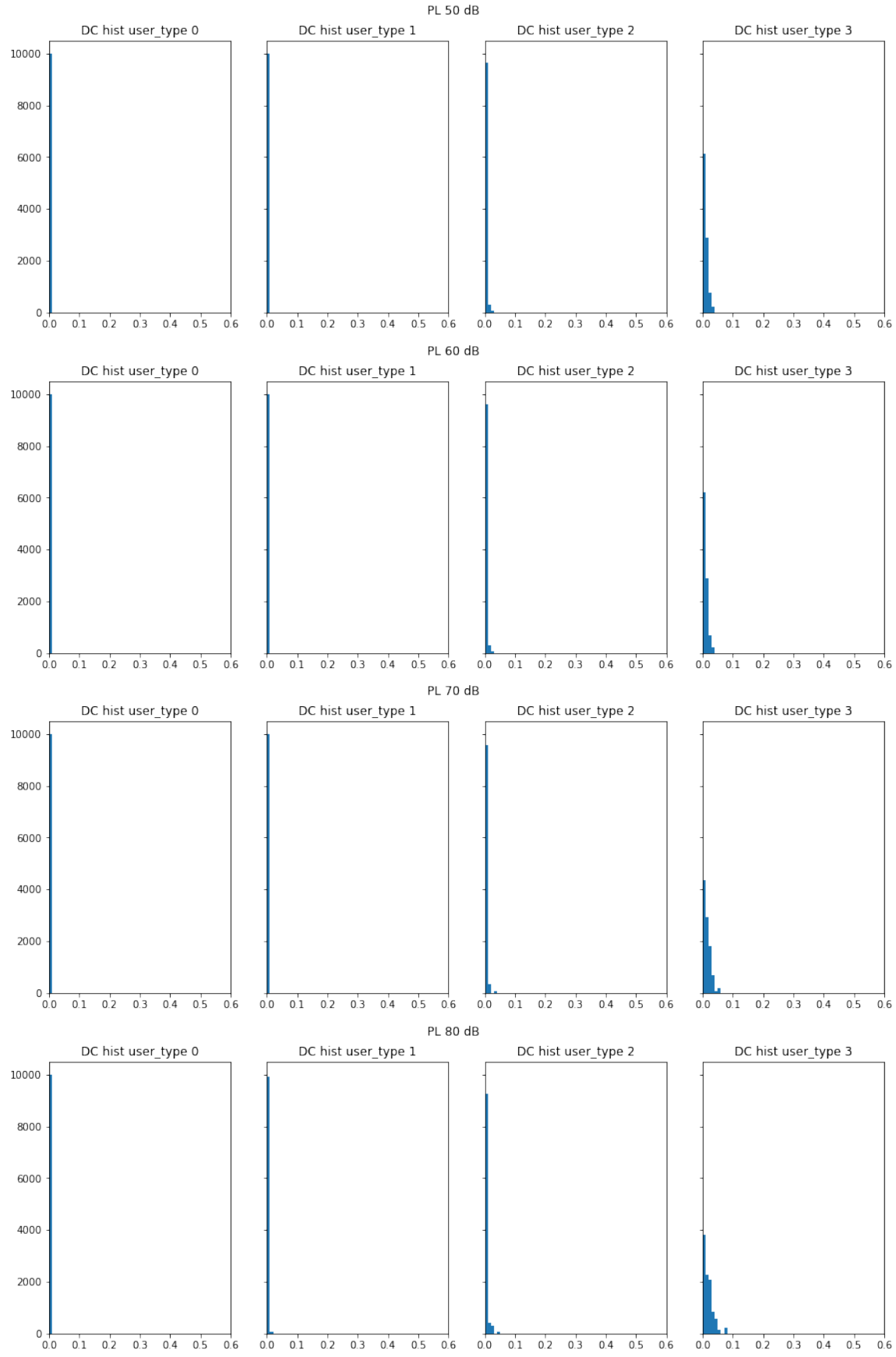

Figure 3: Distributions of 6 minute averaged duty cycles for different user types and path loss levels.

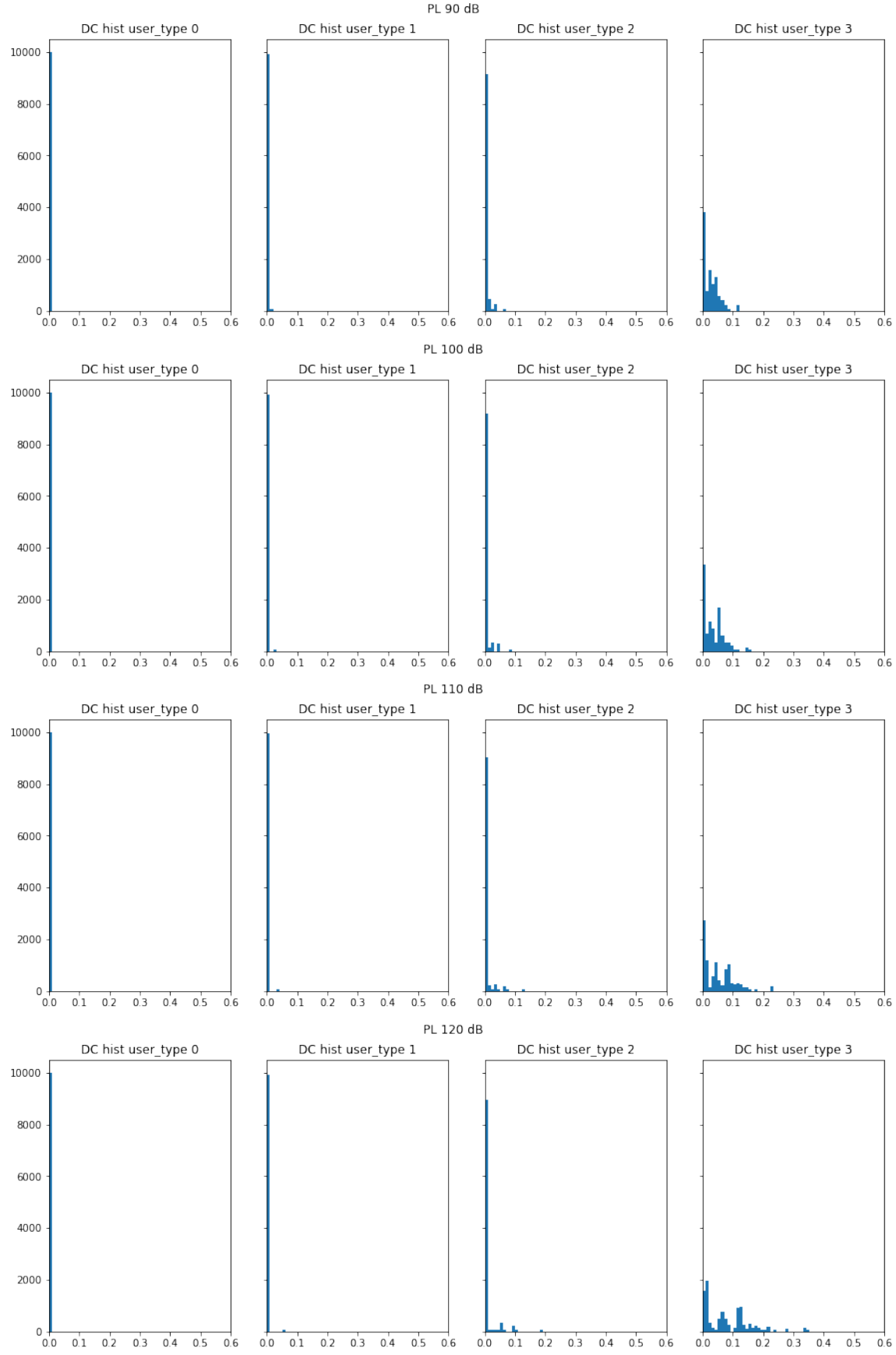

Figure 3: Distributions of 6 minute averaged duty cycles for different user types and path loss levels.

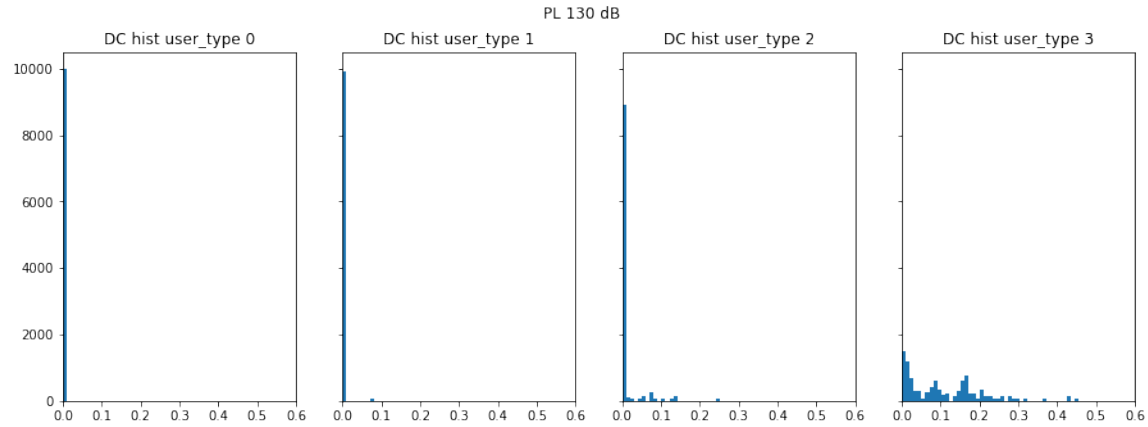

Figure 3: Distributions of 6 minute averaged duty cycles for different user types and path loss levels.

5 Results

5.1 Frequency Dependency of Brain-Region-Specific Exposures

Figure 4 shows the differences in absorbed energy in various brain regions (tissue averaged) in the human head of the MIDA phantom [19], the Ella phantom [20] and the homogeneous SAM phantom with virtual brain regions mapped inside [21] when exposed to generic near-field sources in the frequency range from 700 MHz to 3600 MHz. The results illustrate the absorption characteristics in the human head as a function of frequency. Due to the frequency dependent absorption characteristics, the brain regions are exposed differently at different frequencies. In general, the higher the frequency the lower the penetration of electromagnetic energy into the brain due to the stronger attenuation at higher frequencies (see Figure 6). The tissue-averaged SAR in the outermost region (grey matter) is about a factor of 6 lower at 3.6 GHz than at 700 MHz. However, the local peak SAR (0.1 g average) on the outer surface of the grey matter remains approximately the same (±3 dB) over all frequencies as shown in Figure 5.
The differences in attenuation also lead to changes in the exposure levels of the different brain regions. Due to the frequency dependent attenuation, the difference in the tissue-averaged SAR between the grey matter and the thalamus increases from 3 – 6 dB at 700 MHz to >20 dB at 3.6 GHz.

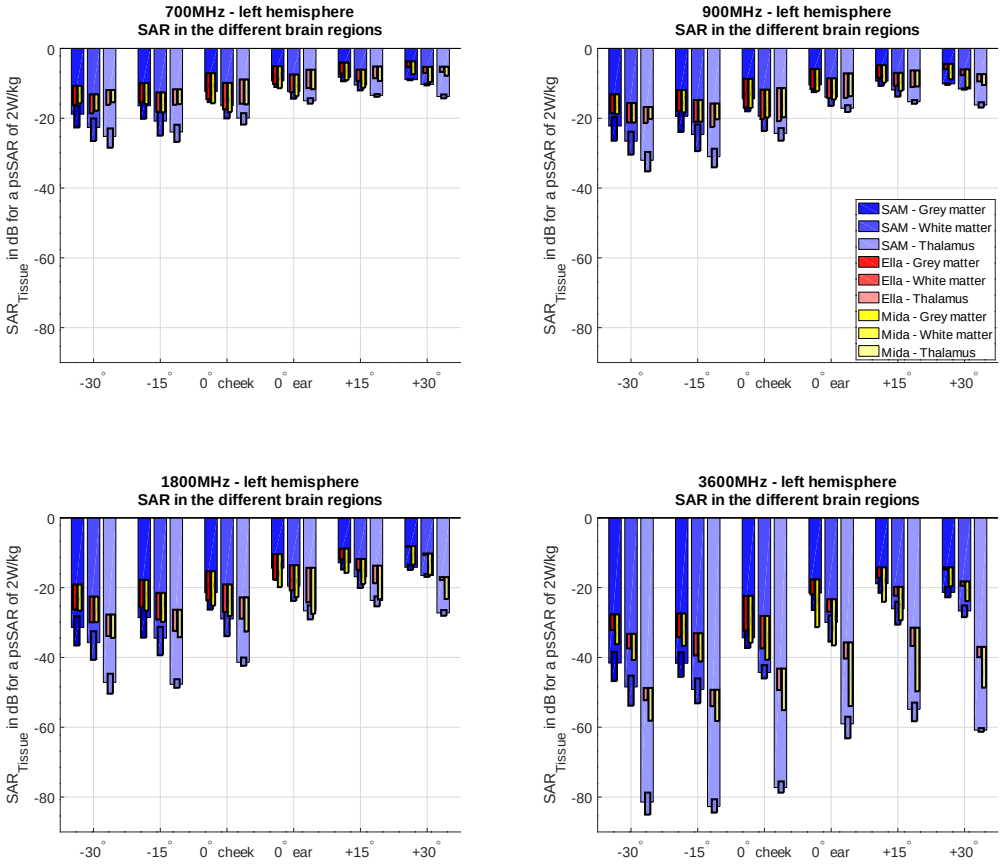

Figure 4: Absorption characteristics (tissue averaged) as a function of frequency (700 – 3600 MHz) in various brain regions (white matter, grey matter and thalamus) in the human head of the SAM phantom that has been defined by standardization bodies for SAR testing [21], the anat omical MIDA phantom [19] and the Ella phantom [20] when exposed to the near-field of generic sources. In each plot, the tissue-averaged SAR is normalized to the psaSAR$_{10g}$ of each exposure configuration. According to IEEE C95.1, the SAR in the pinna of Ella is excluded from the averaging volume. The plots show the average and variability over all source positions for SAM in blue, the variability for Ella in red and for MIDA in yellow.

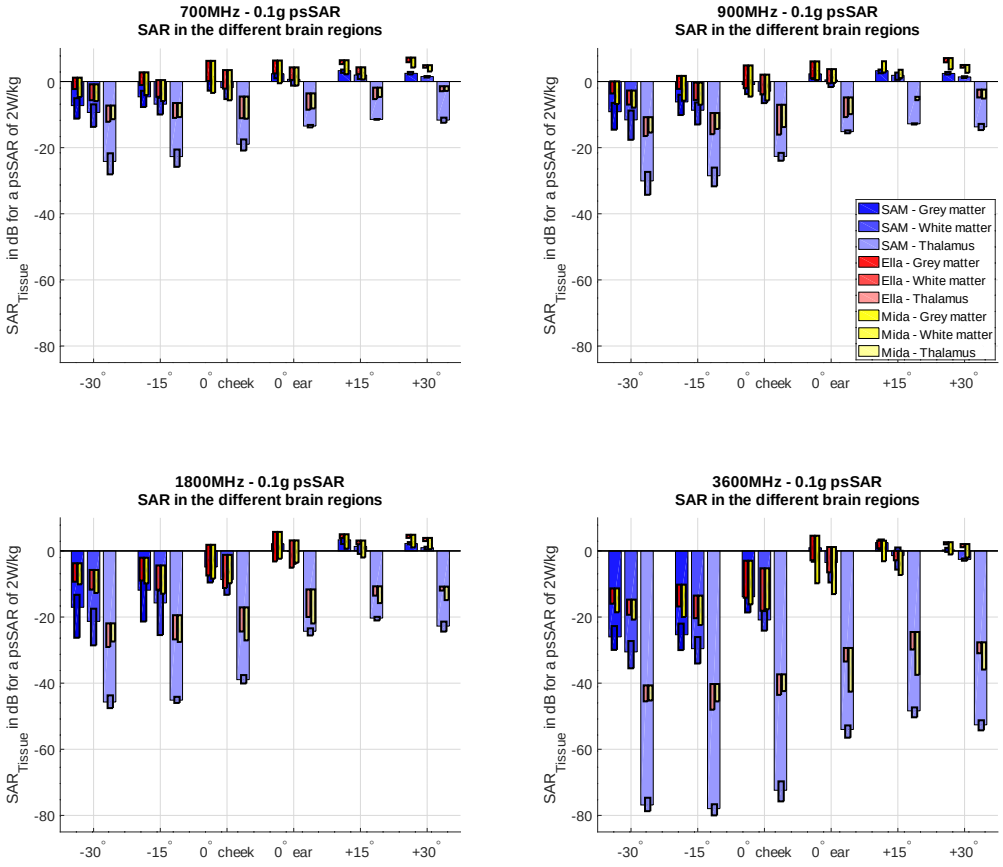

Figure 5: Absorption characteristics (0.1 g SAR peak) as a function of frequency (700 – 3600 MHz) in various brain regions (white matter, grey matter and thalamus) in the human head of the homogeneous SAM phantom [21], the MIDA phantom [19] and the Ella phantom [20] when exposed to the near-field of generic sources. In each plot, the tissue-averaged SAR is normalized to the psaSAR_{10g} of each exposure configuration. According to IEEE C95.1, the SAR in the pinna of Ella is excluded from the averaging volume. The plots show the average and variability over all source positions for SAM in blue, the variability for Ella in red and for MIDA in yellow.

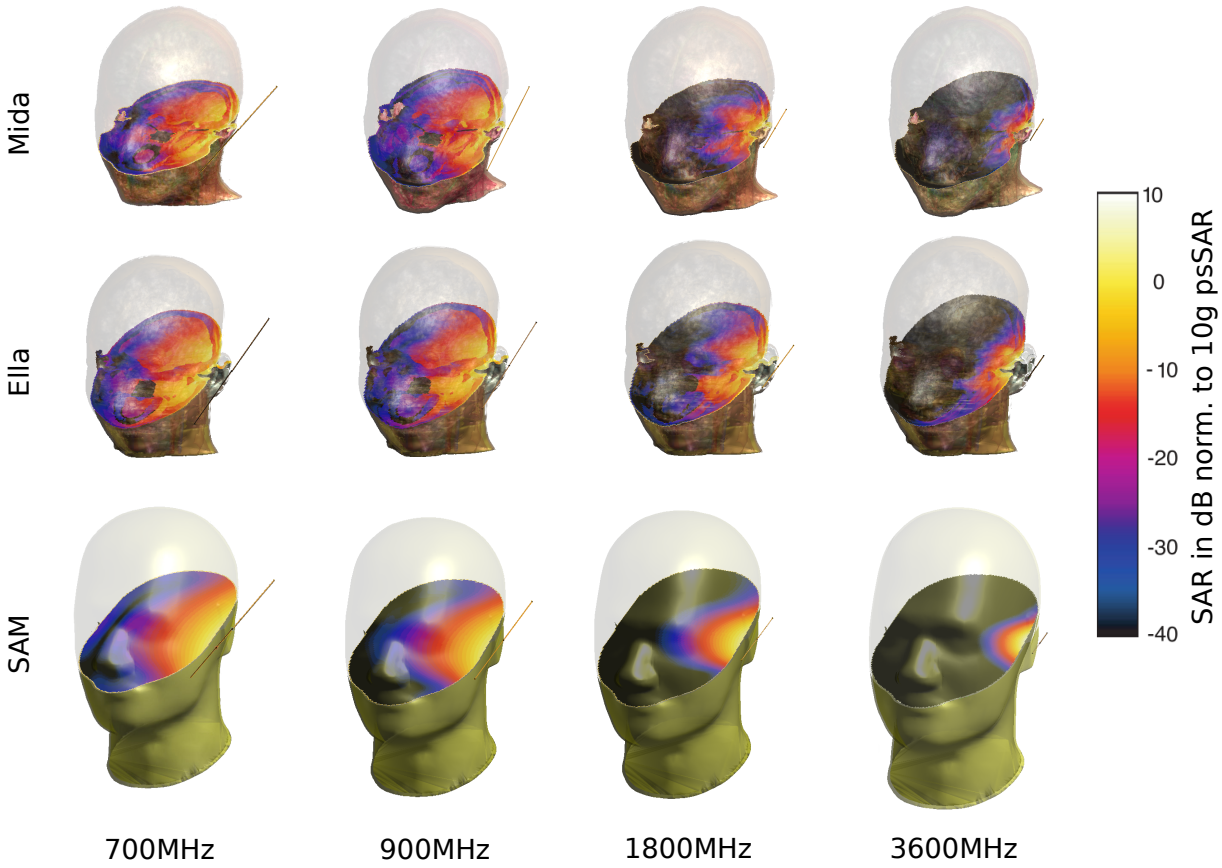

Figure 6: Cut-plane view illustrating the attenuation of the field of the generic source signal inside the human head of the MIDA phantom [19] (top row), the Ella phantom [20] (center row) and the Specific Anthropomorphic Mannequin defined by standardization for SAR evaluations (SAM) phantom [21] (bottom row) at different representative frequencies used in Swiss 5G networks. The SAR in each plot is normalized to the psaSAR_{10g} for each scenario, where the pinna is excluded in the SAR calculation for both SAM and Ella.

5.2 Monte Carlo Simulation Scenarios

Monte Carlo simulations have been used to derive histograms and statistical summaries for the permutations of the following input variables (for $\mathrm{SAR}_{10\mathrm{g}_{\mathrm{total}}}$ averaged over 6 minutes):

- Indoor Coverage Factor (N)
  - 0%
  - 10%
  - 20%
  - 40%
  - 80%
  - 100%
- Usage:
  - 0 MByte/day (non-user)
  - 100 MByte/day (light user)
  - 1 GByte/day (moderate user)
  - 10 GByte/day (heavy user)
- Cell Size Reduction (for $N = 0$, only):
  - 6 dB, 50% (of original cell-size assuming free-space propagation)
  - 12 dB, 25% (of original cell-size assuming free-space propagation)
- Locations:
  - rural
  - suburban
  - urban (macro-cell)
  - urban (mini-cell)
  - urban (micro-cell)
- Bystander Type:
  - rural cell: $r = 25$ m (not of relevance)
  - suburban cell: $r = 10$ m (not of relevance)
  - urban cell:
    - $r = 5$ m
    - $r = 1$ m

A total of 224 scenarios were analyzed with the above input variables and with 10000 to 40000 simulation iterations for each scenario.
The following statistical summaries were calculated:

- histograms and cumulative distribution functions of $10 \cdot \log_{10}(\mathrm{SAR}_{10\mathrm{g}_{\mathrm{total}}})$
- median of $10 \cdot \log_{10}(\mathrm{SAR}_{10\mathrm{g}_{\mathrm{total}}})$
- 95th percentile of $10 \cdot \log_{10}(\mathrm{SAR}_{10\mathrm{g}_{\mathrm{total}}})$

The logarithmic representation was chosen as the underlying data is log-normally distributed.

5.3 Data Histograms and Cumulative Distribution Functions

The complete set of histograms and CDFs computed in this study is available in Appendix A to this report. Figures 7 – 9 depict the results for the urban macro cell scenario. Figure 7 shows the historgrams and the CDFs for varied usage and cell sizes by increasing the minimally required received power level at the cell edge by 6 and 12 dB (for an indoor coverage factor of 0%, i.e., no additional indoor coverage), respectively. Figure 8 shows the histograms and CDFs for the effect of the indoor coverage factor as well the as of the individual data usage behavior for the total exposure.
The red line in the CDF plots indicates the 95^{th} percentile. Summaries in the form of the 95^{th} percentile and median are displayed in Figure 9.
The results confirm the assumption that a person's own mobile device usage dominates the individual total exposure. Both shrinking the cell size and increasing the indoor coverage factor reduces the total exposure of individuals who actively use their mobile devices by a factor of 4 to >10000. Therefore, the higher a person's own usage, the larger the effect of shrinking the cell size or increasing the indoor coverage. As both approaches – shrinking the cell sizes and increasing the indoor coverage – increase the incident signal level at the user, the exposure of the non-users is slightly increased as a result.

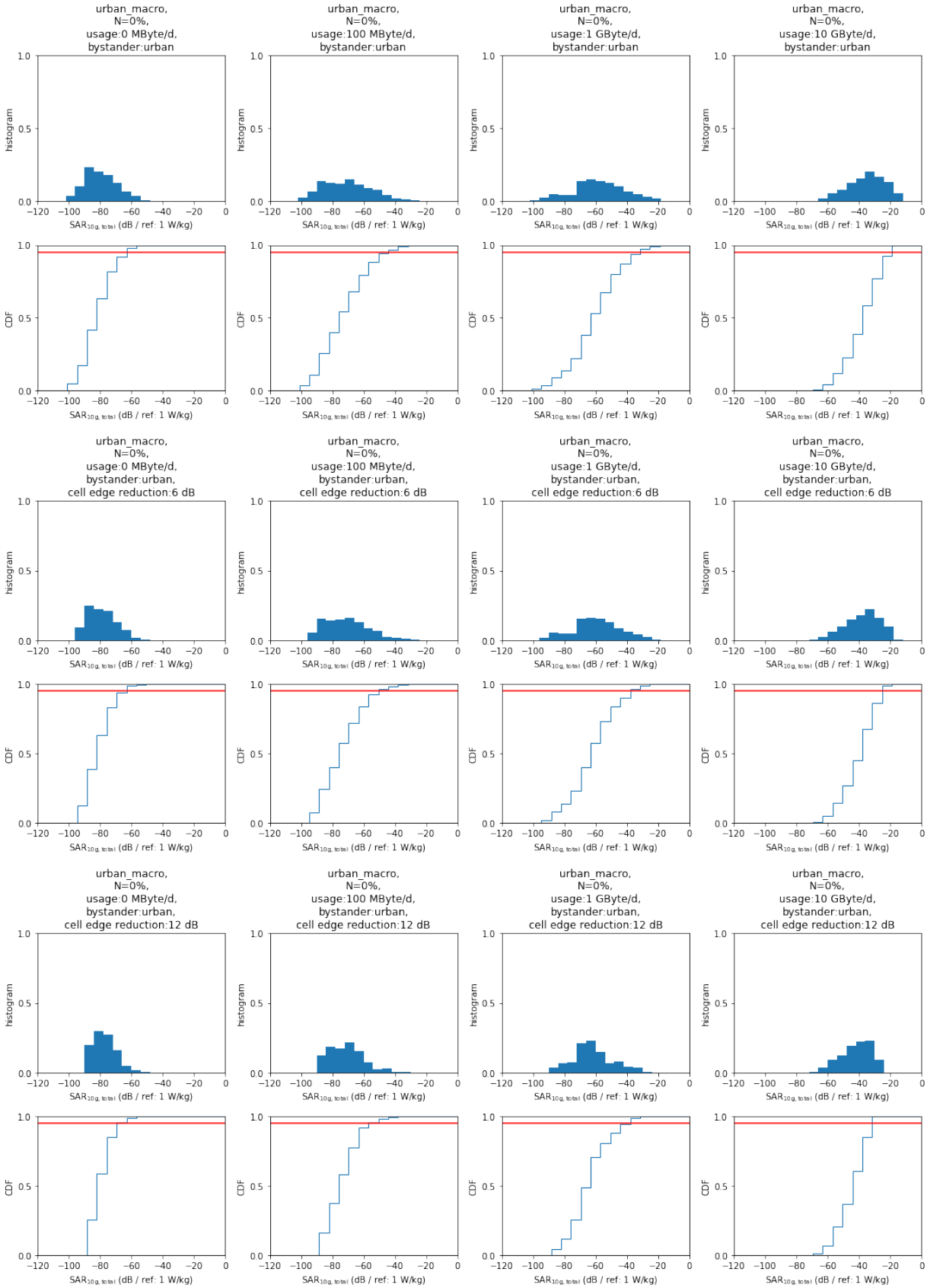

Figure 7: Histograms and CDFs for the urban macro cell scenario with varied cell edge reductions (0, 6, and 12 dB) and usage scenarios (non-user, light user (100 MByte/day), moderate user (1 GByte/day), and heavy user (10 GByte/day)).

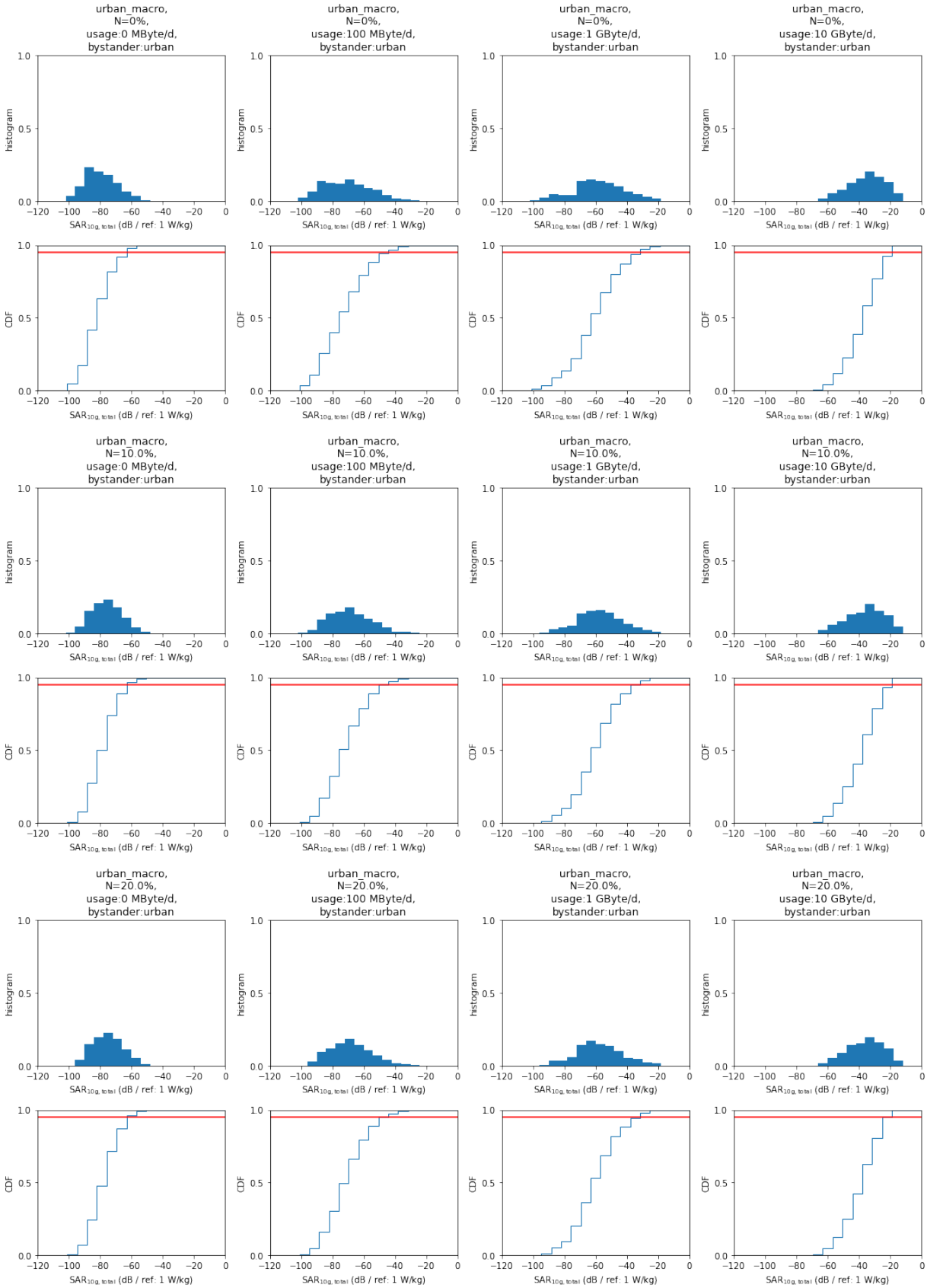

Figure 8: Histograms and CDFs for the urban macro cell scenario with varied indoor coverage factors (N = 0, 10, 20, 40, 80, and 100%)) and usage scenarios (non-user, light user (100 MByte/day), moderate user (1 GByte/day), and heavy user (10 GByte/day)).

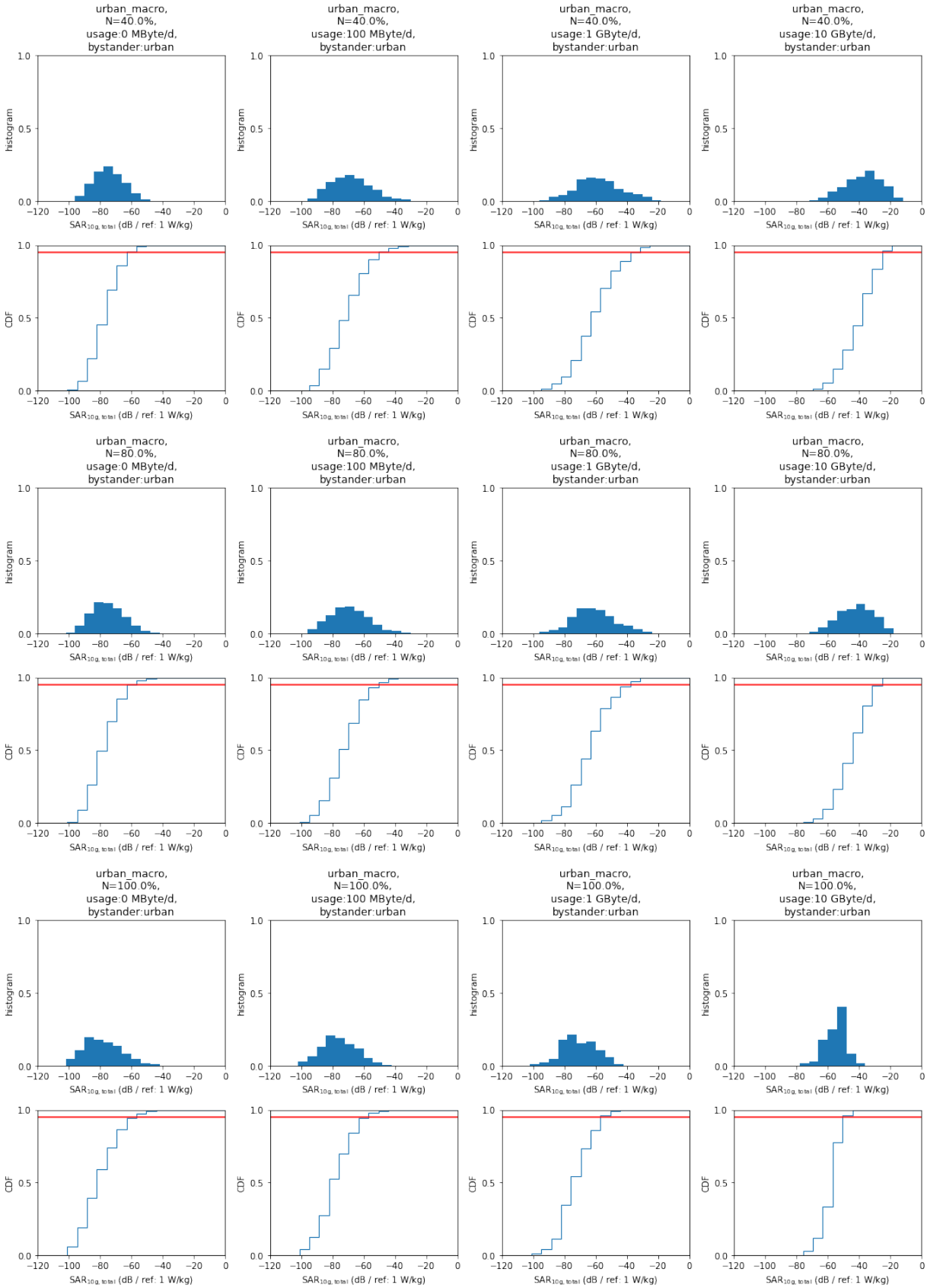

Figure 8: (continued) Histograms and CDFs for the urban macro cell scenario with varied indoor coverage factors (N = 0, 10, 20, 40, 80, and 100%)) and usage scenarios (non-user, light user (100 MByte/day), moderate user (1 GByte/day), and heavy user (10 GByte/day)).

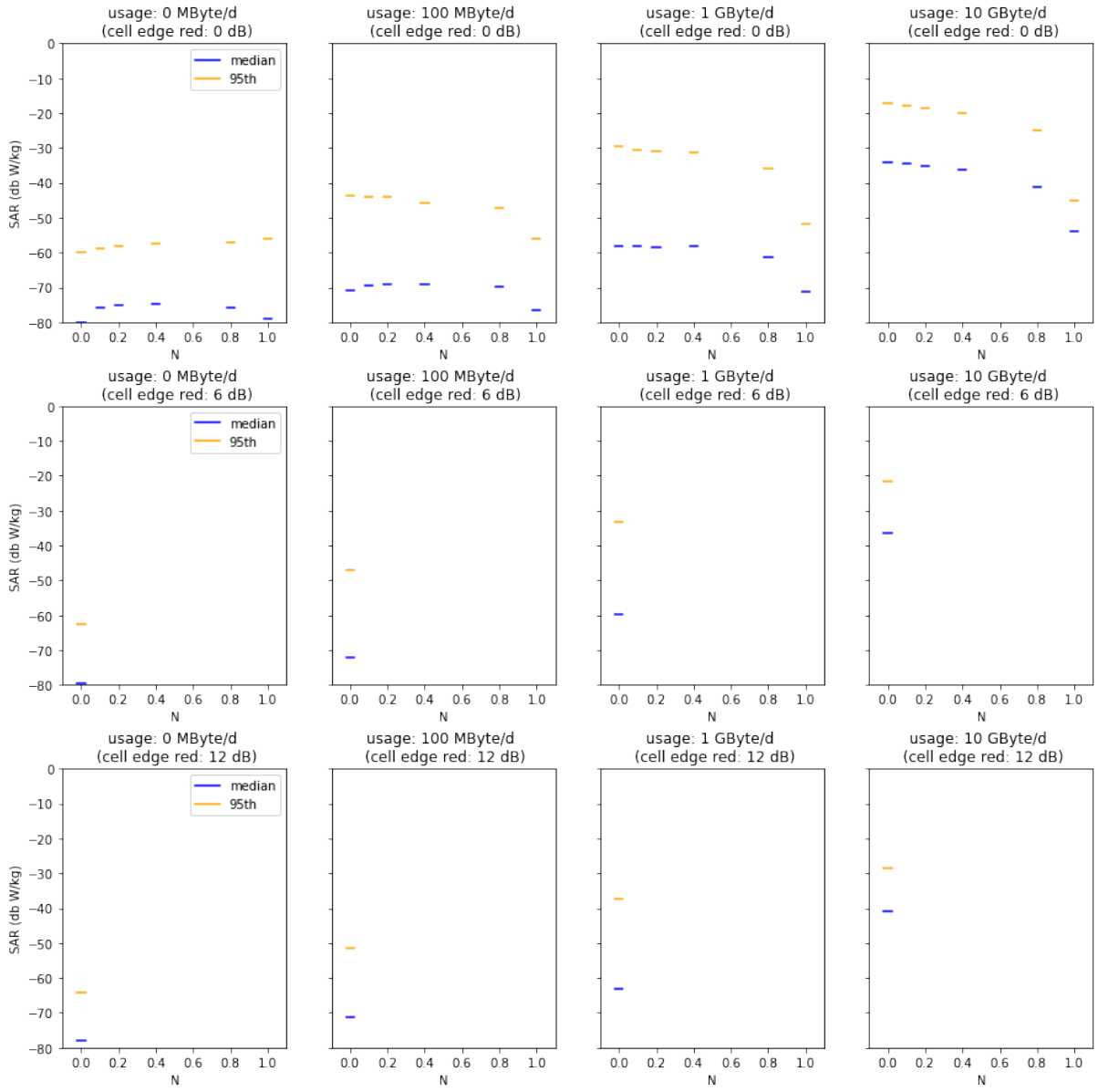

Figure 9: Median and 95$^{\text{th}}$ percentiles for varied usage scenarios (non-user, light user (100 MByte/day), moderate user (1 GByte/day), and heavy user (10 GByte/day)), indoor coverage factors (N = 0, 10, 20, 40, 80, and 100%)), and cell edge reductions (0, 6, and 12 dB) in the urban macro cell scenario.

Table 3: Relative effect (in dB) of increased indoor coverage (increasing N) without cell edge reduction for non-users in different environments and bystander conditions. Shown are the 95^{th} percentiles relative to the case for $N = 0$ in each row.

location	bystander	N: 0	N: 10%	N: 20%	N: 40%	N: 80%	N: 100%
rural_macro	r=25m	0	0.618	1.03	0.8	-0.791	-3
suburban_macro	r=10m	0	0.617	2.02	2.43	2.17	2
urban_macro	r=5m	0	1.62	2.03	2.3	3.51	4
urban_macro	r=1m	0	0.765	0.836	0.762	-0.407	-1.28
urban_mini	r=5m	0	1.97	3.03	3.78	4.12	4
urban_mini	r=1m	0	0.962	1.04	1.46	1.28	1.01
urban_micro	r=5m	0	5.1	7.02	8.78	10.1	11
urban_micro	r=1m	0	4.06	5.43	8.02	10	10

5.4 Effect of Indoor Coverage on Total Exposure

Table 3 shows the effect of added indoor coverage for users who are not using their own mobile devices compared to the the scenario with no additional indoor coverage. As in the rural use case, many usage locations are actually outdoors, and the RSRP values at all of these locations are higher than for indoor coverage, resulting in a slight increase in the exposure of non-users by a factor of 2 – 10) when more indoor cases are added. A similar picture emerges for the suburban case. The effect is less pronounced, as the RSRP statistics for the suburban and the indoor scenarios are in the same range but with a difference in steepness in the CDFs. For all urban scenarios, the RSRP values from macro, mini, and micro cell antennas are lower than those from indoor cells, meaning that the incident fields at non-users are lower. For these scenarios (combinations of indoor and outdoor coverage), increasing the indoor coverage immediately increases the incident field levels from the base stations. This changes, however, for urban macro and mini cells when a nearby (1 m) bystander is present. Adding indoor coverage decreases the exposure due to bystanders, as each bystander's mobile device can reduce its output power in response to reduced path losses towards indoor base stations. For urban micro cells, the incident fields are generally very low (low RSRP). Adding indoor coverage therefore increases the exposure for non-users considerably compared to micro-cells. In addition, the path loss differences between micro cells and indoor cells are the smallest, such that the lower bystander exposure cannot compensate the higher incident fields for non-users.

Table 4 shows the results for cases in which all four user types have been taken into account to the same extent (i.e., each user type is assumed to contribute 25% percent to the average). As even moderate usage of a person's own mobile device dominates the total exposure, there is a general reduction in exposure with increasing indoor coverage. This is simply due to the much smaller path losses for indoor systems than for outdoor systems, such that a person's own device can transmit with lower output power. In the extreme case where only indoor scenarios are considered ($N = 100\%$), the reduction can be in the range of more than 20 dB (or a factor of 100). Once again, the effect is smallest for urban micro cells, which already have a relatively low path loss without additional indoor coverage.

Table 5 illustrates the effect for heavy users (10 GByte/day), where increased indoor coverage reduces the exposure compared to only outdoor coverage and usage.

Table 4: Relative effect (in dB) of increased indoor coverage (increasing N) without cell edge reduction for all user-types (non-user, light user (100 MByte/day), moderate user (1 GByte/day), and heavy user (10 GByte/day)) with the same proportional contributions in different environments and bystander conditions. Shown are the 95^{th} percentiles relative to the case for N=0.

location	bystander	usage	N: 0	N: 10%	N: 20%	N: 40%	N: 80%	N: 100%
rural_macro	r=25m	all	0	-0.711	-1.24	-2.56	-7.2	-22.5
suburban_macro	r=10m	all	0	-0.376	-0.792	-2.64	-6.52	-22.2
urban_macro	r=5m	all	0	-0.283	-0.619	-2.17	-6.86	-25.5
urban_macro	r=1m	all	0	-0.316	-1.02	-2.23	-6.92	-25.7
urban_mini	r=5m	all	0	-0.758	-0.471	-2.22	-6.5	-17.3
urban_mini	r=1m	all	0	-0.66	-1.12	-2.12	-6.29	-17.7
urban_micro	r=5m	all	0	0.0829	-0.506	-1.09	-3.51	-7
urban_micro	r=1m	all	0	-0.14	-0.355	-0.698	-3.23	-7.08

Table 5: Relative effect (in dB) of increased indoor coverage (increasing N) without cell edge reduction for heavy users in different environments and bystander conditions. Shown are the 95^{th} percentiles relative to the case for N=0.

location	bystander	usage	N: 0	N: 10%	N: 20%	N: 40%	N: 80%	N: 100%
rural_macro	r=25m	10 GByte/d	0	-0.482	-0.944	-2.25	-6.77	-25.8
suburban_macro	r=10m	10 GByte/d	0	-0.469	-1.12	-2.39	-6.96	-25.5
urban_macro	r=5m	10 GByte/d	0	-0.659	-1.19	-2.21	-7.13	-27.7
urban_macro	r=1m	10 GByte/d	0	-0.437	-0.94	-2.14	-6.97	-27.6
urban_mini	r=5m	10 GByte/d	0	-0.45	-0.904	-2.12	-6.94	-22
urban_mini	r=1m	10 GByte/d	0	-0.59	-0.95	-2.05	-6.97	-22.2
urban_micro	r=5m	10 GByte/d	0	-0.529	-1.07	-2.13	-6.27	-11
urban_micro	r=1m	10 GByte/d	0	-0.392	-0.882	-2.12	-5.97	-10.8

Table 6: Exposure change (in dB) as a function of the cell size relative to the original cell size. Displayed are the 95th percentiles for different cell scenarios for all four user types (light user (100 MByte/day), moderate user (1 GByte/day), heavy user (10 GByte/day), and non-user (0 MByte/day)), with each user type contributing 25% to the average (all), and with the non-user separately (0 MB/d). All cases were studied without inclusion of indoor coverage (N=0).

location	bystander	usage	N	cell edge reduction 0 dB	cell edge reduction 6 dB	cell edge reduction 12 dB
rural_macro	r=25m	all	[0]	0	-3.89	-8.67
rural_macro	r=25m	0 MB/d	[0]	0	1	3
suburban_macro	r=10m	all	[0]	0	-4.03	-9.35
suburban_macro	r=10m	0 MB/d	[0]	0	0	2
urban_macro	r=5m	all	[0]	0	-2.97	-8.66
urban_macro	r=5m	0 MB/d	[0]	0	-1.86	-3.86
urban_macro	r=1m	all	[0]	0	-3.18	-8.91
urban_macro	r=1m	0 MB/d	[0]	0	-2.07	-6.09
urban_mini	r=5m	all	[0]	0	-3.71	-8.67
urban_mini	r=5m	0 MB/d	[0]	0	0	2
urban_mini	r=1m	all	[0]	0	-3.24	-8.04
urban_mini	r=1m	0 MB/d	[0]	0	-2.76	-1.76
urban_micro	r=5m	all	[0]	0	-4.44	-8.95
urban_micro	r=5m	0 MB/d	[0]	0	1	3
urban_micro	r=1m	all	[0]	0	-4.03	-8.46
urban_micro	r=1m	0 MB/d	[0]	0	0.02	2.01

5.5 Effect of Cell Size Shrinking

Table 6 shows the 95th percentile and Table 7 shows the median values for cell edge reductions of 6 and 12 dB, respectively, relative to the original cell size. The results have been separated for non-users and a mixture of all user types, with each type contributing 25% to the average (all). The data reveal that a reduction in cell size leads to an overall reduction of the exposure for all individuals (all four equally weighted user types) due to the increased RSRP for the mobile devices and lower path losses in the uplinks.

For non-users, the higher incident field levels lead in all cases with cell size reduction >0 to an increased median value of the total exposure (see Table 7). However, for the 95th percentiles, this result is actually not in all cases the same. The reason for this is that the losses in urban cells are high, resulting in steep CDF curves (see Appendix A). By increasing the cell edge RSRP values, essentially many low exposure locations are removed, giving rise to the 95th percentile value.

Table 7: Exposure change (in dB) as a function of the cell size relative to the original cell size. Displayed are the median values for different cell scenarios for all four user types (light user (100 MByte/day), moderate user (1 GByte/day), heavy user (10 GByte/day), and non-user (0 MByte/day)), with each user type contributing 25% to the average (all), and with the non-user separately (0 MB/d). All cases were studied without inclusion of indoor coverage (N=0).

location	bystander	usage	N	cell edge reduction 0 dB	cell edge reduction 6 dB	cell edge reduction 12 dB
rural_macro	r=25m	all	[0]	0	-0.515	-0.526
rural_macro	r=25m	0 MB/d	[0]	0	0.645	3.46
suburban_macro	r=10m	all	[0]	0	-0.835	-1.85
suburban_macro	r=10m	0 MB/d	[0]	0	0.502	2.4
urban_macro	r=5m	all	[0]	0	-0.782	-3.08
urban_macro	r=5m	0 MB/d	[0]	0	0.987	2.02
urban_macro	r=1m	all	[0]	0	-1.62	-3.83
urban_macro	r=1m	0 MB/d	[0]	0	0.0452	2
urban_mini	r=5m	all	[0]	0	-0.972	-1.66
urban_mini	r=5m	0 MB/d	[0]	0	0.655	2.02
urban_mini	r=1m	all	[0]	0	-0.66	-1.73
urban_mini	r=1m	0 MB/d	[0]	0	0.176	2
urban_micro	r=5m	all	[0]	0	-0.373	-0.265
urban_micro	r=5m	0 MB/d	[0]	0	1	3
urban_micro	r=1m	all	[0]	0	-0.816	-0.779
urban_micro	r=1m	0 MB/d	[0]	0	0.945	2.62

Table 8: Total exposure change (in dB) as a function of the data usage relative to the non-user without indoor coverage (i.e., values for $N = 80\%$ have been normalized to the scenario for N=0 with no data usage). Displayed are the 95$^{\text{th}}$ percentile values for all four user types (light user (100 MByte/day), moderate user (1 GByte/day), heavy user (10 GByte/day), and non-user (0 MByte/day)). Situations have been analyzed for N=0 (i.e., no additional indoor coverage) and N=80%, i.e., rather strong indoor coverage.

location	bystander	N	cell edge reduction 0 dB	0 MB/d	100 MB/d	1 GB/d	10 GB/d
rural_macro	r=25m	[0]	[0]	0	7.85	20	33
rural_macro	r=25m	[0.8]	[0]	-0.901	4.03	13.9	26.4
suburban_macro	r=10m	[0]	[0]	0	11	25	37.8
suburban_macro	r=10m	[0.8]	[0]	2.03	8.06	18	30.9
urban_macro	r=5m	[0]	[0]	0	15.6	30.4	42.5
urban_macro	r=5m	[0.8]	[0]	3.06	12	24	35.4
urban_macro	r=1m	[0]	[0]	0	11.2	25.2	37.3
urban_macro	r=1m	[0.8]	[0]	-0.208	6.18	18.6	30.2
urban_mini	r=5m	[0]	[0]	0	10	22.6	36.1
urban_mini	r=5m	[0.8]	[0]	4.07	8.03	16.8	29.3
urban_mini	r=1m	[0]	[0]	0	7.75	19.5	33.5
urban_mini	r=1m	[0.8]	[0]	1.54	5.52	14	26.4
urban_micro	r=5m	[0]	[0]	0	7.06	18.3	30.3
urban_micro	r=5m	[0.8]	[0]	11	12	16.1	24.5
urban_micro	r=1m	[0]	[0]	0	6.16	17.3	29.4
urban_micro	r=1m	[0.8]	[0]	10	10.3	15	23.4

5.6 Effect of a Person's Own Usage on Total Exposure

Table 8 summarizes the 95$^{\text{th}}$ percentile values reflecting the effect of a person's own data usage on total exposure. The data reveals that even small amounts of data usage with a person's own mobile phone dominates the total exposure. A user with low data usage requirements experiences an increase in exposure by 6 – 11 dB compared to a non-user. Moderate and heavy users increase their total exposures by 6 – 25 dB and 25 – 40 dB, respectively, compared to non-users. Increased indoor coverage could lead to reductions in exposure of up to 10 dB for heavy users. In general, exposure for non-users is slightly increased when indoor coverage is added, however, only at levels in the range of 10- to 1000-fold lower than for active users.

Table 9: Total exposure change (in dB) as a function of bystander distance r. Shown are the 95^{th} percentile values for the non-user and light data user (100 MByte/day) relative to the exposure value of the non-user with a bystander 5 m away, for each urban exposure scenario.

location	N	cell edge red (dB)	usage	r=5m	r=1m
urban_macro	[0]	[0]	0 MB/d	0	5.41
urban_macro	[0]	[0]	100 MB/d	15.8	16
urban_mini	[0]	[0]	0 MB/d	0	2.06
urban_mini	[0]	[0]	100 MB/d	9.86	10
urban_micro	[0]	[0]	0 MB/d	0	1
urban_micro	[0]	[0]	100 MB/d	7.02	7.15

5.7 Effect of Bystander on Total Exposure

Table 9 depicts total exposure changes for varied bystander distances and data usages relative to non-user exposure. Only the urban exposure scenarios were analyzed, given that, for suburban and rural scenarios, very close bystanders are unlikely. Results show that a close bystander dominates the exposure from a nearby base station antenna for non-users. As soon as a user generates even small amounts of uplink data traffic, the total exposure increases, and the effect of the bystander becomes negligible ($<$0.2 dB).

6 Discussion

The results of this study are limited due to the network data that has been used and the definition of total exposure as stated earlier in the report. They are further based on the currently relatively limited knowledge about the actual deployment and development of 5G.
This study does not consider the following:

- **The effect of upcoming massive MIMO and multi-user MIMO systems in 5G networks:** MIMO usage is likely to improve the link throughput in 5G networks and hence reduce the local exposure for heavy users. Yet, due to space limitations in realistic handsets, we do not expect MIMO implementations with more than four antennas (4x4 MIMO), i.e., with a theoretical throughput increase of 6 dB in the uplink. Realistically, this value is much smaller. In the downlink, larger MIMO configurations will be implemented. Locally, the beam-steering in the downlink will result in temporal fluctuations of the incident field strength. First experiments suggest a peak to average ratio of approximately 6 dB in 5G MIMO downlink scenarios [22]. For the 6-minute average and the typically relatively high user densities around base stations in Switzerland, large temporal variations for the 6-minute average used in this study are not anticipated. We believe that the current rules in assessing the maximum exposures close to base stations needs to be updated to account for the change in technology. Since the radiation patterns are highly dynamic and not static, a smart time averaging method would be the most appropriate to characterize the exposure and in line with the current safety guidelines based on the basic restrictions. Similar procedures have already been implemented for the power management in the handsets. Spatial averaging is harder to justify with respect to the basic restrictions.

- **Alternative data transmission links - for instance the use of Wireless Local Area Network (WLAN) [23] in homes and offices:** WLAN indoor infrastructure can reduce the exposure to electromagnetic fields in a similar way like indoor 5G infrastructure by reducing the path loss between the access point and the user equipment. However, due to technological and deployment limitations the exposure reduction by WLAN use is limited and in fact to date WLAN is a major source of exposure [24]. Hypothetically, if WLAN [23] systems were replaced by 5G systems, the overall exposure would be further reduced. This is because 5G provides a better power control mechanism and better spectral efficiency than WLAN [23]. Furthermore, with the introduction of 5G, the network planning could be smarter than for WLAN which is deployed uncontrolled and where typically many redundant systems are present that interfere with each other and further reduce their capacities.

- **Millimeter wave frequencies in 5G mobile networks:** The use of millimeter wave frequencies in 5G mobile networks is not considered in this study. Despite that first millimeter wave deployments are expected at the end of 2019, the date of licensing these services in Switzerland remains unclear. However, the use of millimeter waves would dramatically change the exposure compared to the current sub-6 GHz implementation: (i) millimeter waves would require a much denser base station network, (ii) exposure would mainly be superficial (mainly the skin tissues), (iii) it is further expected that strong directivity and beamforming capability of handset antenna arrays reduce the exposure by one's own device. However, a similar study to the current one would be required to estimate the exposure for different usages.

The exposure from a user's own handset is heavily dependent on the position of usage. In this

study, this is partially accounted for by taking the averaged psaSAR value determined over all test positions. The use of mobile devices away from the body (e.g., by placing the device on a desk in front of a user) can reduce the exposure from a person's own device by a factor much larger than 10. It is also not possible to draw conclusions about the actual exposure of sensitive organs like the human brain as the exposure from a user's own device is very local and thus highly dependent on the usage pattern. However, as shown in Section 5.1 the use of higher frequencies is likely to reduce the exposure of deeper brain regions for the head mounted use of mobile devices.

7 Conclusions

The results of this study show that the absorption of energy by the human brain, resulting from exposure to the 3.6 GHz band newly added to the Swiss mobile communication frequencies, is reduced by a factor >6 for the tissue averaged SAR when compared to mobile networks operating at <1 GHz, and by a factor of >2 when compared to the frequency bands at 1.8 – 2 GHz. For deep brain regions, the reduction is much larger.
The reduced exposure for these regions is due to lower penetration depths at higher frequencies. Close to the surface (eyes, testicles, etc.) the exposure can be higher. At the most exposed surface of the grey matter, the values remain approximately ±3 dB over all frequencies whereas the area of high exposure is reduced.
More than 200 Monte Carlo simulated exposure scenarios have been analyzed to evaluate total human exposure in 5G Networks for different topologies and user scenarios. The results show that for all users (except non-users), the total exposure is dominated by a person's own mobile device. Compared to a non-user, the exposure is increased for a light user (with 100 MByte uplink data per day) by 6 – 10 dB (or by a factor 4 to 10), for a moderate user (with 1 GByte uplink data per day) by 13 – 25 dB (or by a factor of 20 to >300), and for a heavy user by 25 – 40 dB (or a factor of 300 to >10000). The peak exposure of non-users is further not defined by exposure to surrounding base stations but by mobile devices of close bystanders in urban areas, resulting in 6 dB (or a factor of 4) higher exposure than from a nearby base station antenna. Reducing the diameter of the mobile cell leads to a decreased overall exposure by a factor of 2 to 10 for people who actively use their mobile devices. At the same time, the reduction in cell size might lead to a small increase by a factor <2 in exposure for non-users. The exposure of active users can be reduced by factors ranging from 4 to 600 by increasing indoor network coverage which, in turn, will be linked to increased exposure of non-users by a factor of 2 to 10. However, such an increase is by a factor 1000 lower than the typical exposure of active users.
The results of this study are limited due to the network data that has been used and the definition of total exposure as stated earlier in this report. This study does not consider (i) the effect of upcoming massive MIMO and multi-user MIMO systems in 5G networks, (ii) alternative data transmission links – for instance the use of Wireless Local Area Network (WLAN) and (iii) millimeter wave frequencies in 5G mobile networks.
In summary, the results of this study show that the user's own mobile device is the dominant source of exposure for the population of active mobile network users. Besides personal usage patterns, total exposure is also closely linked to the network infrastructure. Generally speaking, a network that decreases the path loss by means of smaller cells and additional indoor coverage will help to reduce the total exposure of the population.

References

[1] Swiss Federal Office of Communications. Mobile radio frequencies for 5G awarded in Switzerland. [Online]. Available: https://www.newsd.admin.ch/newsd/message/attachments/55585.pdf

[2] Swiss Federal Institute for the Environment. Mobilfunkanlagen: Anforderungen nach NISV (available in german only). [Online]. Available: https://www.bafu.admin.ch/bafu/de/home/themen/elektrosmog/fachinformationen/massnahmen-elektrosmog/mobilfunkanlagen--anforderungen-nach-nisv.html

[3] I. Guideline, "Guidelines for limiting exposure to time-varying electric, magnetic, and electromagnetic fields (up to 300 ghz)," *Health phys*, vol. 74, no. 4, pp. 494–522, 1998.

[4] Swiss Federal Institute for the Environment. Mobilfunk: Vollzugshilfen zur NISV (available in German and French only). [Online]. Available: https://www.bafu.admin.ch/bafu/de/home/themen/elektrosmog/fachinformationen/massnahmen-elektrosmog/mobilfunk--vollzugshilfen-zur-nisv.html#-815252561

[5] S. Kühn and N. Kuster, "Evaluation of measurement techniques to show compliance with RF safety limits in heterogeneous field distributions," *IEEE Transactions on Electromagnetic Compatibility*, vol. 52, no. 4, pp. 820–828, November 2010.

[6] Swiss Federal Office of Communications. LTE and LTE-Advanced factsheet. [Online]. Available: https://www.bakom.admin.ch/dam/bakom/en/dokumente/faktenblatt_lte.pdf.download.pdf/fact_sheet_lte.pdf

[7] M.-C. Gosselin, S. Kühn, P. Crespo-Valero, E. Cherubini, M. Zefferer, A. Christ, and N. Kuster, "Estimation of head tissue-specific exposure from mobile phones based on measurements in the homogeneous SAM head," *Bioelectromagnetics*, vol. 32, no. 6, pp. 493–505, 2011.

[8] P. Joshi, D. Colombi, B. Thors, L.-E. Larsson, and C. Törnevik, "Output power levels of 4G user equipment and implications on realistic RF EMF exposure assessments," *IEEE Access*, vol. 5, pp. 4545–4550, 2017.

[9] ETSI, "ETSI TS 138 213 V15.3.0 (2018-10) 5G; NR; Physical layer procedures for control (3GPP TS 38.213 version 15.3.0 Release 15)," ETSI, Tech. Rep., October 2018.

[10] I. A. Tomić, M. S. Davidović, and S. M. Bjeković, "On the downlink capacity of LTE cell," in *2015 23rd Telecommunications Forum Telfor (TELFOR)*. IEEE, 2015, pp. 181–185.

[11] Qualcomm. Real-world user experiences with standalone 5G NR. [Online]. Available: https://www.qualcomm.com/news/onq/2018/06/26/real-world-user-experiences-standalone-5g-nr

[12] Rohde and Schwarz. 3GPP categories and data rates up to Release 15 . [Online]. Available: https://www.mobilewirelesstesting.com/wp-content/uploads/2018/11/3GPP_categories_and_data_rates_up_to_Rel_15_po_en_folded_5216-3943-82_v0100.pdf

[13] M. Berg, M. Sonkki, and E. Salonen, "Experimental study of hand and head effects to mobile phone antenna radiation properties," in *2009 3rd European Conference on Antennas and Propagation*, March 2009, pp. 437–440.

[14] J. Ilvonen, O. Kivekas, J. Holopainen, R. Valkonen, K. Rasilainen, and P. Vainikainen, "Mobile terminal antenna performance with the user's hand: Effect of antenna dimensioning and location," *IEEE Antennas and Wireless Propagation Letters*, vol. 10, pp. 772–775, 2011.

[15] M. Pelosi, O. Franek, M. B. Knudsen, M. Christensen, and G. F. Pedersen, "A grip study for talk and data modes in mobile phones," *IEEE Transactions on Antennas and Propagation*, vol. 57, no. 4, pp. 856–865, April 2009.

[16] C. Ide, R. Falkenberg, D. Kaulbars, and C. Wietfeld, "Empirical analysis of the impact of lte downlink channel indicators on the uplink connectivity," in *2016 IEEE 83rd Vehicular Technology Conference (VTC Spring)*. IEEE, 2016, pp. 1–5.

[17] S. Kühn, W. Jennings, A. Christ, and N. Kuster, "Assessment of induced radio-frequency electromagnetic fields in various anatomical human body models," *Physics in Medicine & Biology*, vol. 54, no. 4, p. 875, 2009.

[18] FCC. FCC ID Search. [Online]. Available: https://www.fcc.gov/oet/ea/fccid

[19] M. I. Iacono, E. Neufeld, E. Akinnagbe, K. Bower, J. Wolf, I. V. Oikonomidis, D. Sharma, B. Lloyd, B. J. Wilm, M. Wyss *et al.*, "Mida: a multimodal imaging-based detailed anatomical model of the human head and neck," *PloS one*, vol. 10, no. 4, p. e0124126, 2015.

[20] A. Christ, W. Kainz, E. G. Hahn, K. Honegger, M. Zefferer, E. Neufeld, W. Rascher, R. Janka, W. Bautz, J. Chen *et al.*, "The Virtual Family—development of surface-based anatomical models of two adults and two children for dosimetric simulations," *Physics in Medicine & Biology*, vol. 55, no. 2, p. N23, 2009.

[21] IEC TC106, "IEC 62209-1:2016: Measurement procedure for the assessment of specific absorption rate of human exposure to radio frequency fields from hand-held and body-mounted wireless communication devices - Part 1: Devices used next to the ear (Frequency range of 300 MHz to 6 GHz)," International Electrotechnical Commission, Tech. Rep., 2016.

[22] B. Thors, A. Furuskär, D. Colombi, and C. Törnevik, "Time-averaged realistic maximum power levels for the assessment of radio frequency exposure for 5g radio base stations using massive mimo," *IEEE Access*, vol. 5, pp. 19 711–19 719, 2017.

[23] "Ieee standard for information technology—telecommunications and information exchange between systems local and metropolitan area networks—specific requirements - part 11: Wireless lan medium access control (mac) and physical layer (phy) specifications," *IEEE Std 802.11-2016 (Revision of IEEE Std 802.11-2012)*, pp. 1–3534, Dec 2016.

[24] D. Plets, W. Joseph, K. Vanhecke, G. Vermeeren, J. Wiart, S. Aerts, N. Varsier, and L. Martens, "Joint minimization of uplink and downlink whole-body exposure dose in indoor wireless networks," *BioMed research international*, vol. 2015, 2015.

A Histogram and Cumulative Distribution Functions

A.1 Rural

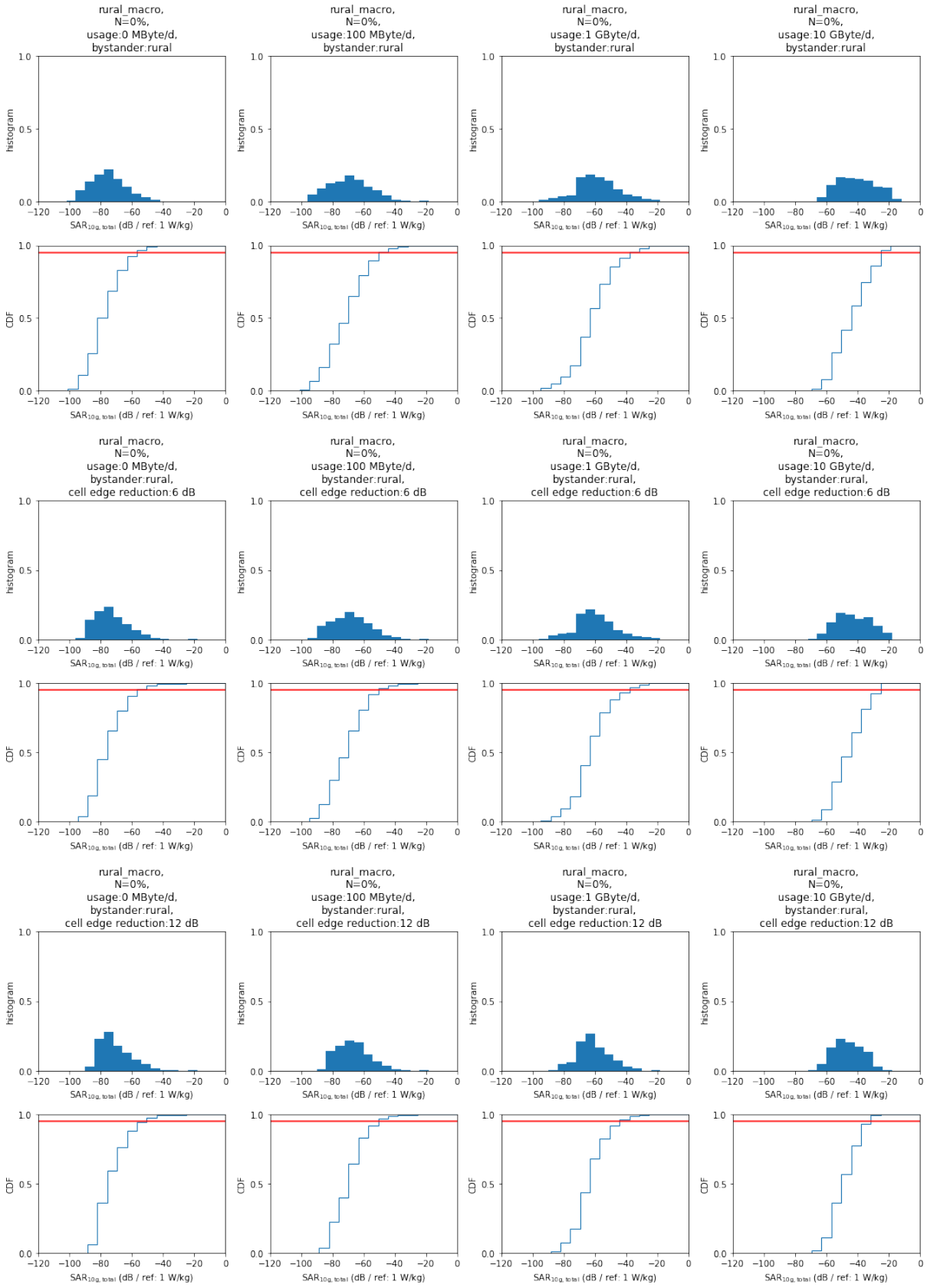

Figure 10: Histograms and cumulative distribution functions for the rural cell scenario with varied cell edges and usage scenarios.

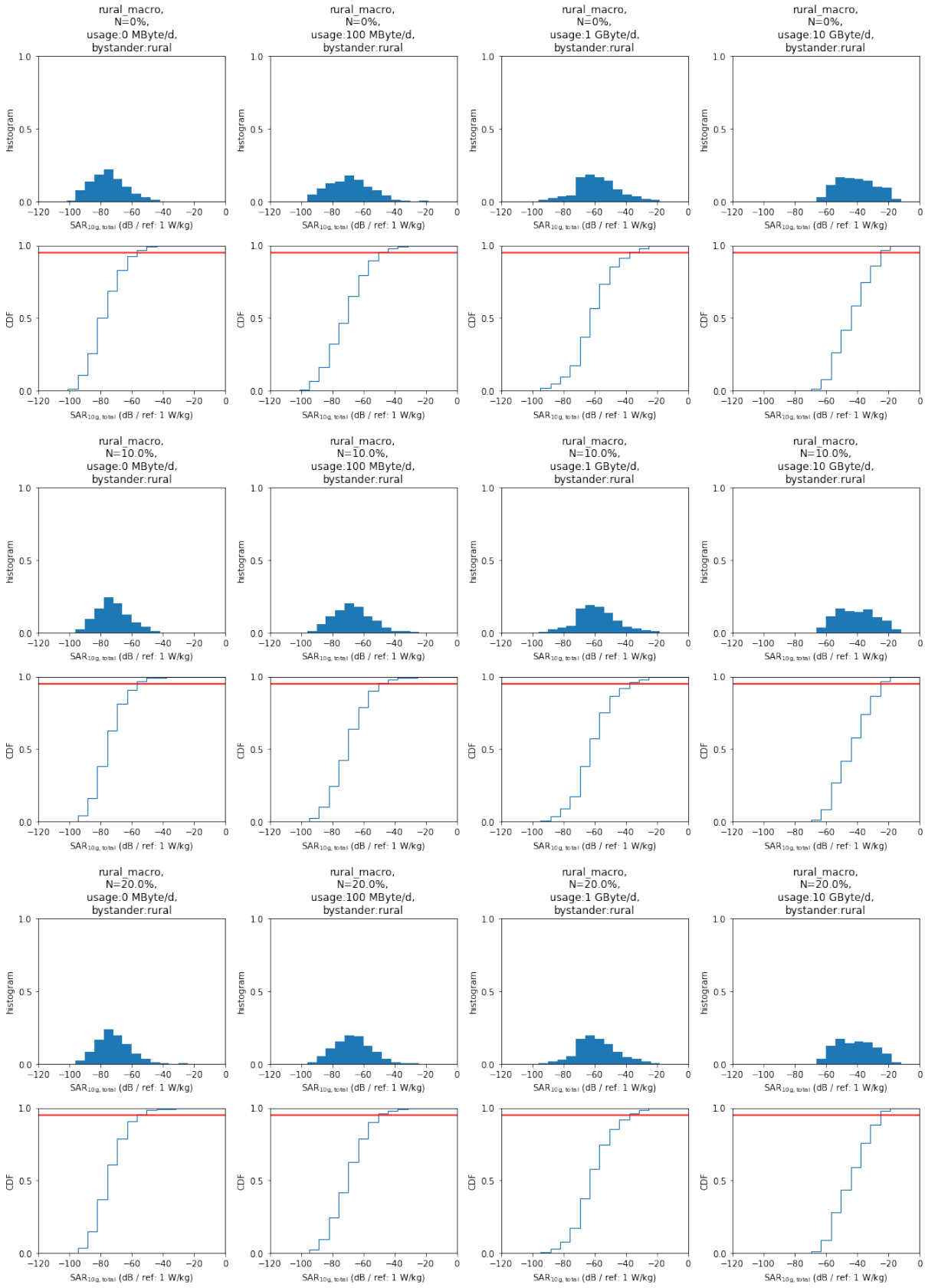

Figure 11: Histograms and cumulative distribution functions for the rural cell scenario with varied indoor coverage factors (N) and usage scenarios.

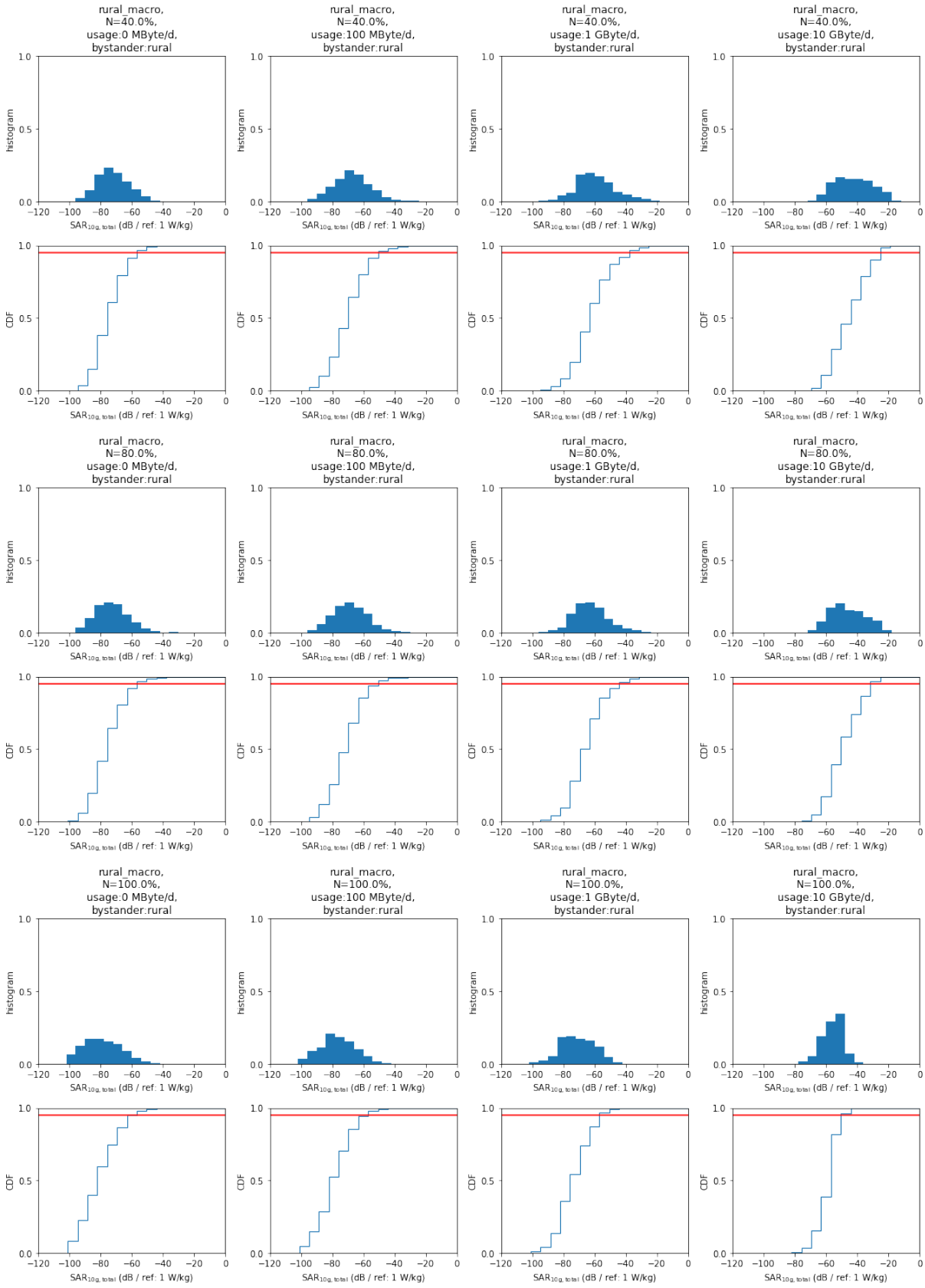

Figure 11: Histograms and cumulative distribution functions for the rural cell scenario with varied cell edges and usage scenarios.

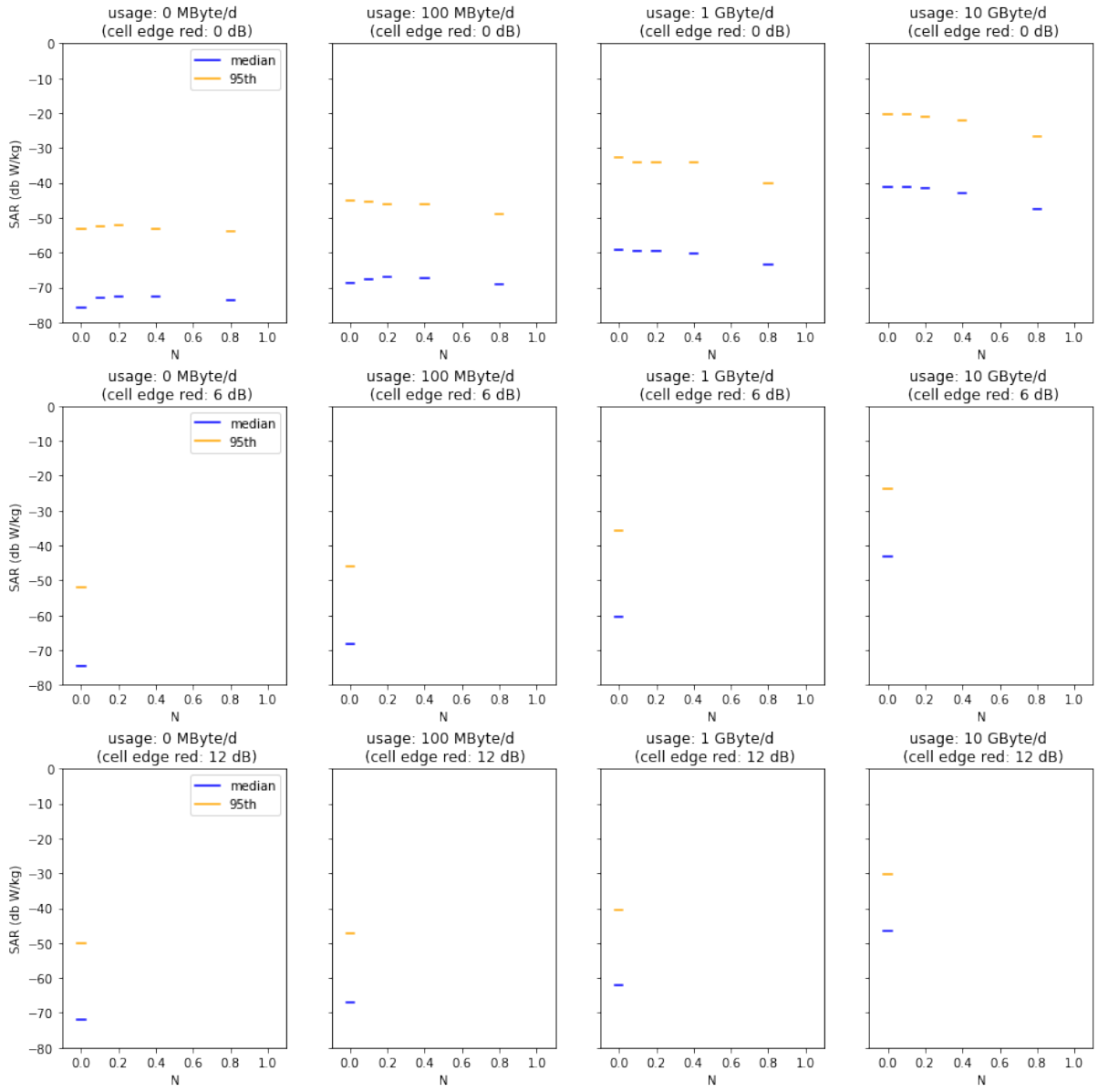

Figure 12: Median and 95$^{\text{th}}$ percentiles for varied usage, indoor coverage factor N, and cell size reductions in the rural cell scenario.

A.2 Suburban

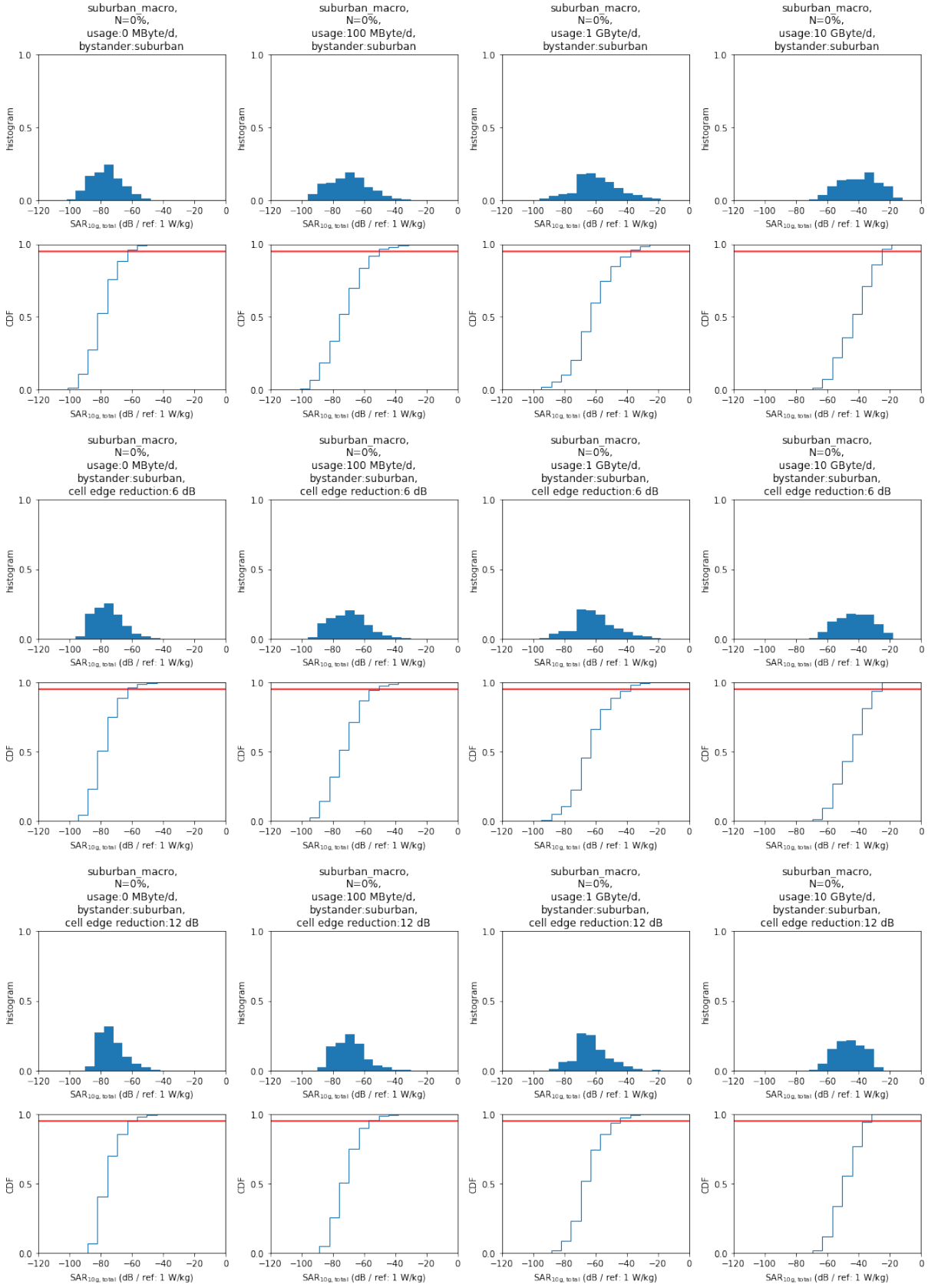

Figure 13: Histograms and cumulative distribution functions for the suburban cell scenario with varied cell edges and usage scenarios.

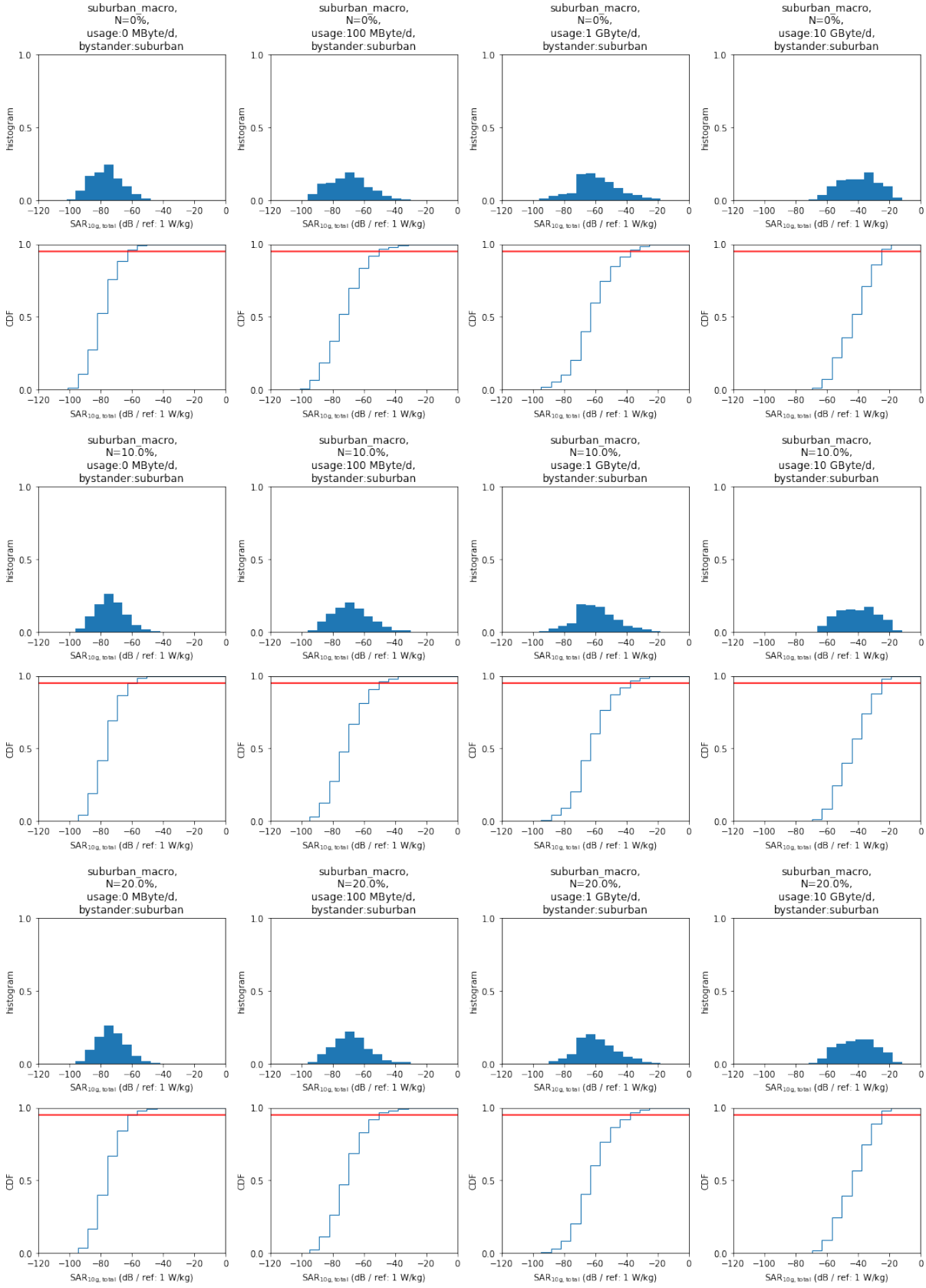

Figure 14: Histograms and cumulative distribution functions for the suburban cell scenario with varied indoor coverage factors (N) and usage scenarios.

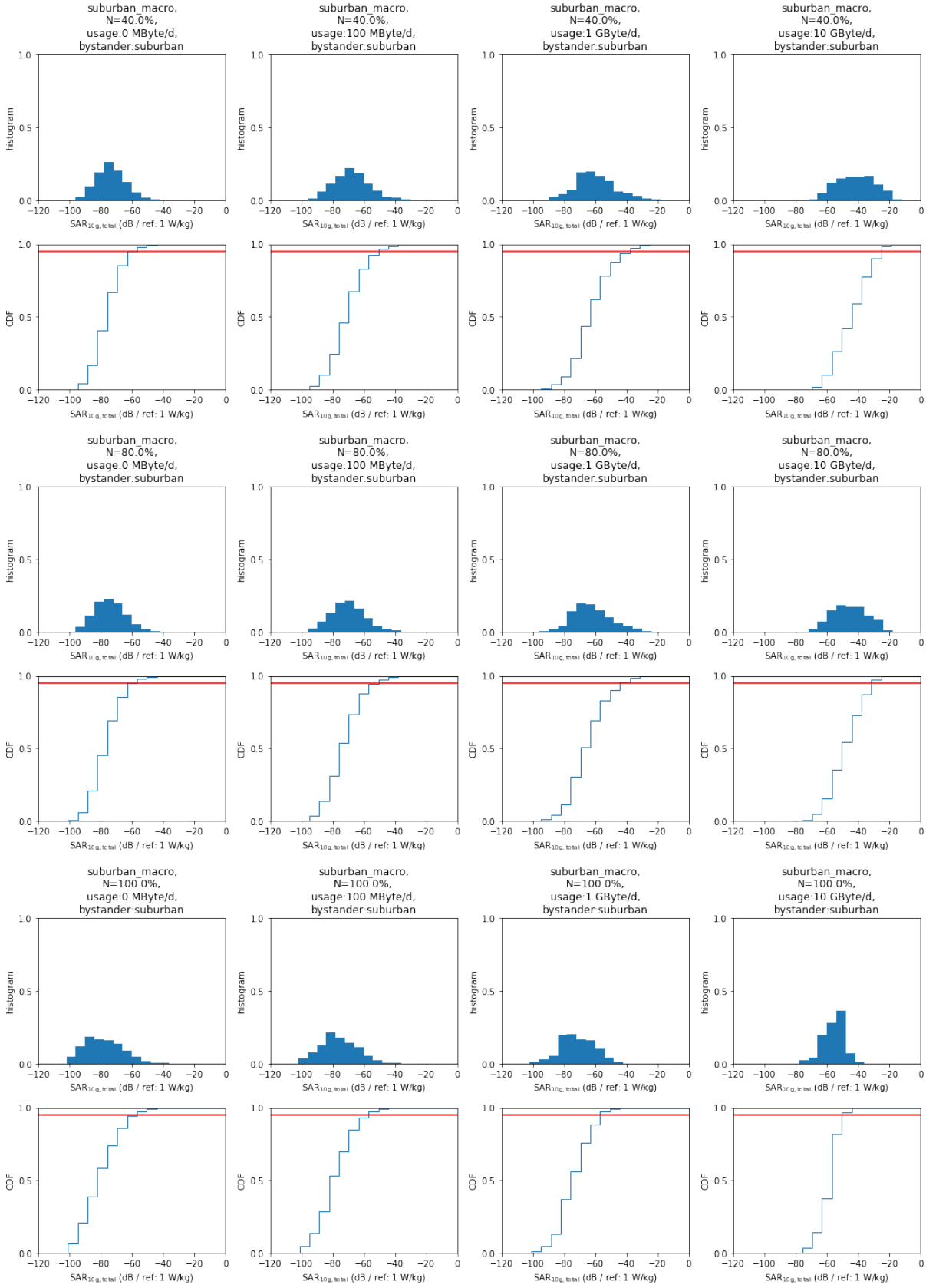

Figure 14: Histograms and cumulative distribution functions for the suburban cell scenario with varied cell edges and usage scenarios.

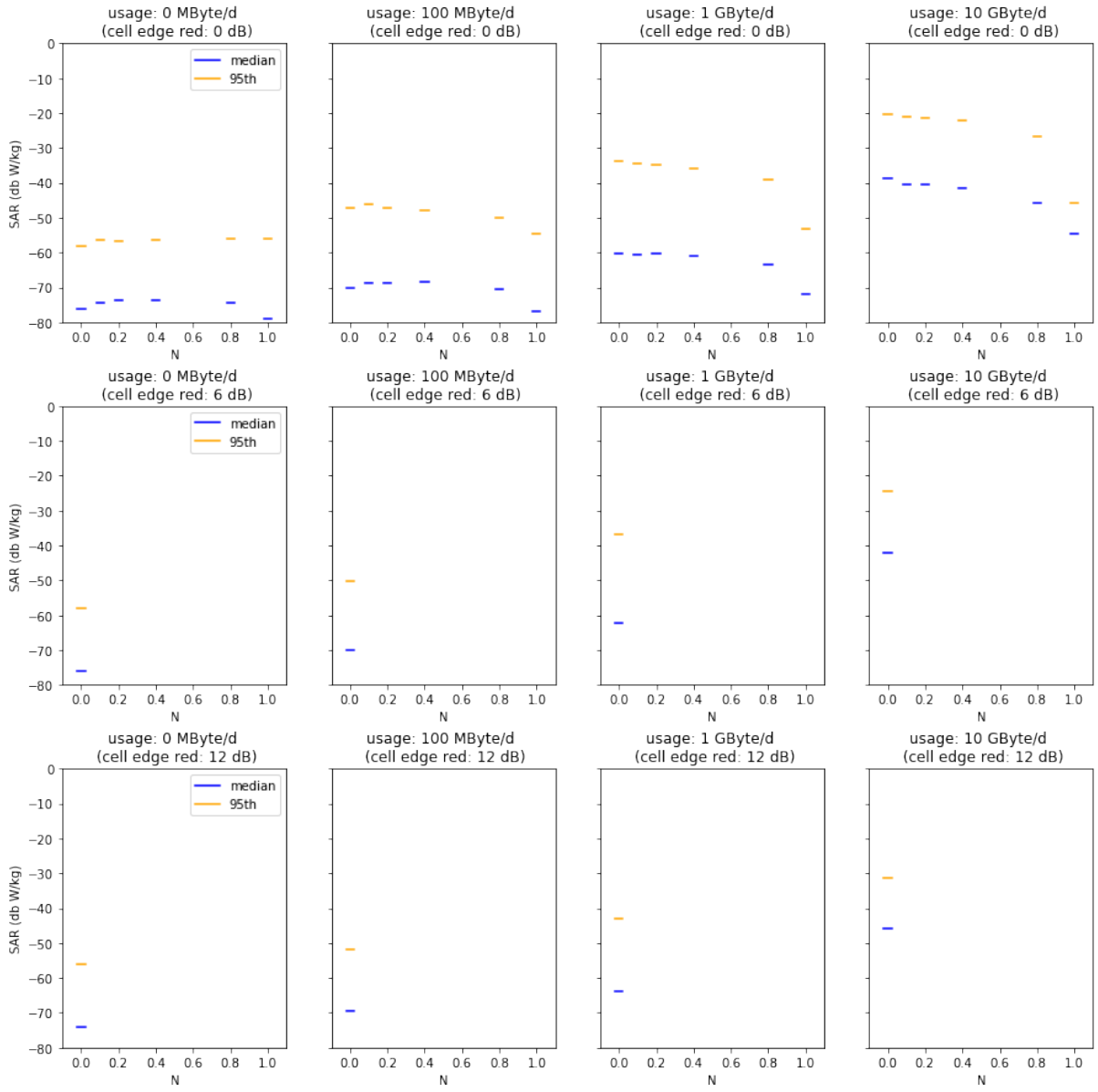

Figure 15: Median and 95$^{\text{th}}$ percentiles for varied usage, indoor coverage factor N, and cell size reductions in the suburban cell scenario.

A.3 Urban Macro Cell

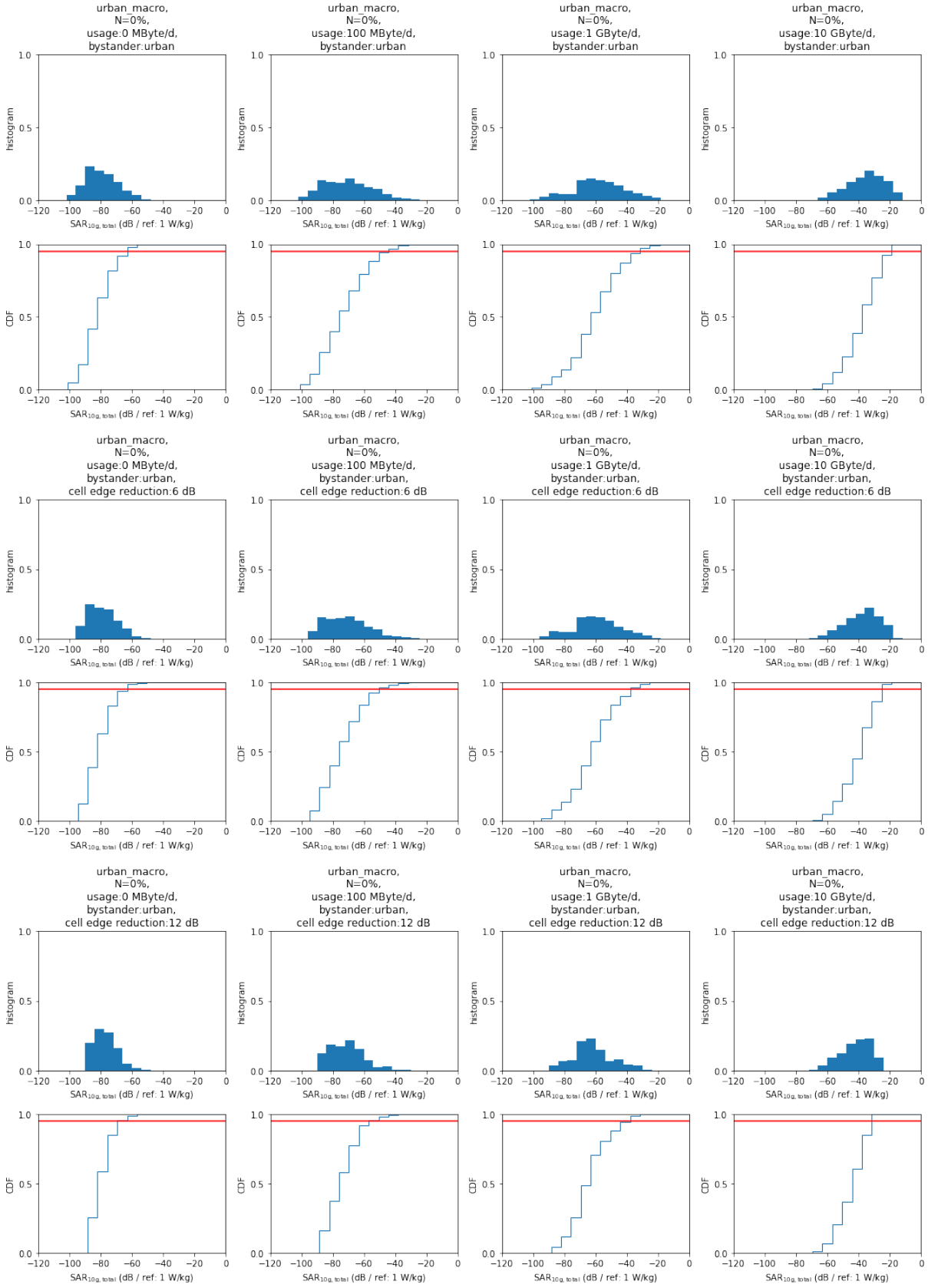

Figure 16: Histograms and cumulative distribution functions for the urban macro cell scenario with varied cell edges and usage scenarios for bystander 5 m away.

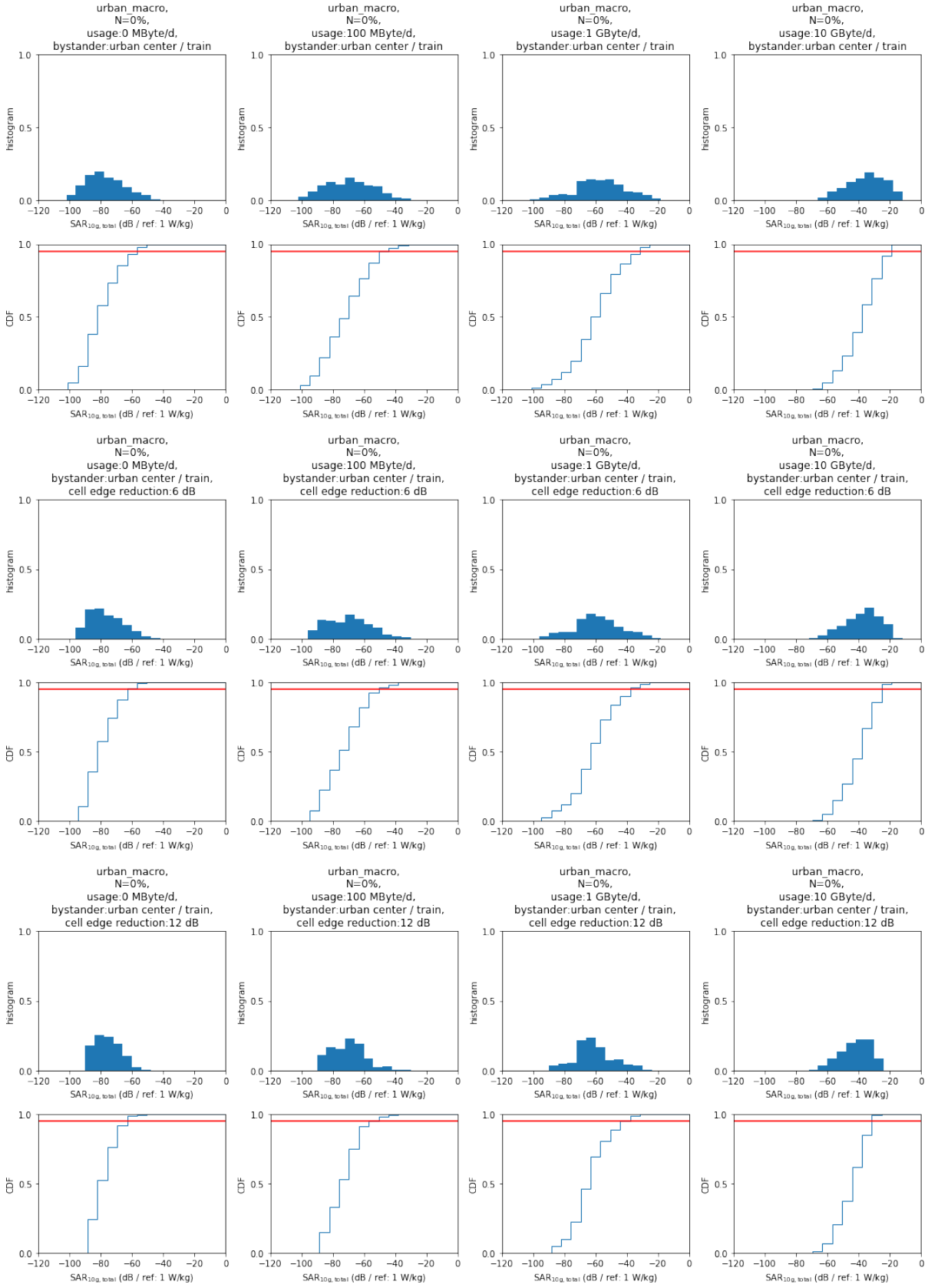

Figure 17: Histograms and cumulative distribution functions for the urban macro cell scenario with varied cell edges and usage scenarios for bystander 1 m away.

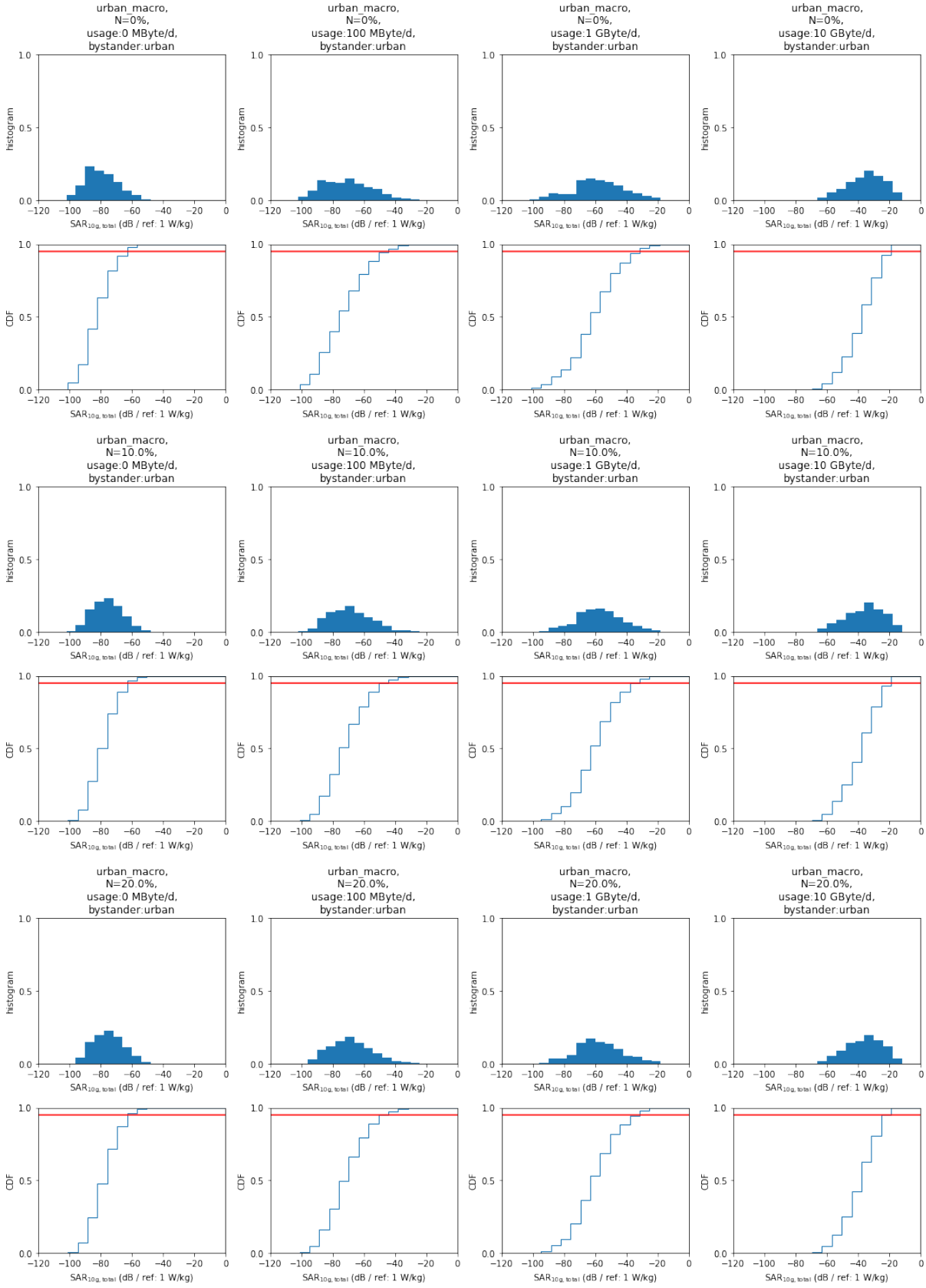

Figure 18: Histograms and cumulative distribution functions for the urban macro cell scenario with varied indoor coverage factors (N) and usage scenarios for bystander 5 m away.

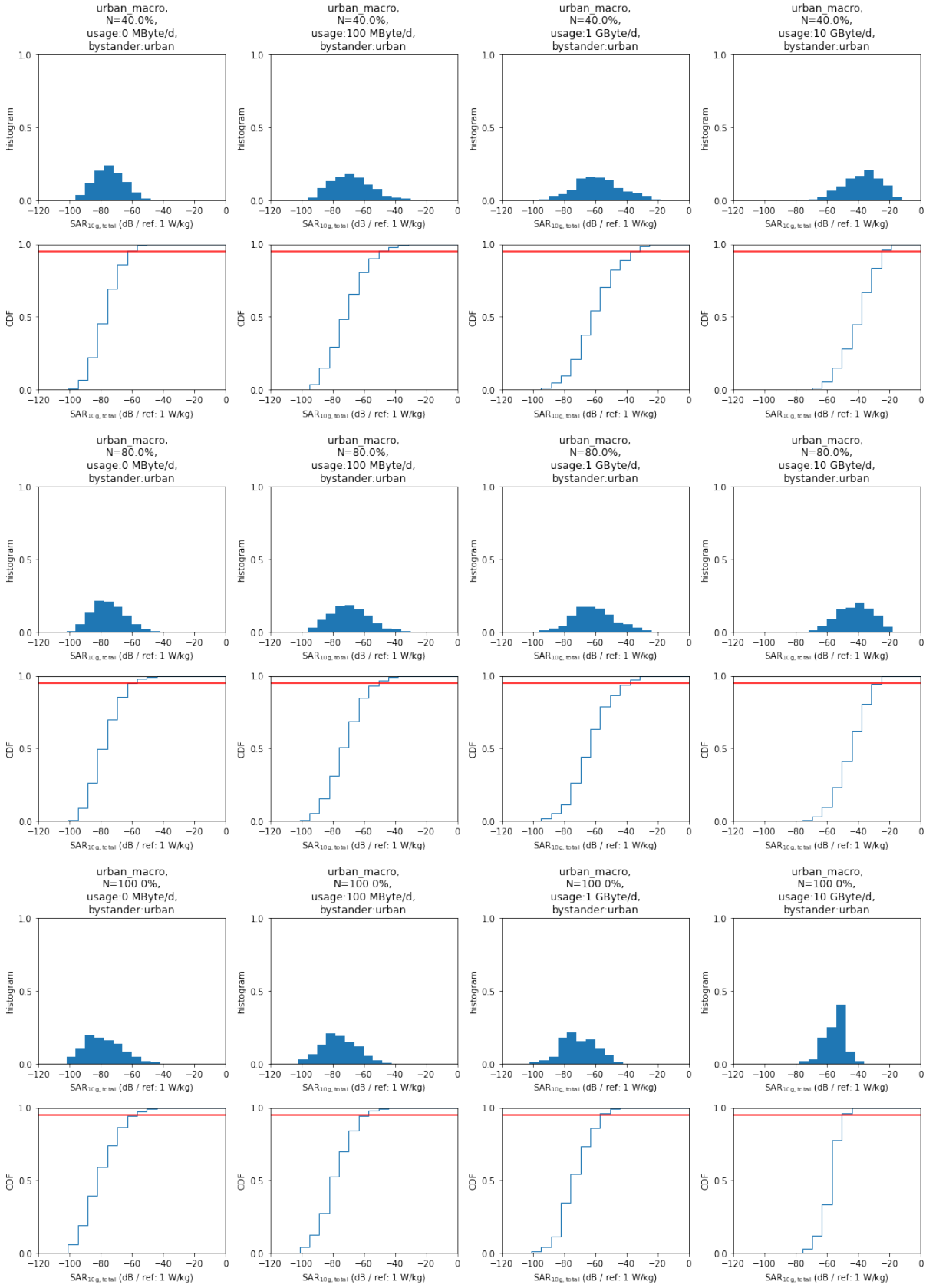

Figure 18: Histograms and cumulative distribution functions for the urban macro cell scenario with varied cell edges and usage scenarios for bystander 5 m away.

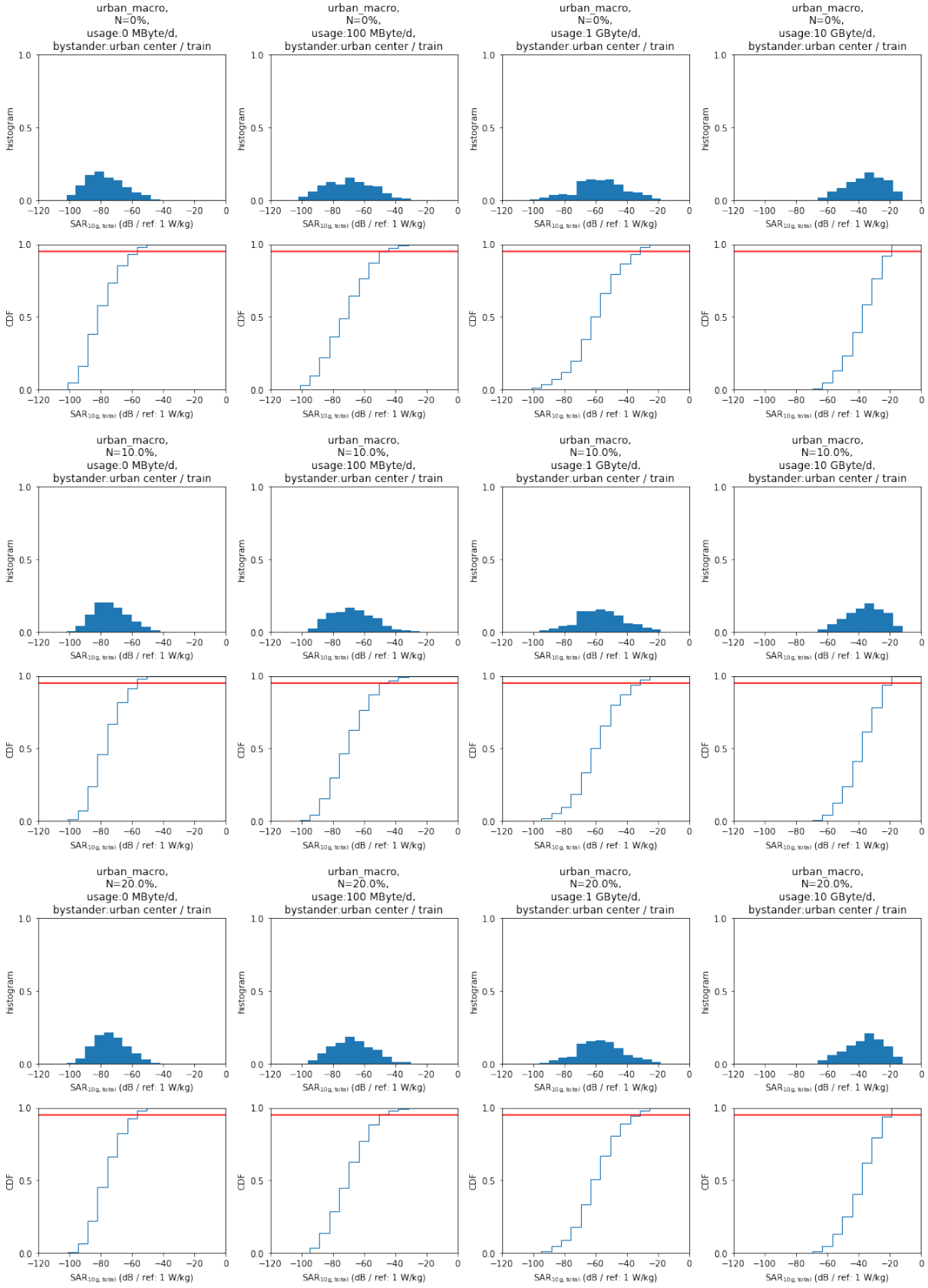

Figure 19: Histograms and cumulative distribution functions for the urban macro cell scenario with varied indoor coverage factors (N) and usage scenarios for bystander 1 m away.

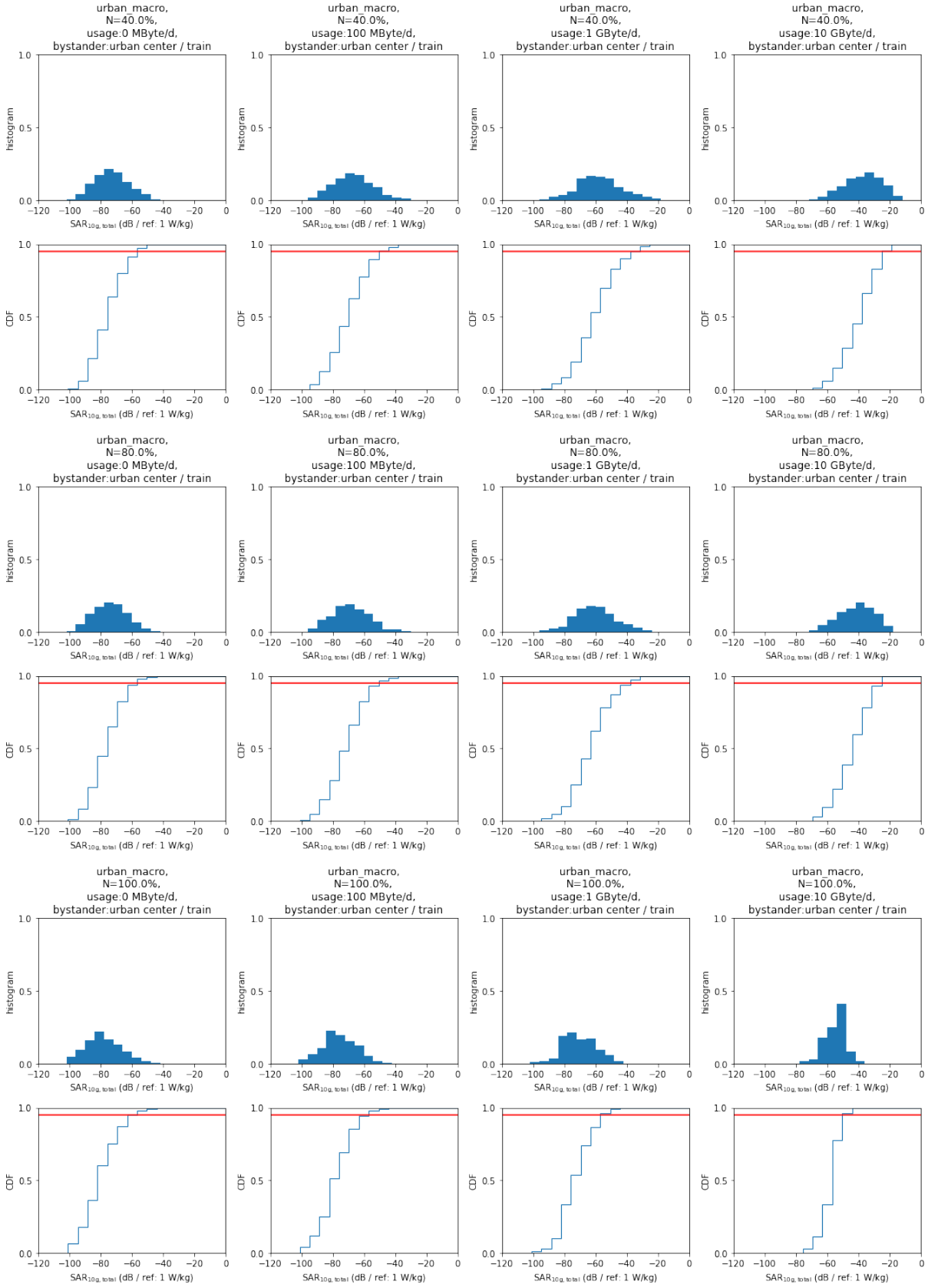

Figure 19: Histograms and cumulative distribution functions for the urban macro cell scenario with varied cell edges and usage scenarios.

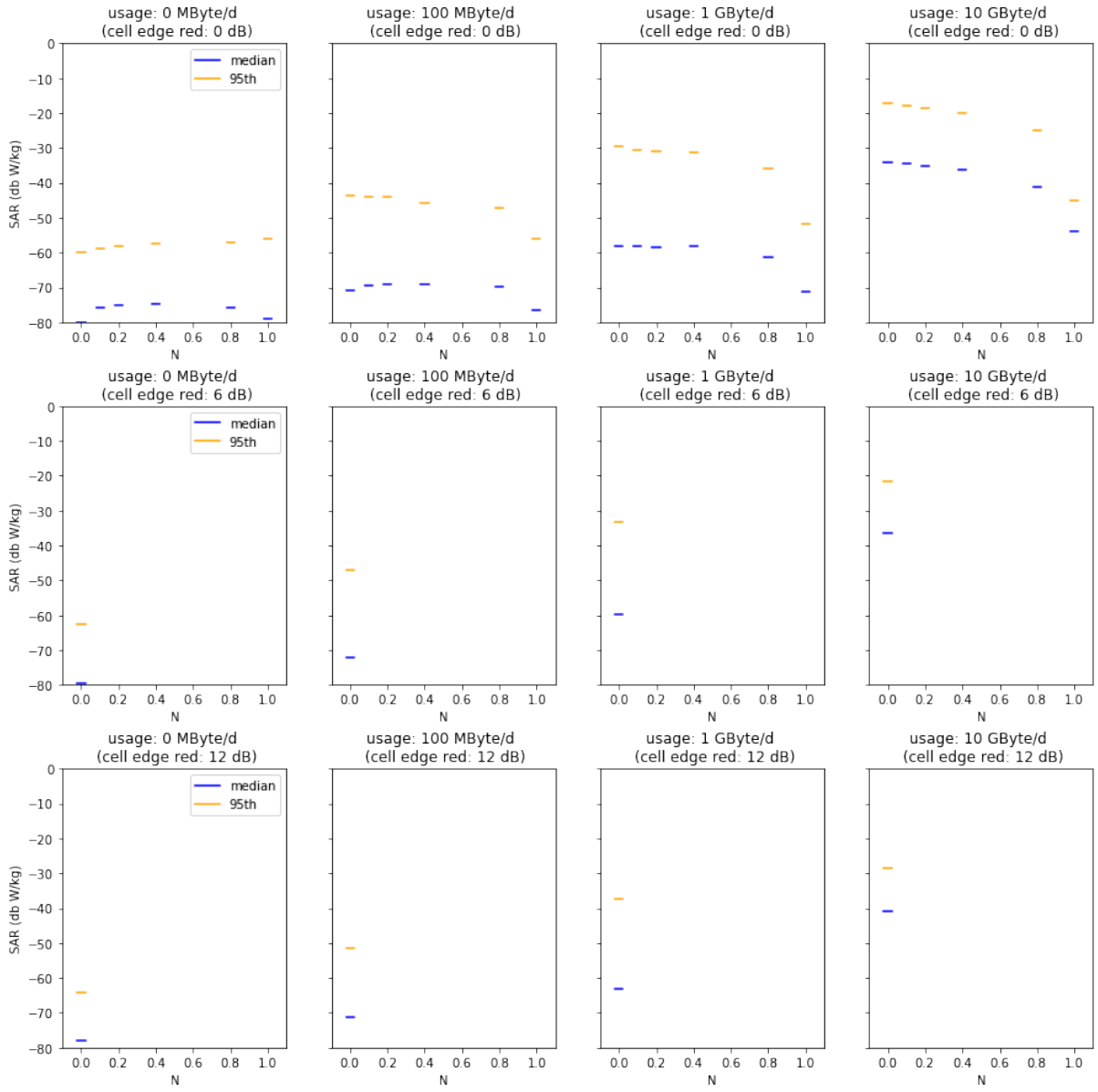

Figure 20: Median and 95$^{\text{th}}$ percentiles for varied usage, indoor coverage factor N and cell size reductions in the urban macro cell scenario for a bystander 5 m away.

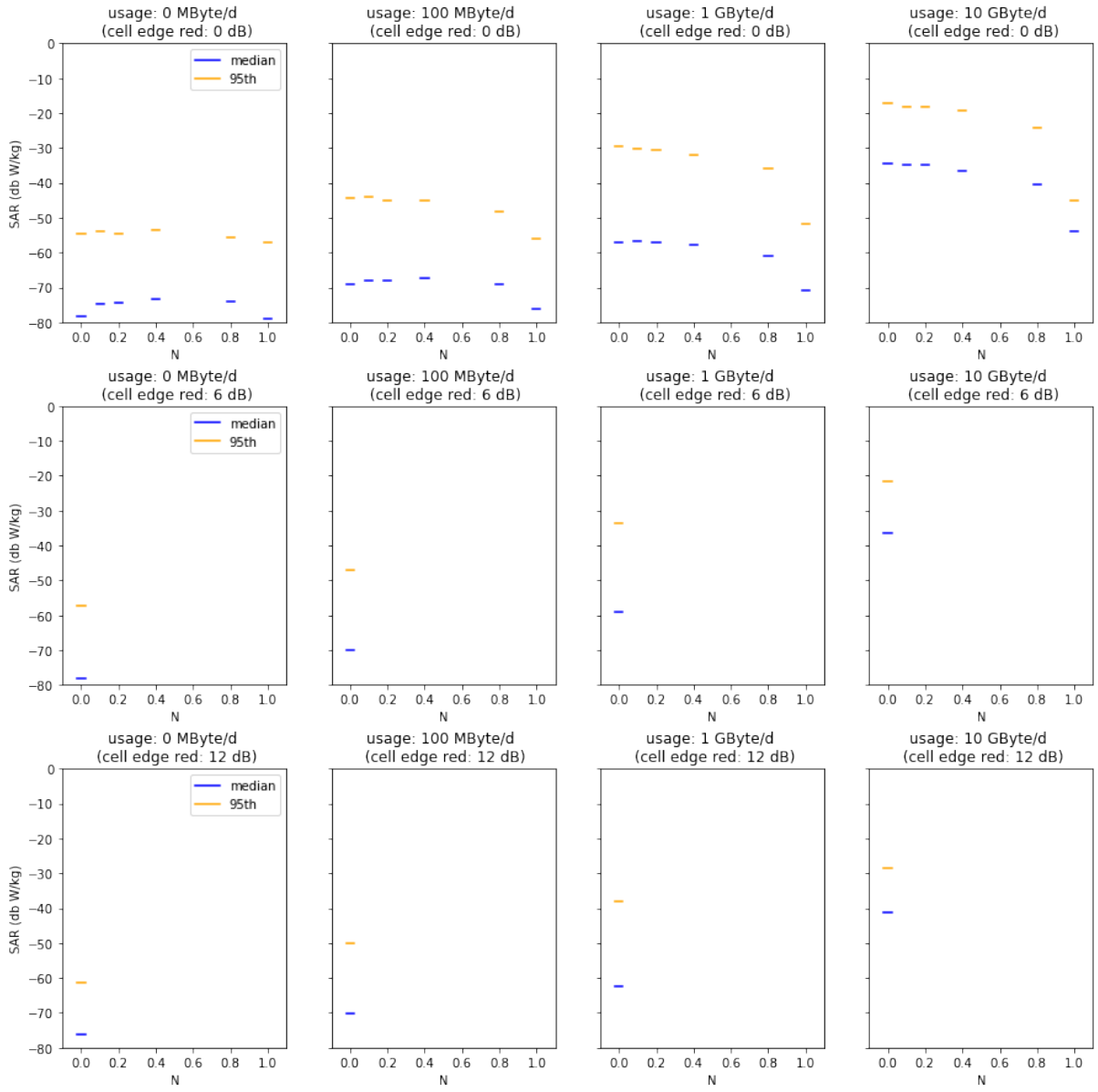

Figure 21: Median an 95^{th} percentiles for varied usage, indoor coverage factor N and cell size reductions in the urban macro cell scenario for bystander 1 m away.

A.4 Urban Mini Cell

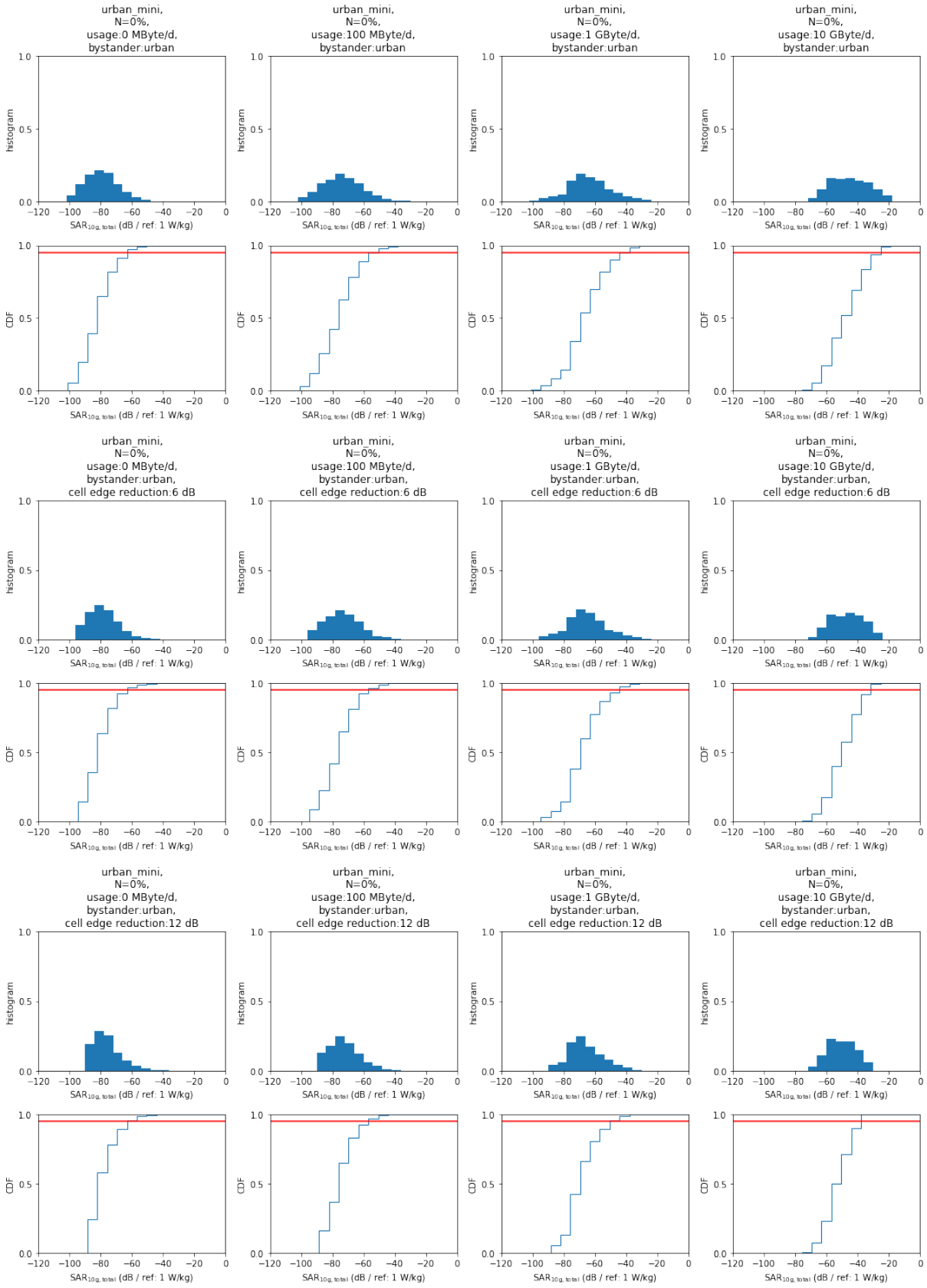

Figure 22: Histograms and cumulative distribution functions for the urban mini cell scenario with varied cell edges and usage scenarios for bystander 5 m away.

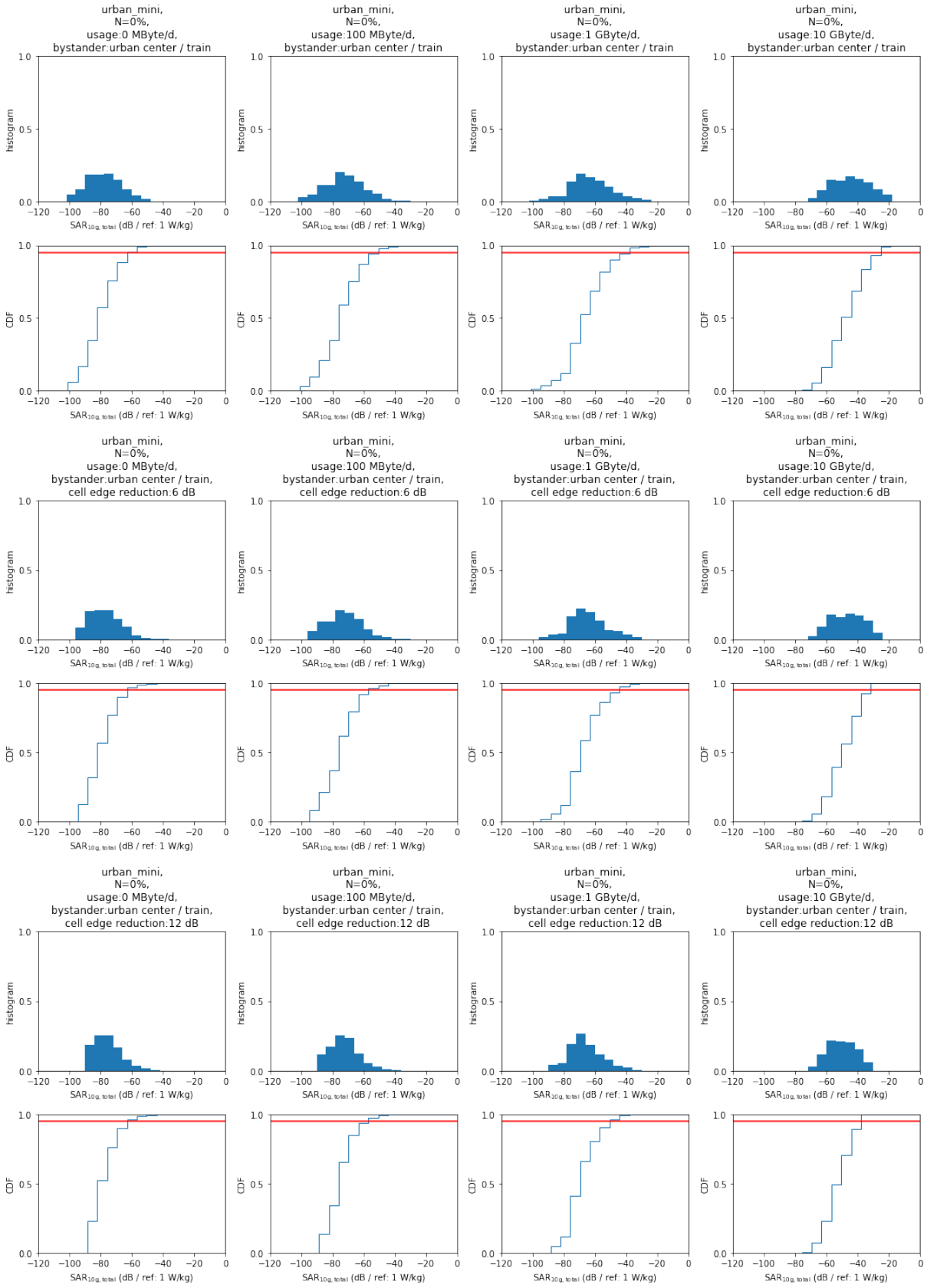

Figure 23: Histograms and cumulative distribution functions for the urban mini cell scenario with varied cell edges and usage scenarios for bystander 1 m away.

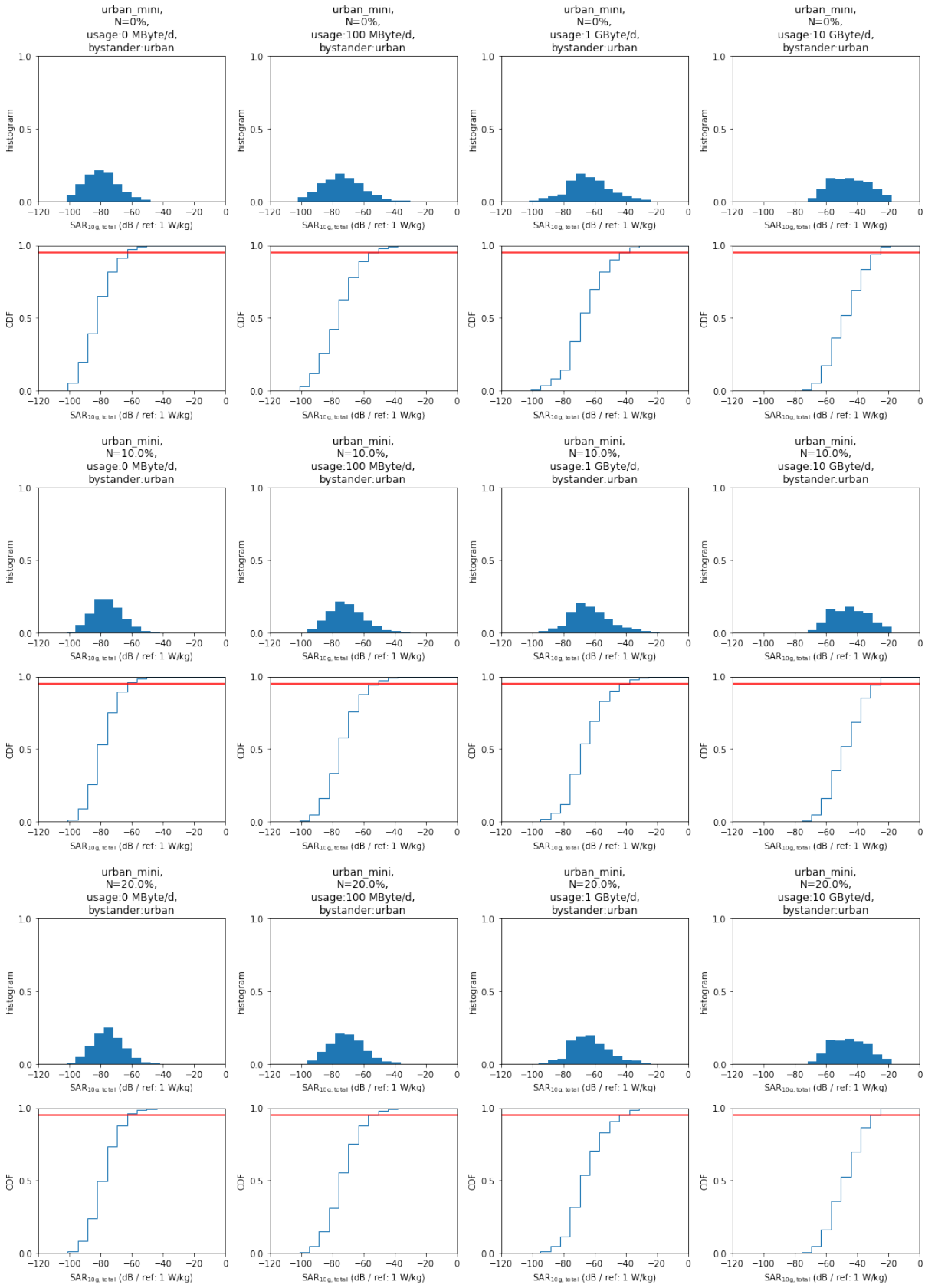

Figure 24: Histograms and cumulative distribution functions for the urban mini cell scenario with varied indoor coverage factors (N) and usage scenarios for bystander 5 m away.

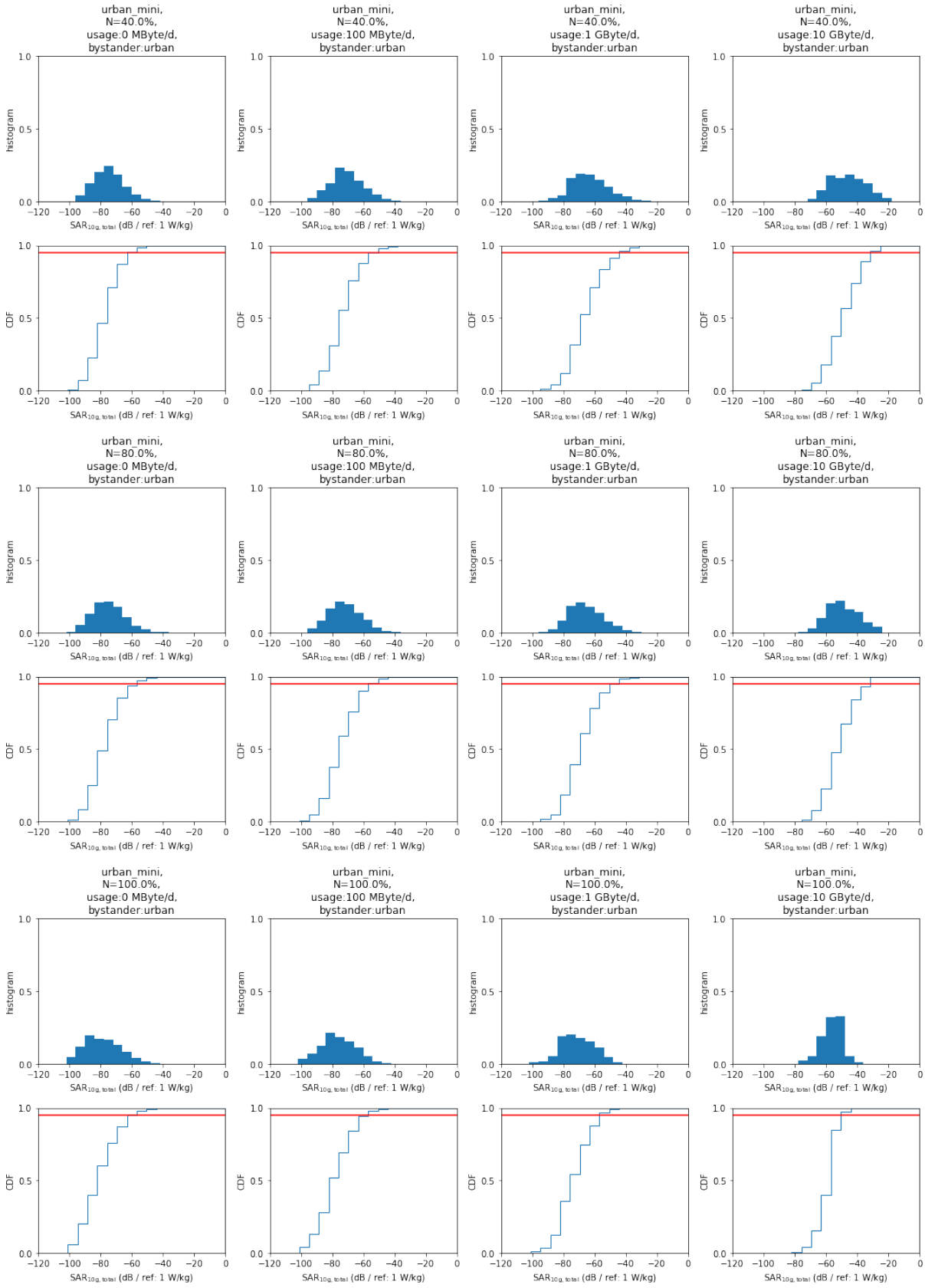

Figure 24: Histograms and cumulative distribution functions for the urban mini cell scenario with varied cell edges and usage scenarios for bystander 5 m away.

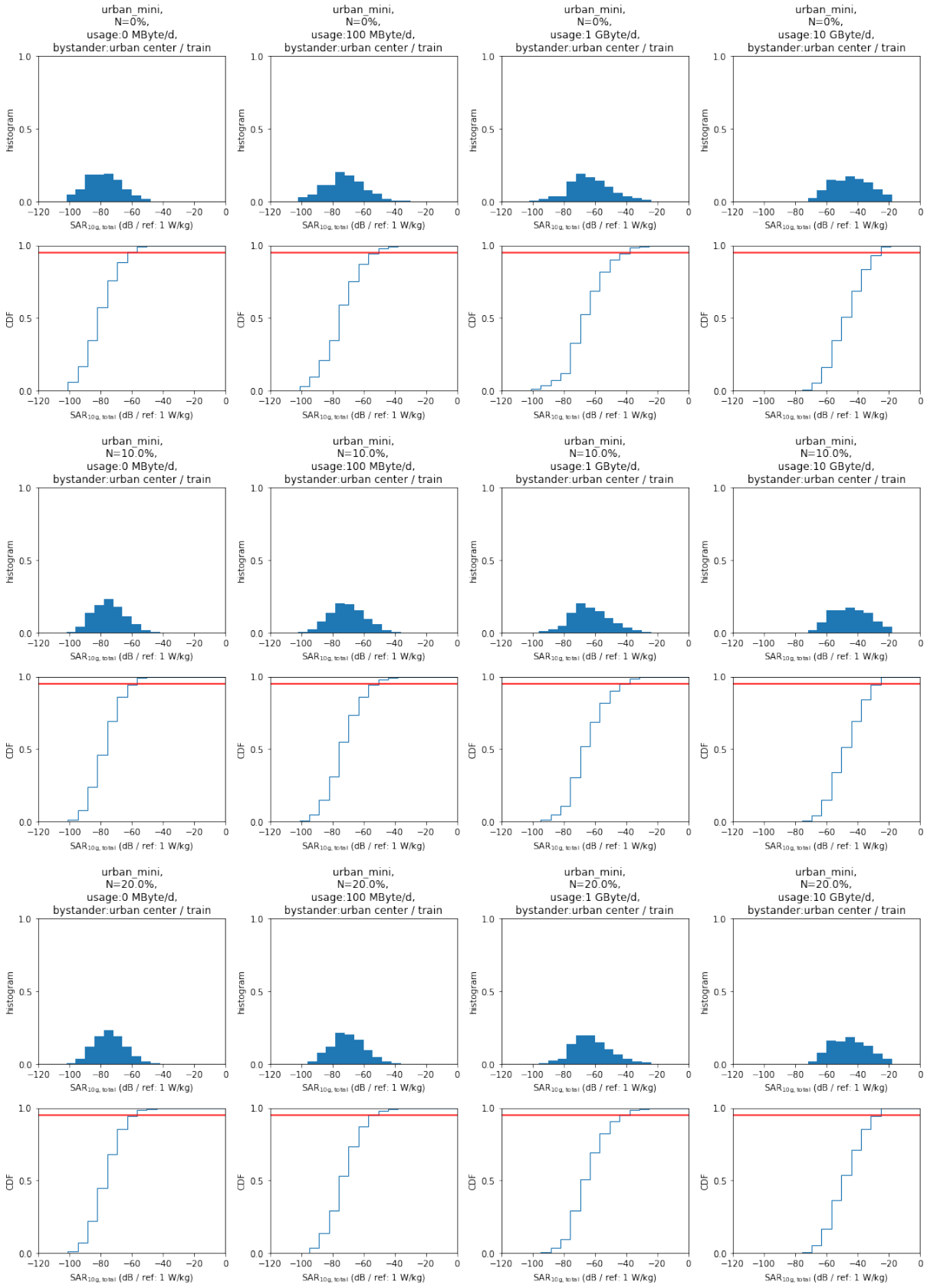

Figure 25: Histograms and cumulative distribution functions for the urban mini cell scenario with varied indoor coverage factors (N) and usage scenarios for bystander 1 m away.

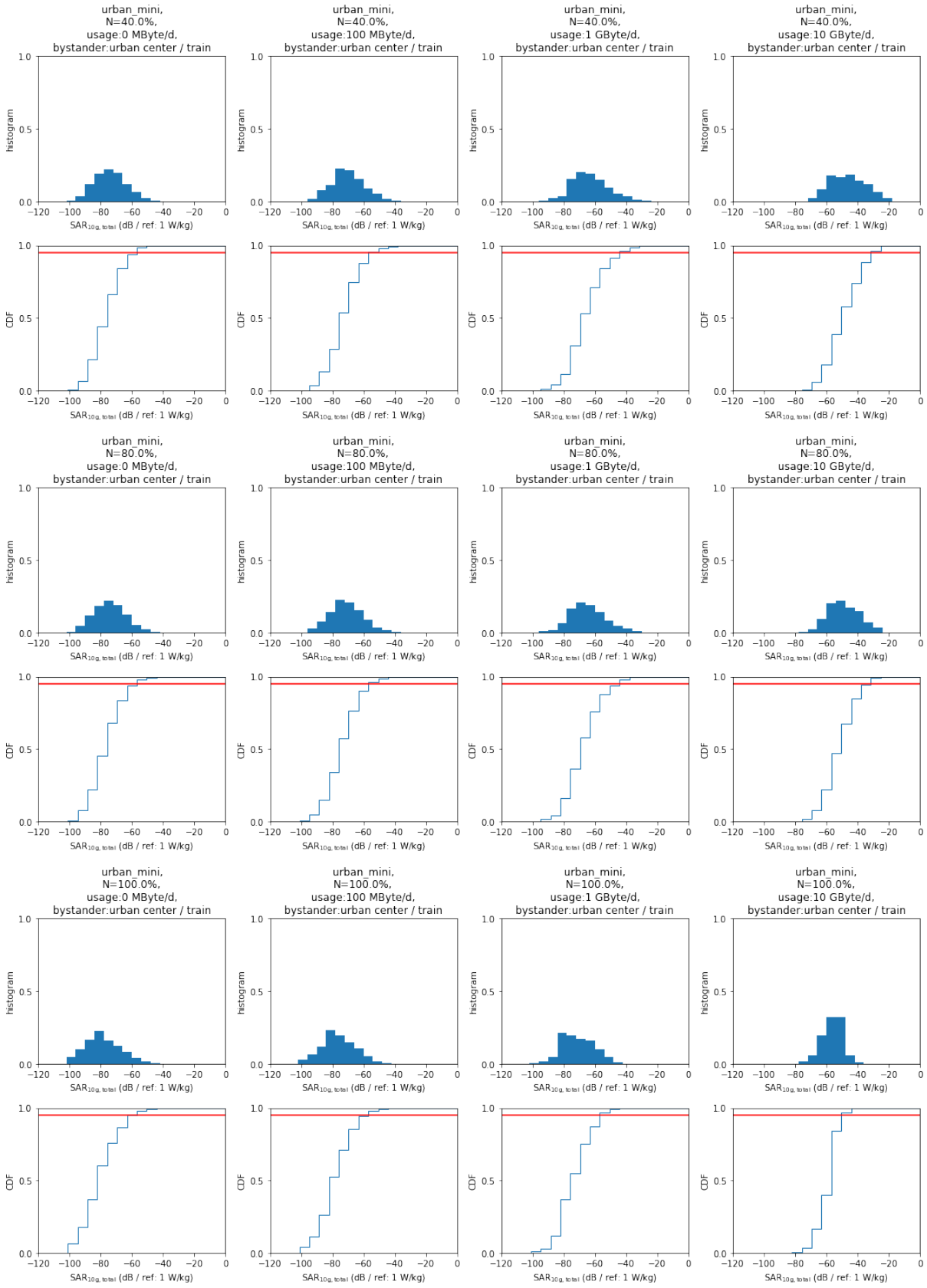

Figure 25: Histograms and cumulative distribution functions for the urban mini cell scenario with varied cell edges and usage scenarios.

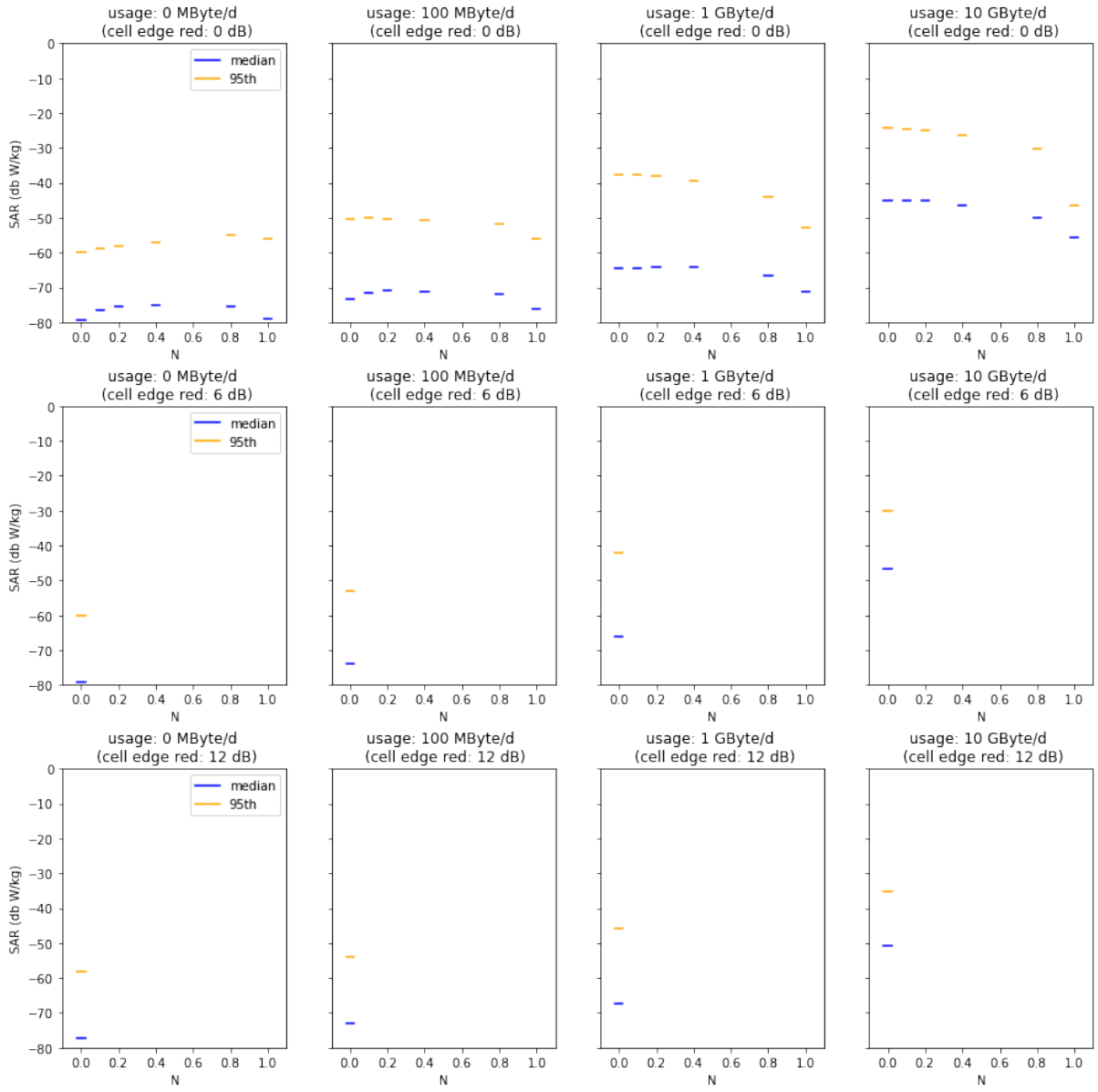

Figure 26: Median and 95$^{\text{th}}$ percentiles for varied usage, indoor coverage factor N and cell size reductions in the urban mini cell scenario for a bystander 5 m away.

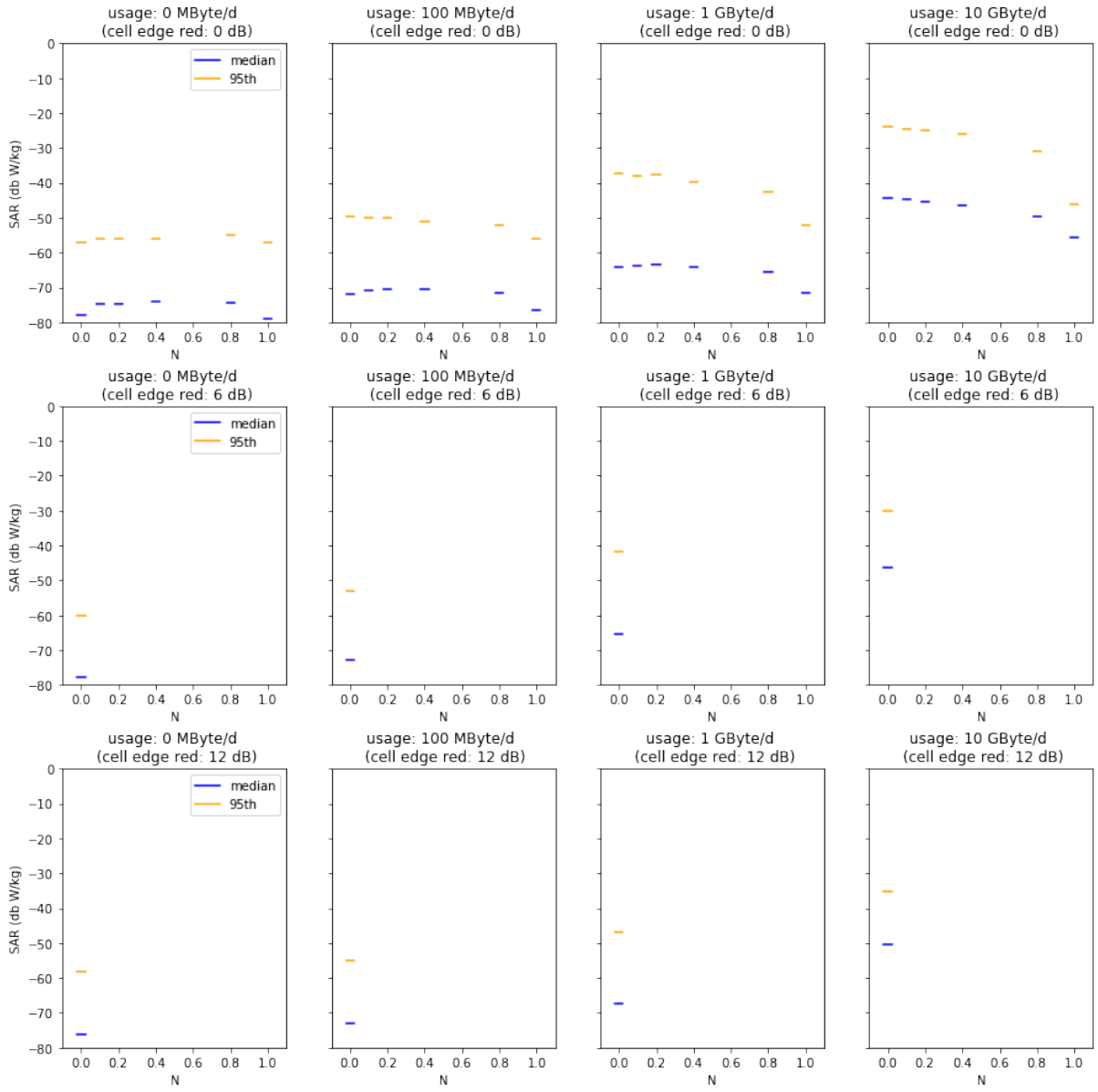

Figure 27: Median and 95$^{\text{th}}$ percentiles for varied usage, indoor coverage factor N, and cell size reductions in the urban mini cell scenario for a bystander 1 m away.

A.5 Urban Micro Cell

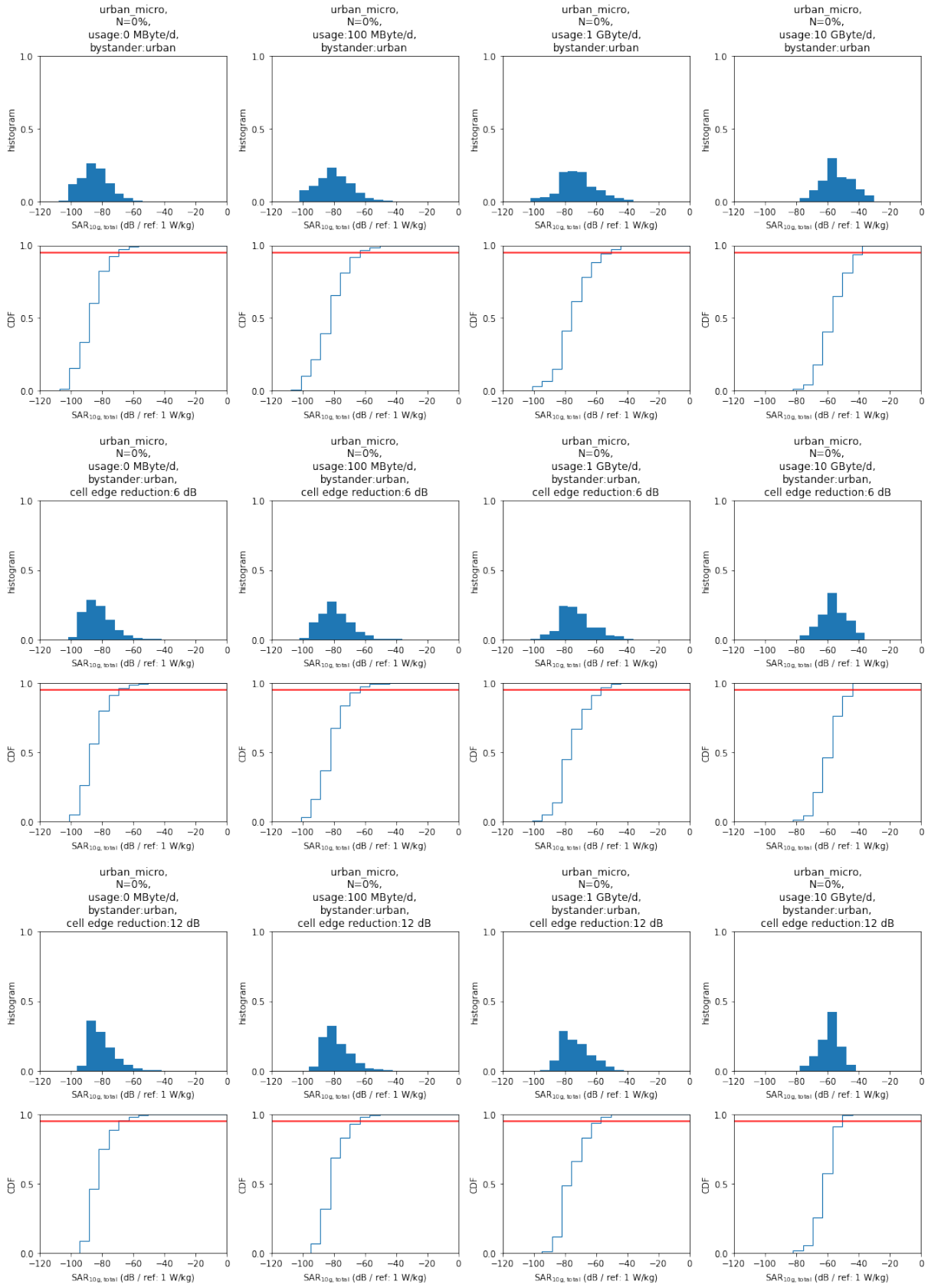

Figure 28: Histograms and cumulative distribution functions for the urban micro cell scenario with varied cell edges and usage scenarios for bystander 5 m away.

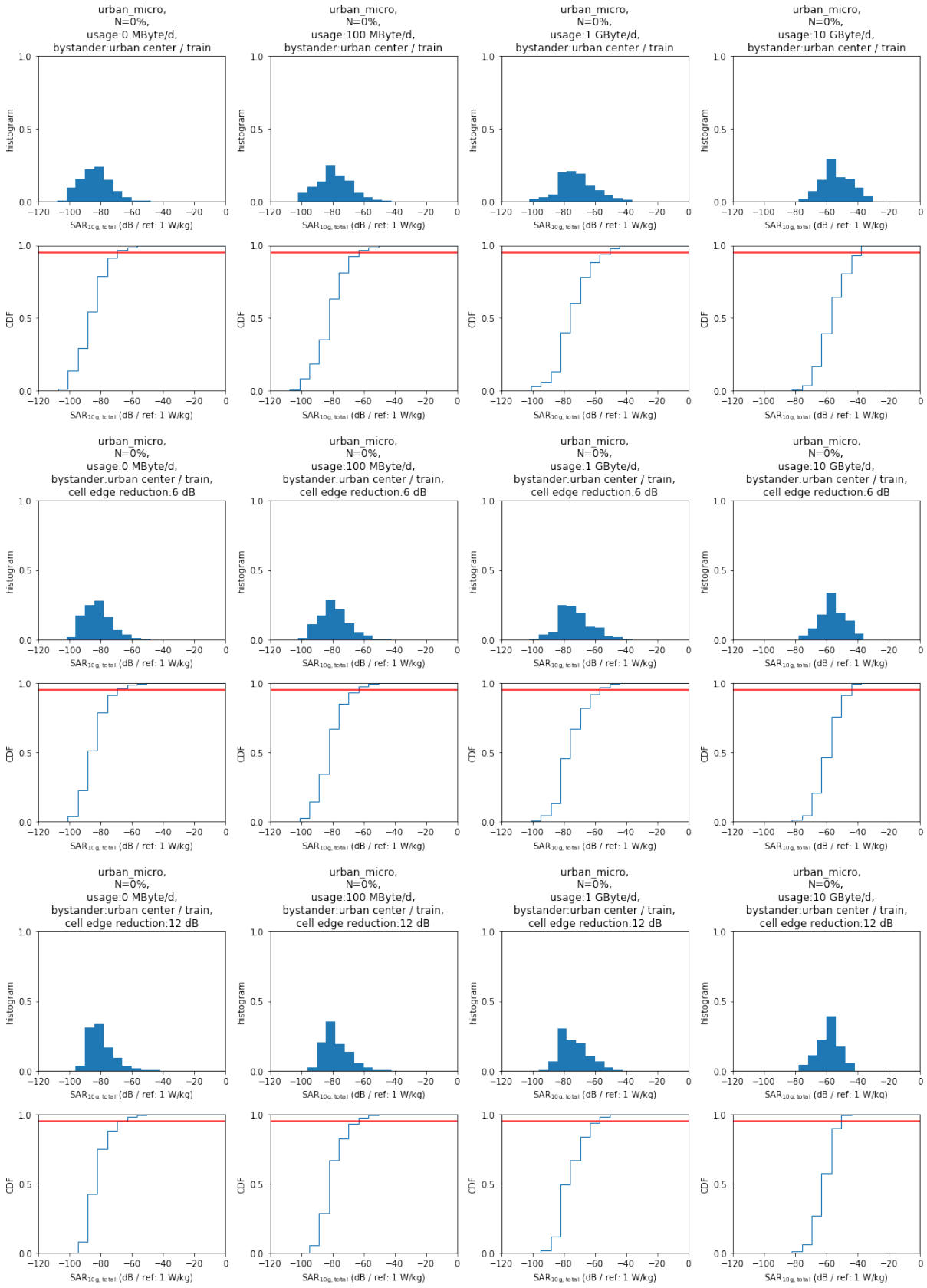

Figure 29: Histograms and cumulative distribution functions for the urban micro cell scenario with varied cell edges and usage scenarios for bystander 1 m away.

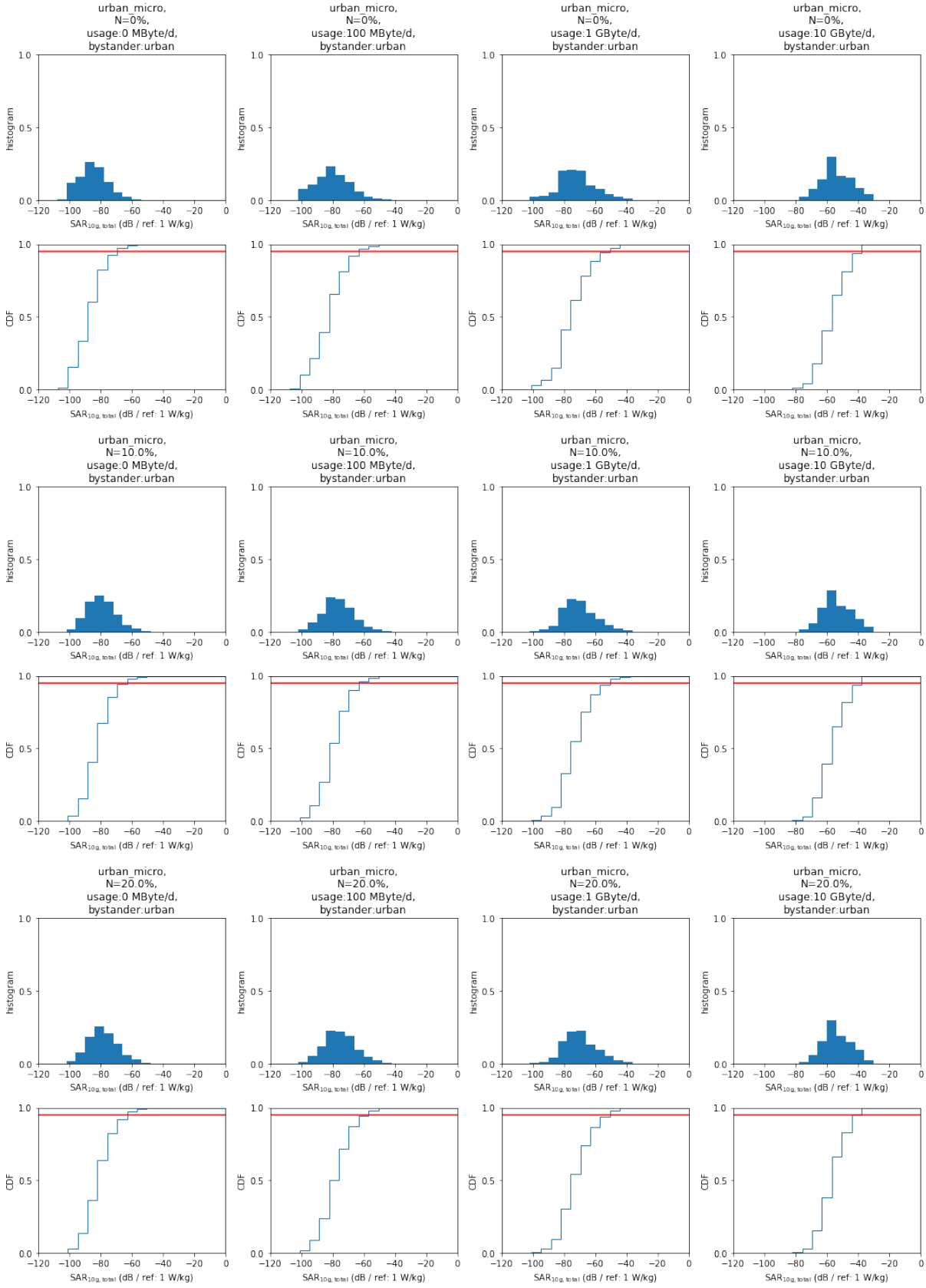

Figure 30: Histograms and cumulative distribution functions for the urban micro cell scenario with varied indoor coverage factors (N) and usage scenarios for bystander 5 m away.

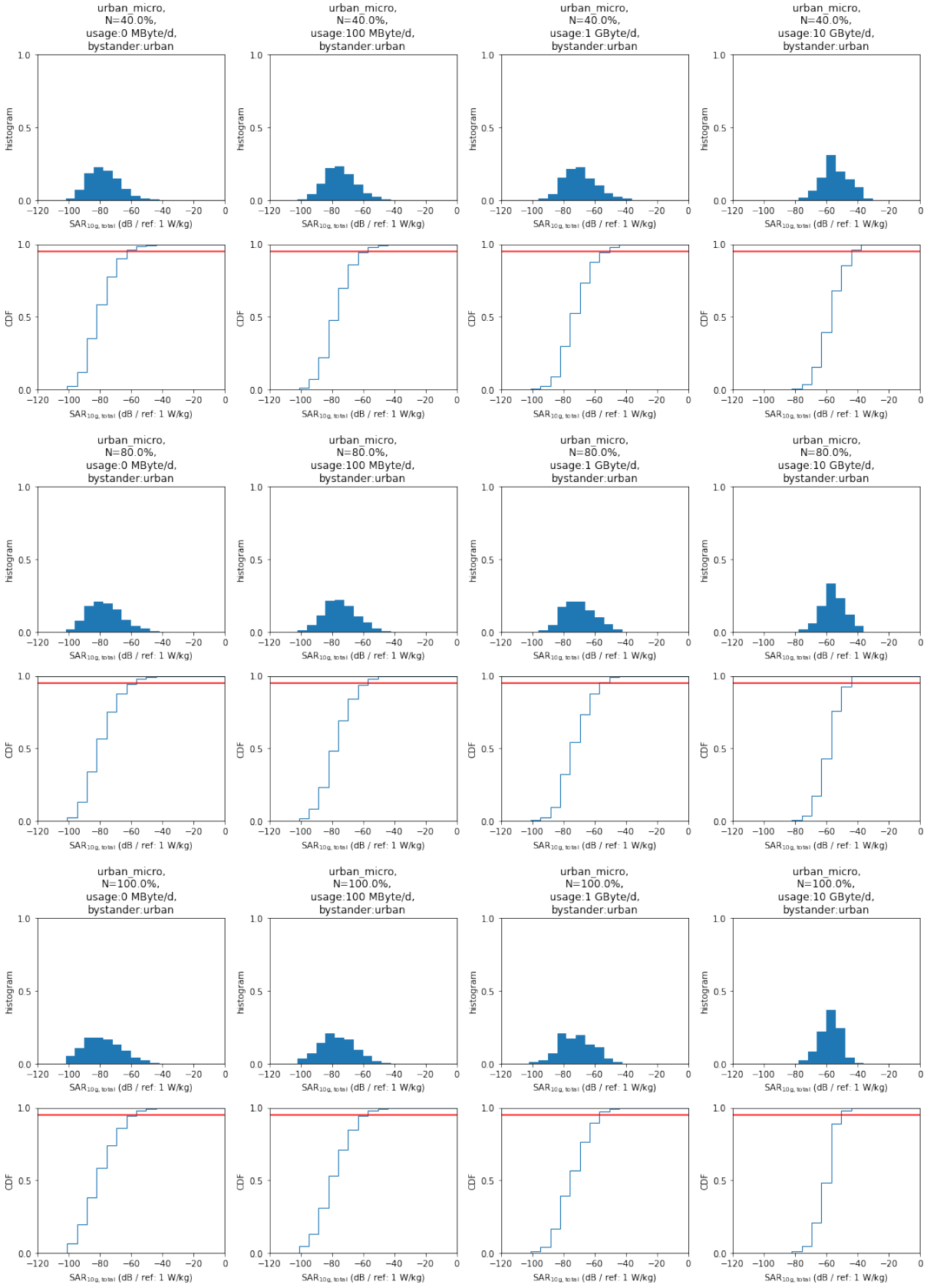

Figure 30: Histograms and cumulative distribution functions for the urban micro cell scenario with varied cell edges and usage scenarios for bystander 5 m away.

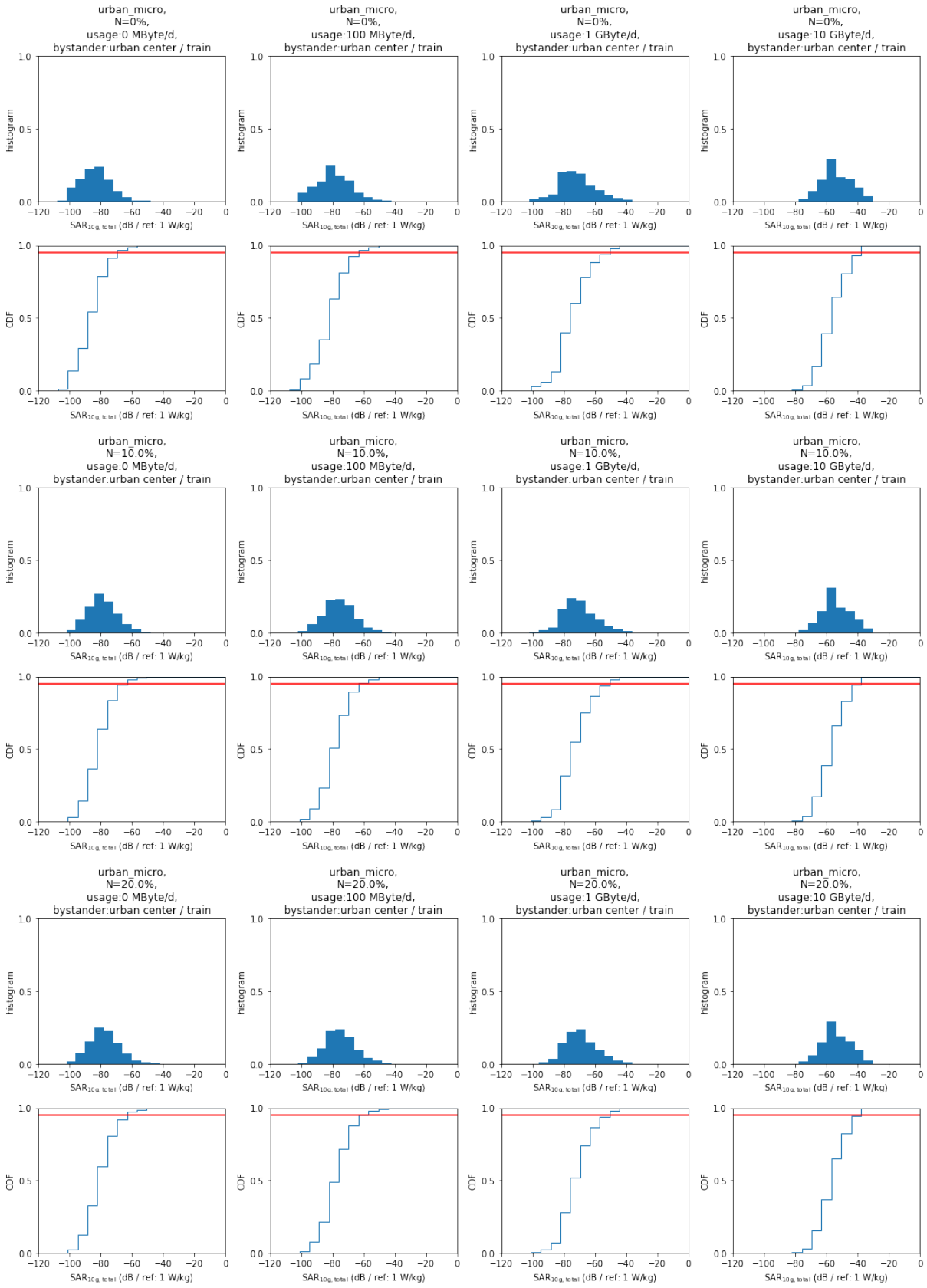

Figure 31: Histograms and cumulative distribution functions for the urban micro cell scenario with varied indoor coverage factors (N) and usage scenarios for bystander 1 m away.

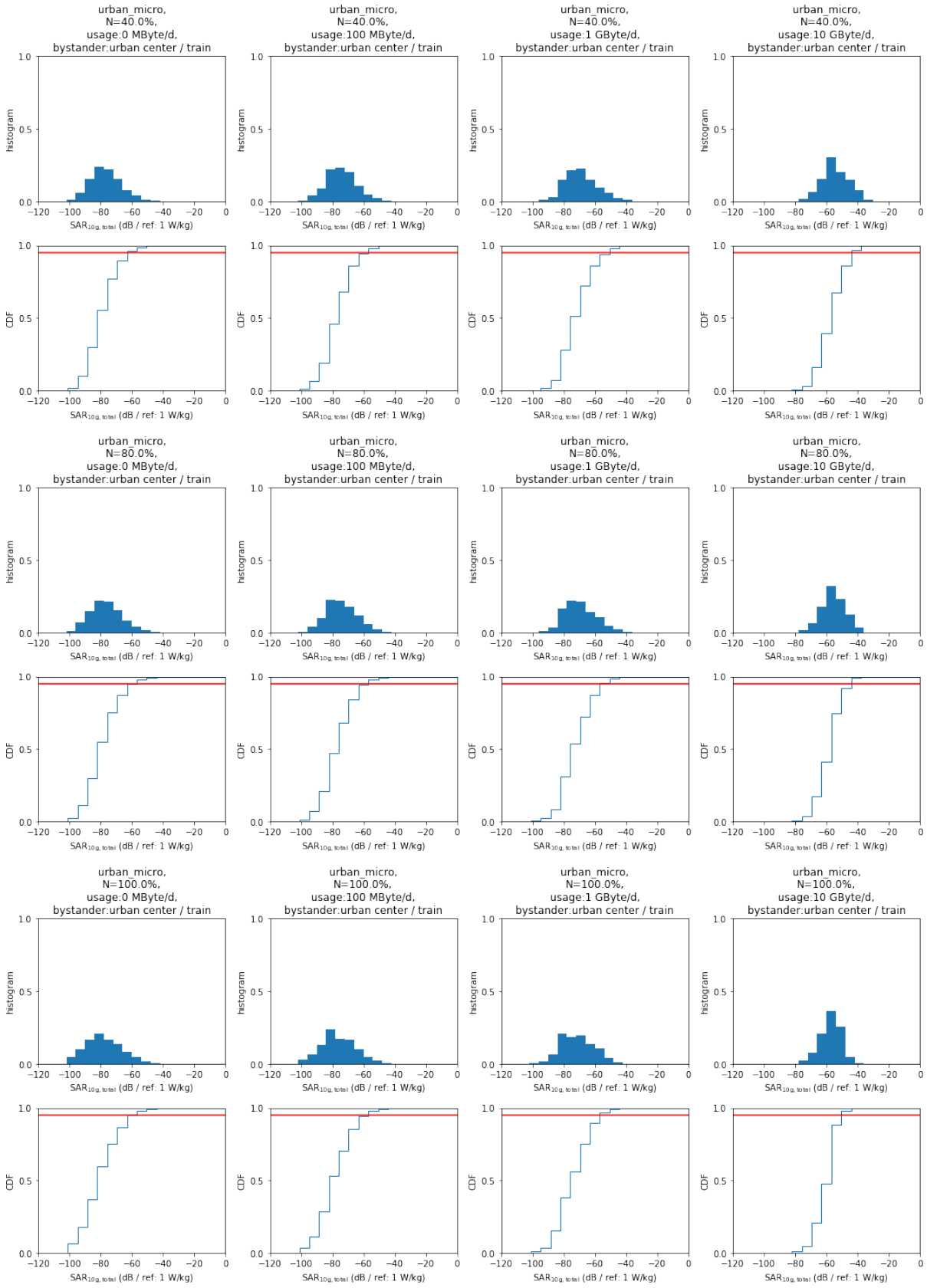

Figure 31: Histograms and cumulative distribution functions for the urban micro cell scenario with varied cell edges and usage scenarios.

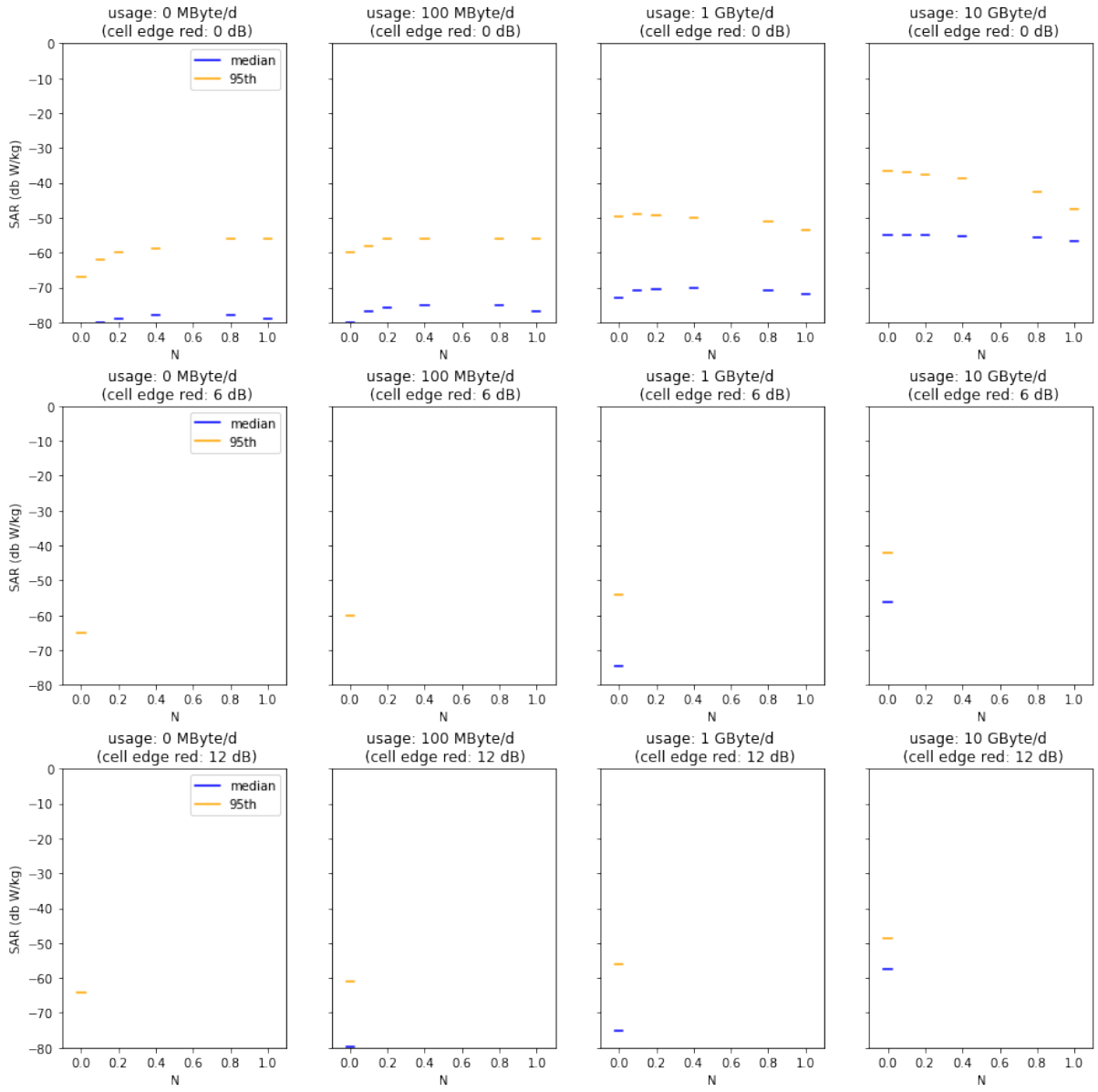

Figure 32: Median and 95$^{\text{th}}$ percentiles for varied usage, indoor coverage factor N, and cell size reductions in the urban micro cell scenario for a bystander 5 m away.

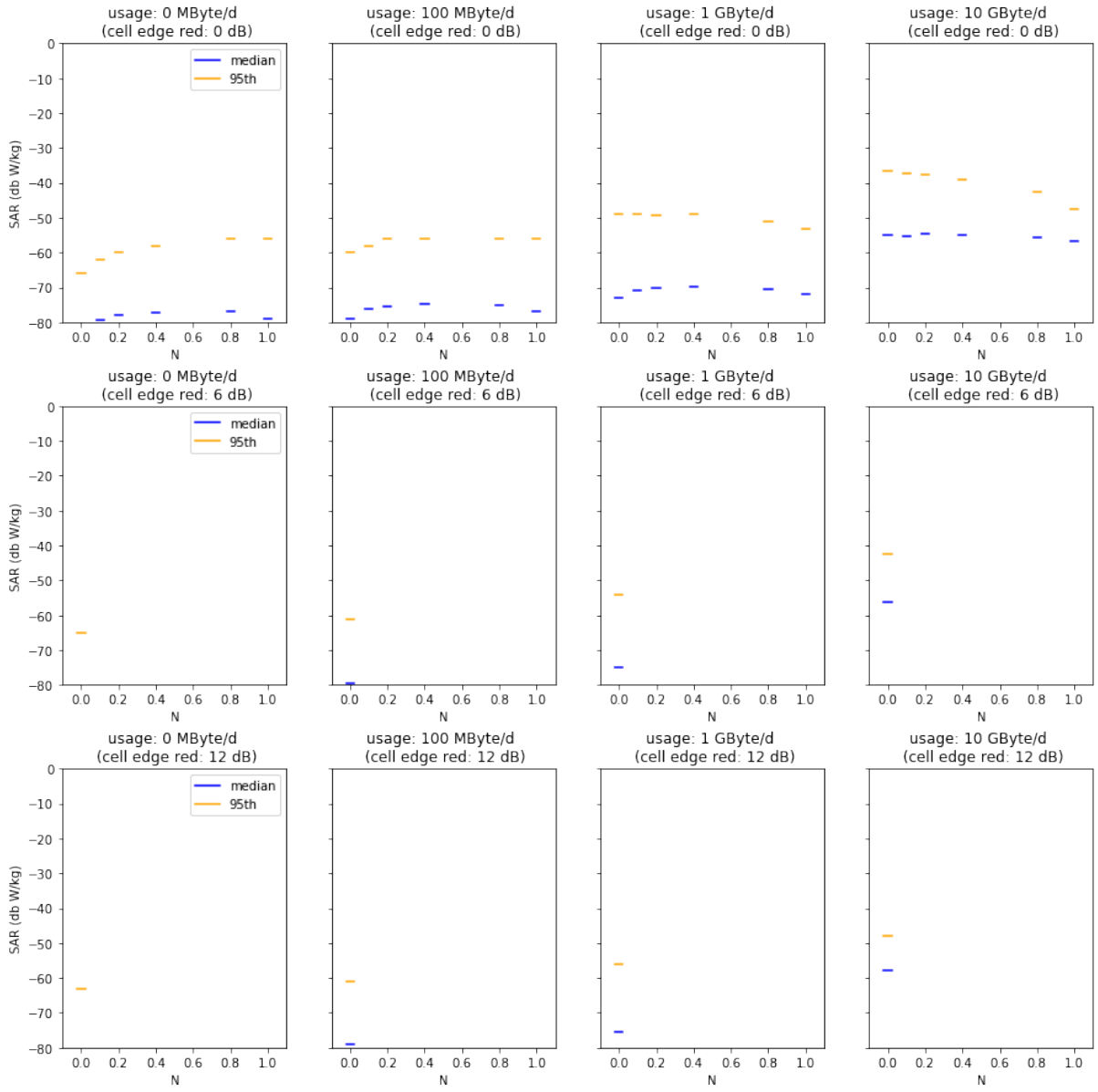

Figure 33: Median and 95$^{\text{th}}$ percentiles for varied usage, indoor coverage factor N, and cell size reductions in the urban micro cell scenario for a bystander 1 m away.